

# Dissertation

Expression of higher plant photosynthetic proteins in  
the cyanobacterium *Synechocystis* sp. PCC 6803



Dissertation der Fakultät für Biologie der Ludwig-Maximilians-  
Universität München

vorgelegt von

**Stefania Viola**

23.01.14

# Expression of higher plant photosynthetic proteins in the cyanobacterium *Synechocystis* sp. PCC 6803

Dissertation

zur Erlangung des Doktorgrades der Fakultät für Biologie  
der Ludwig-Maximilians-Universität München

**Stefania Viola**

Erstgutachter: Prof. Dr. Dario Leister

Zweitgutachter: Prof. Dr. Jörg Nickelsen

Tag der Einreichung: 18.12.2013

Tag der mündlichen Prüfung: 23.01.2014

## Summary

In plants, oxygenic photosynthesis occurs in chloroplasts, specialized organelles that originated from the endosymbiosis of an ancestral cyanobacterium. During evolution, the photosynthetic apparatus of higher plants underwent several changes in order to adapt to the new environmental light and oxygen conditions. The biogenesis and function of the photosynthetic complexes require many auxiliary and regulatory proteins that evolved in land plants, together with novel physiological mechanisms, in order to optimize the photosynthetic efficiency. The identification of these newly-evolved photosynthetic proteins is hampered by technical and biological limits of the plant model organisms. Here, we show the establishment of new tools for the study of higher plant photosynthesis that rely on the expression of *Arabidopsis* proteins in the unicellular cyanobacterium *Synechocystis* sp. PCC 6803. The use of a cyanobacterial platform benefits from the possibility to perform targeted gene manipulation, homologous complementation experiments and its short generation time. In this study, the PsaA and PsaB core subunits of *Synechocystis* photosystem I (PSI) have been replaced with the homologs from *Arabidopsis* and were shown to partially complement their function, although no functional PSI could form. The CURT1A protein from *Arabidopsis*, responsible for the curvature of the thylakoid grana margins, was expressed in *Synechocystis* in addition to or in replacement of the bacterial synCURT1 homolog. CURT1A functionally interacted with and partially complemented synCURT1, showing membrane-bending properties that increased when removing the bulky cyanobacterial phycobilisomes. In order to easily perform the elaborate gene manipulations required to substitute the *Synechocystis* photosynthetic apparatus, an alternative single-vector based marker-less gene replacement strategy was developed. The strategy was applied to introduce the *Arabidopsis* PGRL1 and PGR5 proteins in *Synechocystis*. These proteins are responsible for the antimycin A-sensitive variant of cyclic electron flow in plants. The expressed proteins caused changes in the PSI oxidation-reduction kinetics, interacting with the electron transport chain in a manner that needs to be further elucidated. The strategy also proved to be useful to sequentially disrupt and replace the *Synechocystis* *psaA* gene with the *Arabidopsis* evolutionary descendant.

## Zusammenfassung

Die oxygene Photosynthese der Pflanzen findet in spezialisierten Organellen, den Chloroplasten, statt, welche durch ein endosymbiotisches Ereignis entstanden sind. Als Folge der Anpassung an die neue zelluläre Umgebung erfuhr der Chloroplast cyanobakteriellen Ursprungs im Laufe der Evolution eine deutliche Veränderung. Diese ging mit dem Erwerb neuartiger Proteine und physiologischen Mechanismen einher, die die Biogenese und Funktion der Photosynthesekomplexe an die eukaryotische Situation angepasst haben. Die Identifizierung dieser neu entstandenen, photosynthetischen Proteine wird durch technische und biologische Limitierungen der pflanzlichen Modellorganismen erschwert. Im Rahmen dieser Arbeit wurden daher neue Methoden für die Untersuchung der Photosynthese höherer Pflanzen entwickelt, die den Transfer und die Expression von Proteinen aus *Arabidopsis* in dem Cyanobakterium *Synechocystis* sp. PCC 6803 erlauben. Die Vorteile dieses Einzellers liegen vorwiegend in der relativ kurzen Generationszeit sowie in der Möglichkeit zur gezielten Genmanipulation und homologen Komplementation. In dieser Arbeit wurden die Untereinheiten des Photosystems I (PSI) aus *Synechocystis*, PsaA und PsaB, durch die homologen Proteine aus *Arabidopsis* ersetzt. Hierbei wurde gezeigt, dass sich die Funktion dieser Proteine durch deren Homologe aus *Arabidopsis* teilweise ersetzen lässt, auch wenn kein funktionstüchtiges PSI assembliert werden konnte. Desweiteren wurde das CURT1A-Protein aus *Arabidopsis*, welches für die Biegung der Thylakoidmembran in den Randbereichen der Granastapel zuständig ist, in *Synechocystis* zusätzlich oder als Ersatz für dessen homologes synCURT1-Protein exprimiert. CURT1A war in der Lage, mit synCURT1 zu interagieren und dessen membranbiegende Funktion teilweise zu ersetzen. Die membranbiegende Fähigkeit ließ sich zudem durch das Entfernen der voluminösen Phycobilisomen deutlich verstärken. Ein weiteres Ziel dieser Arbeit bestand in der Etablierung einer alternativen Genaustauschstrategie, welche die aufwändige, mehrstufige Genmanipulationen von *Synechocystis* vereinfacht und auf dem Transfer eines Marker-freien Einzelvektors beruht. Unter Verwendung dieser Strategie konnten die Proteine PGRL1 und PGR5 von *Arabidopsis*, die für den Antimycin A-empfindlichen zyklischen Elektronentransport verantwortlich sind, in *Synechocystis* exprimiert werden. Die Expression dieser Proteine führte zu Veränderungen in der PSI-Redox-Kinetik, wobei der genaue Wirkungsmechanismus unbekannt ist und weitere Analysen erforderlich sind. Diese Strategie wurde zudem erfolgreich angewandt, um das endogene *psaA*-Gen in *Synechocystis* zu stören und anschließend durch dessen evolutionären Nachkommen aus *Arabidopsis* zu ersetzen.

## Index

<b>Summary</b> .....	<b>i</b>
<b>Zusammenfassung</b> .....	<b>ii</b>
<b>Index</b> .....	<b>iii</b>
<b>List of Figures</b> .....	<b>vi</b>
<b>List of Tables</b> .....	<b>vii</b>
<b>Abbreviations</b> .....	<b>viii</b>
<b>1. Introduction</b> .....	<b>1</b>
1.1. <u>Endosymbiotic origin of plant chloroplasts</u> .....	1
1.2. <u>Higher plant photosynthesis in the light of evolution</u> .....	2
1.3. <u>Evolution of PSI</u> .....	7
1.4. <u>Evolution of the thylakoid membrane architecture</u> .....	12
1.5. <u>Limitations of plant photosynthesis research</u> .....	14
1.6. <u>Designing a cyanobacterial platform to study higher plant photosynthesis</u> .....	16
1.7. <u><i>Synechocystis</i> as a model organism</u> .....	16
1.8. <u>Aim of the work</u> .....	19
<b>2. Materials and Methods</b> .....	<b>20</b>
2.1. <u>Chemicals, enzymes and radioactive substances</u> .....	20
2.2. <u>Bacterial strains and vectors</u> .....	21
2.3. <u>Generation of recombinant plasmids</u> .....	23
2.4. <u><i>Synechocystis</i> transformation</u> .....	30
2.5. <u><i>Synechocystis</i> counter-selection and frequency calculation of second recombinants</u> .....	30
2.6. <u>Plant cultivation and growth conditions</u> .....	31
2.7. <u>Nucleic acid manipulation</u> .....	31
2.7.1. <u>Standard and high-fidelity PCR</u> .....	31
2.7.2. <u>Genomic DNA isolation</u> .....	31
2.7.3. <u>RNA isolation</u> .....	32
2.7.4. <u>Plant cDNA synthesis</u> .....	33
2.7.5. <u>Southern analyses</u> .....	33
2.7.6. <u>Northern analyses</u> .....	35

2.8. <u>Protein manipulation</u> .....	36
2.8.1. <u>Protein preparation and immuno-blot analyses</u> .....	36
2.8.2. <u>Blue-Native analyses of thylakoid protein complexes</u> .....	36
2.8.3. <u>In vivo translation assay</u> .....	37
2.9. <u>Spectroscopic and fluorimetric analyses</u> .....	38
2.9.1. <u>P700 oxidation-reduction kinetics measurements</u> .....	38
2.9.2. <u>Bacterial whole-cell absorbance spectra</u> .....	38
2.9.3. <u>Low temperature (77 K) fluorescence emission spectra</u> .....	39
2.10. <u>Luciferase assay</u> .....	39
2.11. <u>TEM analyses</u> .....	39
2.12. <u>Database analyses and software tools</u> .....	39
<b>3. Results and Discussion</b> .....	<b>41</b>
3.1. <u>Replacement of the <i>Synechocystis</i> PSI complex</u> .....	41
3.1.1. <u>Generation of the PSI core subunits PsaA and PsaB mutants</u> .....	42
3.1.2. <u>Molecular analysis of the PSI core mutants</u> .....	44
3.1.3. <u>Discussion: <i>Arabidopsis</i> PsaA and PsaB can partially complement the function of the <i>Synechocystis</i> homologs</u> .....	50
3.2. <u>Effects of CURT1 proteins levels on the thylakoid architecture in <i>Synechocystis</i></u> .....	54
3.2.1. <u>Generation of <i>Synechocystis</i> mutants with altered CURT1 protein levels</u> .....	55
3.2.2. <u>Knockout of phycobilisomes in <i>CURTIA syncurt1</i></u> .....	57
3.2.3. <u>Discussion: <i>Synechocystis</i> and <i>Arabidopsis</i> CURT1 proteins have a conserved function in determining the thylakoid architecture</u> .....	60
3.3. <u>Development of a single vector-based based strategy for marker-less gene replacement in <i>Synechocystis</i></u> .....	60
3.3.1. <u>Design of the strategy</u> .....	60
3.3.2. <u>Confirmation of the strategy: introduction of the luciferase reporter system</u> .....	63
3.3.3. <u>Application of the strategy: 1. Introduction of <i>Arabidopsis</i> PGRL1 and PGR5 proteins</u> .....	67
3.3.4. <u>Application of the strategy: 2. The <i>psaA</i> gene</u> .....	72

3.3.5. <u>Discussion: advantages of the single-step replacement strategy....</u>	75
<b>4. Conclusions.....</b>	<b>78</b>
4.1. <u>Dissecting the molecular function of known proteins: the CURT1 family and the PGRL1/PGR5-mediated CEF.....</u>	79
4.2. <u>Generating a cyanobacterium with a plant-type photosynthetic machinery: replacement of PSI.....</u>	80
4.3. <u>Improving the molecular tools for large-scale gene knockout and replacement in <i>Synechocystis</i>.....</u>	81
<b>References.....</b>	<b>84</b>
<b>Acknowledgements.....</b>	<b>95</b>
<b>Curriculum vitae.....</b>	<b>96</b>
<b>Declaration / Eidesstattliche Erklärung.....</b>	<b>98</b>

## List of Figures

Figure 1.1 Scheme of linear electron transport (LEF).....	3
Figure 1.2 Major protein and protein complexes of the photosynthetic apparatus of <i>Arabidopsis thaliana</i> and the cyanobacterium <i>Thermosynechococcus elongatus</i> (Adapted and reprinted from Trends in Plant Science, <b>16</b> , Allen, J.F., de Paula, W.B., Puthiyaveetil, S., and Nield, J., A structural phylogenetic map for chloroplast photosynthesis., pages 645-655, 2011, with permission from Elsevier).....	5
Figure 1.3 Scheme of cyclic electron transport (CEF) in higher plants.....	11
Figure 1.4 Schematic depiction of the classical double recombination strategy...	18
Figure 3.1 Analysis of the <i>psaA-psaB</i> mutant strains.....	45
Figure 3.2 Expression and translation analysis in the <i>psaA-psaB</i> strains.....	47
Figure 3.3 Analyses of photosynthetic complexes in the WT, $\Delta$ <i>psaA</i> and <i>AB_opt</i> strains.....	49
Figure 3.4 Characteristics of CURT1 proteins.....	54
Figure 3.5 Analysis of the <i>CURT1</i> strains.....	56
Figure 3.6 Analysis of thylakoid structure of <i>CURT1</i> mutants by TEM.....	57
Figure 3.6 Analysis of the phycobilisome mutant strains.....	58
Figure 3.7 Analysis of thylakoid structure of $\Delta$ <i>apc</i> mutants by TEM.....	59
Figure 3.8 Schematic depiction of the single-step double recombination strategy	62
Figure 3.9 Analysis of the <i>lux</i> strains.....	65
Figure 3.10 Analysis of the <i>PGRL1</i> strains.....	68
Figure 3.11 Physiological characterization of the <i>PGRL1</i> strains.....	70
Figure 3.12 Analysis of the <i>psaA</i> strains.....	73



## List of Tables

Table 1.1 List of the photosystem I subunits in <i>Arabidopsis thaliana</i> and their homologs from <i>Synechocystis</i> sp. PCC 6803.....	8
Table 2.1 Strains used in this study.....	21
Table 2.2 Plasmid vectors used in this study.....	22
Table 2.3 Primers used in the PSI project.....	24
Table 2.4 Primers used in the CURT1 project.....	26
Table 2.5 Primers used in the marker-less gene replacement project.....	28
Table 3.1 Frequency of the second recombination event in independent <i>lux<sup>prim</sup></i> strains.....	63
Table 3.2 Luciferase activity relative to OD <sub>730</sub> in <i>Synechocystis lux<sup>prim</sup></i> and <i>lux<sup>sec</sup></i> mutants.....	66

## Abbreviations

<i>A. thaliana</i>	<i>Arabidopsis thaliana</i>
AA	antimycin A
A	absorbance
ATP	adenosine triphosphate
ATPase	ATP synthase
$\beta$ -DM	n-dodecyl $\beta$ -D-maltoside
BN	blue-native
bp	base pair
BSA	bovine serum albumin
CAI	Codon Adaptation Index
cDNA	complementary deoxyribonucleic acid
CEF	cyclic electron flow
Chl ( <i>a/b</i> )	chlorophyll ( <i>a/b</i> )
cTP	chloroplast transit peptide
cyt	cytochrome
DBMIB	2,5-dibromo-3-methyl-5-isopropyl-7-benzoquinone
DCMU	3-(3,4-dichlorophenyl)-1,1-dimethylurea
DNA	deoxyribonucleic acid
DTT	dithiothreitol
EDTA	ethylene diamine tetraacetic acid
Fd	ferredoxin
FNR	ferredoxin-NADP <sup>+</sup> -oxido-reductase
LAHG	Light Activated Heterotrophic Growth
LB	lysogeny broth
LDS	lithium dodecyl sulphate
LEF	linear electron flow
LHC (I/II)	light harvesting complex (I/II)
mRNA	messenger ribonucleic acid
NADP <sup>+</sup> /H	Nicotinamide adenine dinucleotide phosphate
NDH	NADPH dehydrogenase complex
OD	optical density
ORF	open reading frame

P680	PSII reaction centre
P700	PSI reaction centre
PAGE	polyacrylamide gel electrophoresis
PAM	pulse amplitude modulation
PC	plastocyanin
PCR	polymerase chain reaction
PGR5	PROTON GRADIENT REGULATION 5
PGRL1	PROTON GRADIENT REGULATION 5-LIKE 1
PQ(H <sub>2</sub> )	plastoquinone oxidised (reduced)
PS (I/II)	photosystem (I/II)
RNA	ribonucleic acid
rRNA	ribosomal RNA
RT-PCR	reverse transcriptase PCR
<i>Synechocystis</i>	<i>Synechocystis</i> sp. PCC 6803
SDS	sodium dodecyl sulphate
T-DNA	transfer-DNA
TM	transmembrane domain
Tris	tris (hydroxymethyl) aminomethane
tRNA	transfer RNA
WT	wild type

### Units

°C	degree Celsius
Da	Dalton
g	gram
<i>g</i>	gravity
h	hour
K	Kelvin
k	kilo
l	litre
μ	micro
M	molar
m	metre
min	minutes

ml	millilitre
mM	millimolar
mol	molar
nm	nanometre
rmp	rounds per minute
sec	second
v	volume
w	weight

## 1. INTRODUCTION

### 1.1. Endosymbiotic origin of plant chloroplasts

Oxygenic photosynthesis evolved about 2.7 billion years ago (Holland, 2006), when cyanobacteria started to use the energy of sunlight to extract electrons from water and channel them through two photosystems in series (photosystem II and photosystem I) to generate high-energy chemical bonds and reducing power as final products. In photosynthetic eukaryotes (algae and plants), this process takes place inside specialized organelles called chloroplasts that are now widely believed to derive from an endosymbiotic relationship between an ancestral cyanobacterium and a heterotrophic eukaryote. Like mitochondria, these so-called “primary” plastids are probably monophyletic and derive from a single endosymbiotic event (Howe et al., 2003; Douglas and Raven, 2003). Although chlorophyll *b* and *c*, photosynthetic pigments present in chloroplasts, are found only in certain cyanobacteria called prochlorophytes, this appears not to be an unequivocal proof for this specific clade to be the plastidial ancestor. Indeed, prochlorophytes are no monophyletic group by themselves (Lewin, 2002) and this suggests that chlorophyll *b* or *c* emerged independently several times during evolution. In contrast, it was recently shown that chloroplasts share the highest genetic similarity with the cyanobacterium *Nostoc punctiforme* (Meeks et al., 2001).

From the comparison of different cyanobacterial and plant chloroplast genomes, it can be concluded that the latter are strongly reduced in size and encode less genes than their evolutionary ancestors. Indeed, the genome length of *Nostoc punctiforme* approaches 9 Mbp and contains up to 7500 ORFs (Meeks et al., 2001), while the chloroplast genome from *Arabidopsis thaliana*, a well-characterized angiosperm, is 154 kb long and contains 87 putative protein-coding genes, 4 rRNA genes and 37 tRNA genes (Sato et al., 1999). In addition to the products of the few annotated plastidial genes, the *Arabidopsis* chloroplast proteome comprises about 2-3000 proteins, most of which are encoded by nuclear genes. On the other hand, up to 4500 (18 %) of *Arabidopsis* nuclear genes have direct homologs in cyanobacteria (Martin et al., 2002). Indeed, after the endosymbiotic event that originated chloroplasts, many genes became transferred from the plastidial to the nuclear genome of the host cell (Kleine et al., 2009). In this scenario, while the genetic autonomy of the organelles was reduced, new mechanisms required for the functionality of the transferred genes arose in the host cell. The newly evolved nuclear genes needed to be coupled with adequate DNA

regulatory elements (promoters, terminators) in order to be transcribed by the eukaryotic transcription machinery. Once translated in the cytosol, the proteins needed to be re-targeted to the organelle of origin in order to complete their function (Cavalier-Smith and Lee, 1985; Martin, 2003). Some of these genes acquired targeting elements that enabled them to be imported into the chloroplast while some others were not re-targeted to plastids anymore and gained new functions in other organelles or pathways of the host cell. Moreover, copies of the same gene deriving from duplication events diverged in their function, occasionally generating new metabolic pathways via their interaction with host proteins (Leister, 2003; Timmis et al., 2004). The integration process of the endosymbiont also included the targeting to the new organelle of nuclear genes that were not of cyanobacterial origin. Because of the gene transfer, the chloroplast protein complexes and supercomplexes are mosaics of plastid- and nuclear-encoded proteins, therefore making it necessary to efficiently coordinate the gene expression in both genetic compartments to guarantee a correct plastid development and functionality (reviewed in Pesaresi et al., 2007; Woodson and Chory, 2008). Indeed, the assembly of the chimeric protein complexes, their cofactors and the stoichiometric adaption of the photosynthetic machinery to the changing environmental conditions require an intricate bidirectional communication between the organelle and the nucleus. Therefore, integration of the photosynthetic endosymbiont in the host cell led to the rise of new plant-specific regulatory, signalling and transport functions, thus introducing new levels of complexity in eukaryotic photosynthesis.

Cyanobacteria and plant chloroplasts, although basically performing the same photosynthetic reaction, find themselves facing different environmental conditions and the various biological challenges that derive from them. Plants are sessile organisms and cannot avert drastic or unfavourable changes in the surrounding environment. Therefore, they needed to evolve new strategies to modulate the photosynthetic process in order to maintain its efficiency and avoid damages. Modern plant chloroplasts differ from modern cyanobacteria in many aspects and all of them can be understood in the light of evolution.

## 1.2. Higher plant photosynthesis in the light of evolution

Oxygenic photosynthesis is the process in which solar energy is used to synthesize carbon compounds from water and carbon dioxide. During the photosynthetic light reactions, the light energy is used to photolyse H<sub>2</sub>O and to generate reducing power (NADPH) and high-energy chemical bonds (ATP).

In cyanobacteria and chloroplasts, light energy is converted into chemical energy by the concerted action of different protein complexes, all of which are embedded in the thylakoid membranes (Hill and Bendall, 1960). As described schematically in Figure 1.1, light energy drives the electron transfer from photosystem II (PSII) via the cytochrome  $b_6f$  complex (Cyt  $b_6f$ ) and photosystem I (PSI) to the final electron acceptor  $\text{NADP}^+$ . Coupled with the linear electron transport, protons ( $\text{H}^+$ ) are transported into the thylakoid lumen by the Q-cycle at the Cyt  $b_6f$  complex and a proton gradient is thus created across the photosynthetic membrane. The protons accumulate in the lumen and create an electrochemical potential, which is balanced by the diffusion of the protons through the ATP synthase (ATPase). The proton flux through the ATPase is the motive force required for synthesis of ATP, a process that occurs in the chloroplast stroma or in the cyanobacterial cytosol. ATP and NADPH are subsequently used during the dark reactions for the biosynthesis of carbohydrates from  $\text{CO}_2$  and  $\text{H}_2\text{O}$ .

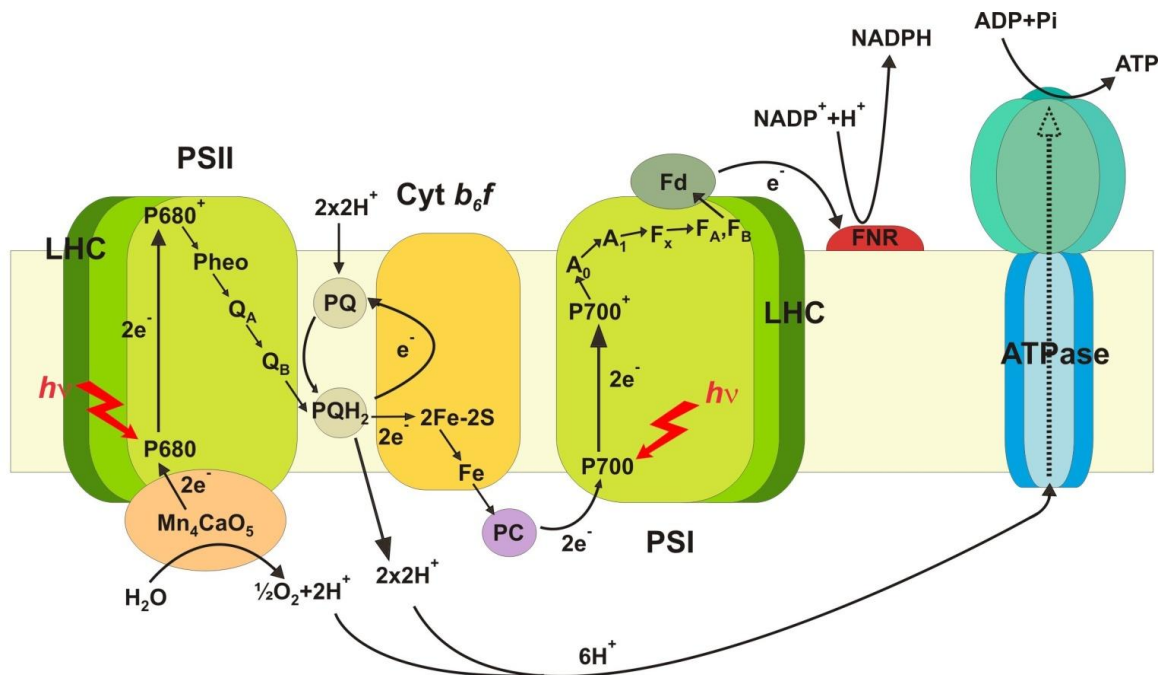


Figure 1.1 Scheme of linear electron transport (LEF). Photosystem II (PSII); Pheophytin a (Pheo); oxidised/reduced form of plastoquinone (PQ/PQH<sub>2</sub>); cytochrome  $b_6f$  complex (Cyt  $b_6f$ ); plastocyanin (PC); photosystem I (PSI); ferredoxin (Fd); ferredoxin-NADPH oxidoreductase (FNR); ATP synthase (ATPase).

The principal photoreceptor in photosynthesis is chlorophyll, a cyclic tetrapyrrole able to harvest light and convert the energy of the photons into higher excitation states of its electrons and to transmit it to neighbouring molecules by excitation transfer. In both cyanobacteria and plant chloroplasts, chlorophyll  $a$  (Chl  $a$ ) defines the charge-separation properties of the photosystem I and photosystem II reaction centres (RCs), each possessing a so-called “special pair” of chlorophylls (Oie et al., 1982). The chlorophylls of the PSII reaction centre (P680)

have an excitation wavelength peak at 680 nm and transfer electrons from water to the primary acceptor pheophytin (Pheo) (Debus, 1992). From PSII, the electrons are transferred by the plastoquinones, lipid-soluble electron carriers, to the Cyt  $b_6f$  complex. This, in turn, transfers them to the luminal soluble carrier plastocyanin, replaced by the cytochrome  $c_6$  in cyanobacteria under copper deficiency conditions (reviewed in Kerfeld and Krogmann, 1998). The photosystem I (PSI) complex catalyzes the oxidation of plastocyanin and the reduction of ferredoxin or flavodoxin, a small iron-sulphur protein located in the stroma of chloroplasts or in the cytosol in cyanobacteria. In PSI the primary photochemistry is initiated by a Chl  $a$  dimer, P700, with an excitation peak at 700 nm and the charge separation of P700 transfers electrons to a chlorophyll  $a$  monomer (Ao). In addition 4Fe-4S centres serve as electron carriers in PSI (van der Est et al., 1994).

Although they perform the same fundamental process, the photosynthetic machineries of cyanobacteria and higher plant evidently display many differences in both their structure and their physiology, as shown in Figure 1.2 (modified from Allen et al., 2011). To increase the absorption cross-section of the chlorophylls located in the photosynthetic RCs, light-harvesting antenna systems are normally associated with them. In contrast to PSII, many of the antenna chlorophyll molecules in PSI are bound to the proteins of the reaction centre and, therefore, the antennas serving the two photosystems are also different (Rakhimberdieva et al., 2001). The antenna systems of cyanobacteria and land plants present an extraordinary variety of protein structures and pigments, suggesting that they diverged during evolution to adapt to different light environments. In cyanobacteria, the light-harvesting antennas are constituted by the phycobilisomes (PBSs), protein-pigment complexes peripherally associated with the thylakoid membrane (external antenna) (Liu et al., 2013). Phycobilisomes are constituted by a core of allophycocyanin (APC), which is connected to the membrane through linker polypeptides and is surrounded by six rods of chromophorylated phycocyanin (PC) and phycoerythrin (PE) proteins (reviewed in Adir, 2005). All chlorophylls in cyanobacteria are exclusively localized in the core antennas of PSI and PSII, whereas the chromophores associated with the PSBs are the bilins, a class of open-chained tetrapyrrols that are responsible for the blue-green colour of cyanobacteria. Pigments of lateral rods transfer the excitation energy via APC to the terminal acceptor of energy (also APC) which, in turn, relays the excitation to antenna chlorophylls of PSII and PSI localized within the membrane (Mullineaux, 2008).

In higher plants, the Light Harvesting Complexes (LHCs) are associated with Chl  $a$  and Chl  $b$  and therefore belong to the CAB (chlorophyll  $a/b$ -binding) protein class. Although Chl  $a$  is



present in both reaction centres and LHCs, Chl *b* is restricted to LHCs (Dolganov et al., 1995). The plant LHC proteins are composed of three transmembrane helices and are embedded into the thylakoid membrane, where they are associated with the RCs.

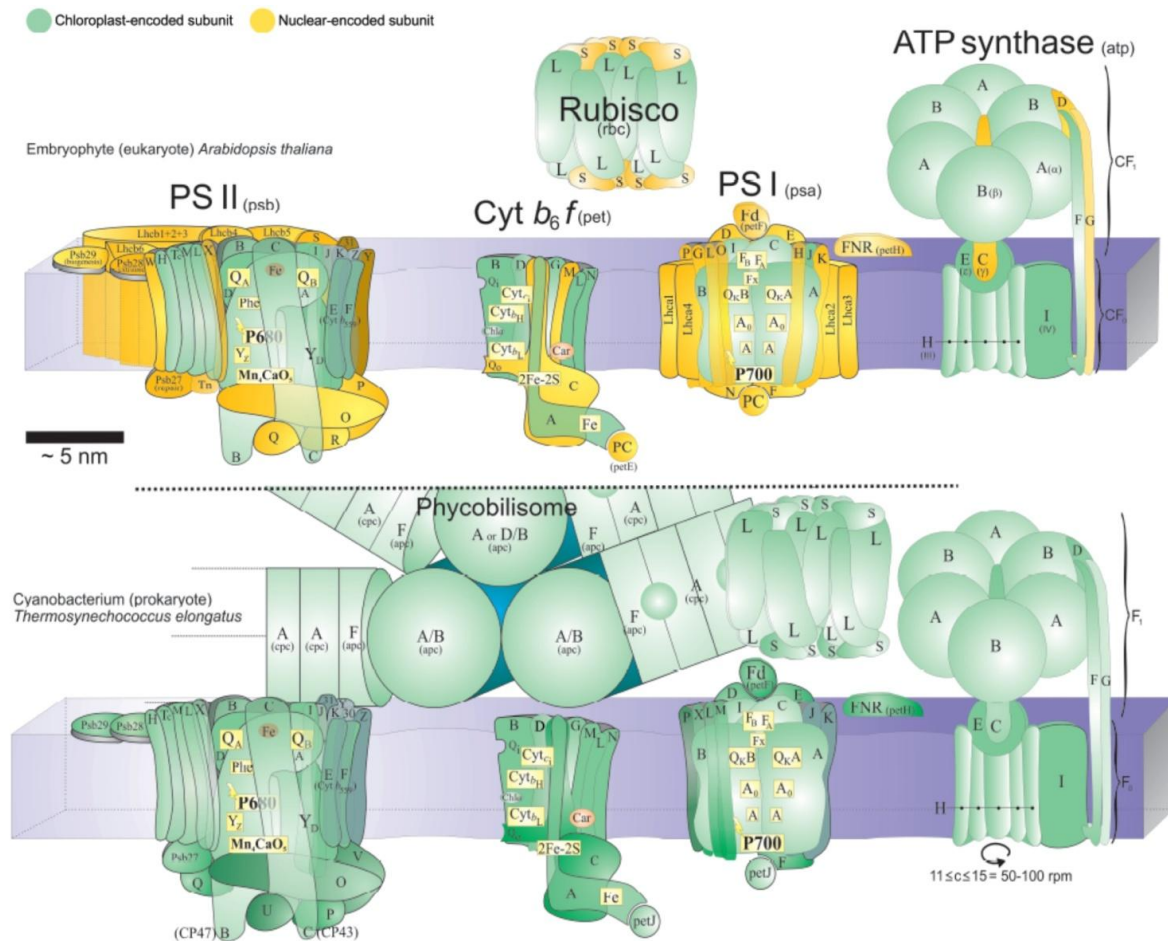


Figure 1.2 Major protein and protein complexes of the photosynthetic apparatus of *Arabidopsis thaliana* and the cyanobacterium *Thermosynechococcus elongatus*. Protein subunits encoded by the plastidial or cyanobacterial genome are coloured in green, the plant subunits encoded by nuclear genes are coloured in yellow (Adapted from Allen et al., 2011).

Whereas trimeric in cyanobacteria, the PSI of higher plants is monomeric (Jensen et al., 2007) and binds the additional membrane peripheral antenna called LHCI. This antenna consists of four Lhca polypeptides (Lhca1–4) that associate in a crescent supercomplex with a protein mass of around 25 kDa, linked to the PSI core complex at positions that in cyanobacteria are excluded from the trimer interface (Amunts and Nelson, 2009).

The peripheral antenna proteins associated with plant PSII can be distinguished in two types. The most abundant complex is the so-called „major“ LHCII antenna complex. This complex is composed of various combinations of the Lhcb1, Lhcb2 and Lhcb3 protein subunits that occur in a trimeric association state (Butler et al., 1988). In addition, there are three „minor“ antenna

proteins, called Lhcb4 (CP29), Lhcb5 (CP26) and Lhcb6 (CP24) that normally occur in monomeric aggregation states. The LHC antennas arose during the evolutionary divergence from the cyanobacterial ancestor to adapt to the highly variable light conditions plants had to face with terrestrial life. Indeed, the redistribution of the mobile LHCI pool between PSII and PSI, called state transition, enables chloroplasts to modulate the excitation pressure on the two photosystems, thus maintaining the optimal photochemical efficiency (Kargul et al., 2005). The LHCI redistribution process involves phosphorylation/dephosphorylation events (Depege et al., 2003) and a structural reorganization of the photosynthetic complexes and of the thylakoids themselves.

Although more conserved than the antenna systems, the photosynthetic reaction centres differ between cyanobacteria and chloroplasts in terms of their spatial distribution, stoichiometry, supermolecular organization and subunit composition. Adjustments in the relative amounts of the two photosystems represent another mechanism through which cyanobacteria and plants redistribute the excitation energy along the electron transport chain (Murakami, 1997; Allen and Pfannschmidt, 2000). PSII is the complex responsible for the photolysis of water, the hallmark and starting point of oxygenic photosynthesis and its main physiological form in both plants and cyanobacteria is a dimer (Holzenburg et al., 1993). The plant and bacterial PSII complexes have a slightly different subunit composition (Hankamer et al., 2001) but an overall similar structure (Büchel and Kühlbrandt, 2005). In both classes of organisms, the biogenesis of PSII is a highly regulated process and the subsequent events that lead to the assembly of the complex have been investigated in detail, as well as the integration of the cofactors (for a review, see Nickelsen and Rengstl, 2013). Additionally, a plethora of trans-acting PSII assembly factors are known and most of them have been conserved throughout evolution, not surprisingly since the PSII subunits and their assembly order are highly conserved. Those that are not conserved represent plant-specific factors that might have evolved either as substitutes to cyanobacterial counterparts or, especially the repair factors, in response to the new conditions of the life on land (Komenda et al., 2012). In the biogenesis of PSII and of PSI, a further regulatory level derives from the plant-specific compartmentalization inside the cell that requires the post-translational targeting of the nuclear-encoded subunits to the chloroplast and the concerted biosynthesis and integration of the cofactors, as well as the coordinated expression of the nuclear and the chloroplast genes. Whereas the molecular details of PSII structure and physiology have been studied and dissected extensively, the biogenesis and assembly of PSI are still poorly understood in higher

plants, particularly because of the difficulties in identifying the assembly intermediates and because of the lethality caused by PSI depletion.

### 1.3. Evolution of PSI

Photosystem I is the plastocyanin-ferredoxin oxidoreductase in the thylakoid membranes of cyanobacteria and chloroplasts that catalyses the last step of the photosynthetic electron transport. It is one of the most complex membrane protein complexes known in nature and its quantum efficiency in the transfer of electrons is close to 1.0 (Nelson and Ben-Shem, 2002). PSI has a longer half-life than PSII (Yao et al., 2011) and is less susceptible to photodamage, because PSI-catalyzed reactions do not occur at extremely oxidizing redox potentials (Powles, 1984). Because of these characteristics, PSI is studied by many groups from different disciplines, with a focus on energy utilization and the design of photosensors (Carmeli et al., 2007; Terasaki et al., 2007). Probably for the same reason, it is highly conserved along the green lineage, although some key modifications arose in the PSI of land plants to adapt to different ecological niches.

Eukaryotic PSI structurally consists of two membrane complexes: the reaction centre (RC), composed of 15 subunits, and the LHCI antenna system, composed of 4 subunits (Amunts et al., 2007). The currently known PSI-LHCI supercomplex therefore consists of a total of 19 protein subunits and approximately 200 cofactors, non-covalently bound to the core complex and to the antennas (Jensen et al., 2007). The plant PSI-LHCI supercomplex is much larger than the cyanobacterial PSI that lacks the surrounding antenna proteins and is composed of 12 subunits and 127 associated cofactors (Jordan et al., 2001). The protein components of the PSI core complexes from *Arabidopsis thaliana*, together with their homologs in *Synechocystis* sp. PCC 6803, are listed in Table 1.1. The cyanobacterial PsaM and PsaX subunits are not conserved in higher plants in which, in return, the four additional subunits PsaG, PsaH, PsaN and PsaO evolved.

Of the 15 genes encoding the subunits of the higher plant PSI reaction centre, only 4 (encoding PsaA, PsaB, PsaC and PsaJ) are located in the chloroplast genome, while the other 11 are scattered throughout the nuclear chromosomes (Table 1.1). The nuclear genes encode for proteins translated in the cytoplasm and subsequently imported in the chloroplast (Soll and Schleiff, 2004) to be assembled with the cofactors and the plastid-encoded proteins. Therefore, additional steps of regulation are needed, with respect to cyanobacteria, for the biogenesis of a functional PSI.

Table 1.1 List of the photosystem I subunits in *Arabidopsis thaliana* and their homologs from *Synechocystis* sp. PCC 6803

PSI subunit	<i>Arabidopsis</i> gene		<i>Synechocystis</i> gene		Protein Identity	Features
<b>Core</b>						
PsaA	<i>AtCg00350</i>	2253 bp	<i>slr1834</i>	2256 bp	80 %	
PsaB	<i>AtCg00340</i>	2205 bp	<i>slr1835</i>	2196 bp	80 %	
<b>Fd docking</b>						
PsaC	<i>ArthCp075</i>	246 bp	<i>ssl0563</i>	246 bp	90 %	
PsaD	<i>At4g02770</i> <i>At1g03130</i>	835 bp 892 bp	<i>slr0737</i>	426 bp	64 %	Plants: probably direct interaction with FNR in stroma
PsaE	<i>At4g28750</i> <i>At2g20260</i>	1204 bp 1034 bp	<i>ssr2831</i>	225 bp	46 %	
<b>PC docking</b>						
PsaF	<i>At1g31330</i>	1214 bp	<i>sll0819</i>	498 bp	42 %	Additional N-term. (positively charged aminoacids) domain in plants
PsaN	<i>At1g49975</i>	796 bp	/			
<b>Anchor for LHCI binding</b>						
PsaG	<i>At1g55670</i>	780 bp	/			
<b>PSI stability</b>						
PsaJ	<i>ArthCp042</i>	135 bp	<i>sml0008</i>	123 bp	48 %	
<b>LHCII interaction in state transition</b>						
PsaH	<i>At3g16140</i> <i>At1g52230</i>	973 bp 833 bp	/			In plants it prevents trimerization
PsaI	<i>ArthCp032</i>	114 bp	<i>smr0004</i>	123 bp	45 %	
PsaL	<i>At4g12800</i>	1349 bp	<i>slr1655</i>	474 bp	44 %	For trimerization in cyanobacteria
PsaO	<i>At1g08380</i>	1016 bp	/			
<b>Interaction with LHCI</b>						
PsaK	<i>At1g30380</i>	1050 bp	<i>ssr0390</i> <i>sll0629</i>	261 bp 387 bp	28 %	

In both organisms, the PSI core is a heterodimer formed by the two large subunits PsaA and PsaB that consists of 22 transmembrane helices and harbours most of the cofactors of the electron transport chain, together with 80 Chl *a* molecules forming an internal antenna system. The stromal subunit PsaC carries the two terminal 4Fe-4S clusters of the electron transport chain and is, like the two core subunits, encoded by the chloroplast genome and extremely conserved in plants and cyanobacteria (90 % of protein identity for PsaC, 80 % for

PsaA and PsaB). The assembly of the core dimer starts with the co-translational insertion in the thylakoid membrane of PsaA and PsaB. This reaction centre (165 kDa) constitutes almost half of the molecular mass of the PSI complex (390 kDa) and forms the docking site for the subsequent assembly of the peripheral subunits PsaC, PsaD and PsaE. In the stroma, these three subunits form the docking site for the final electron acceptor ferredoxin, the reduction of which seems to have been optimized in plants with respect to cyanobacteria (Hanley et al., 1996; Fischer et al., 1998). Moreover, the plant ferredoxin:NDP<sup>+</sup> oxidoreductase (FNR) seems to accept electrons from ferredoxin by directly interacting with PSI, whereas this direct interaction has never been detected in cyanobacteria (Vallejos et al., 1984; Andersen et al., 1992). The site of interaction of the electron donor plastocyanin on the luminal side of PSI was also refined by evolution (Hippler et al., 1996), with the introduction of an extension in the luminal N-terminus of the plant PsaF subunit. PsaF is an integral membrane protein and its exposed luminal region contains the positively charged patch responsible for plastocyanin interaction (Hippler et al., 1998). The order and modality with which the other subunits are assembled into the plant PSI complex is still unclear (Ozawa et al., 2010), because their small sizes make it difficult to resolve assembly intermediates by mass-based separation techniques. Identification of auxiliary proteins involved in PSI biogenesis is also problematic and, to date, only a limited number of regulatory factors specifically involved in PSI assembly have been identified, as reviewed in Schöttler et al. (2011) and Chi et al. (2012). Although these factors are generally conserved in chloroplasts and cyanobacteria, the functions of some of them evolved together with eukaryotic photosynthesis. The plastid-encoded proteins YCF3 (Schwabe and Kruij, 2000; Naver et al., 2001) and YCF4 (Wilde et al., 1995; Krech et al., 2012) are highly conserved in cyanobacteria and, in both organisms, they have been proposed to function as molecular chaperones during the formation of the PSI complex. In chloroplasts, lack of these proteins causes a complete loss of PSI (Boudreau et al., 1997; Ruf et al., 1997), while PSI amount are only reduced in *Synechocystis ycf4* mutants (Wilde et al., 1995). Two additional factors involved in the assembly of the plant PSI subunits are the nuclear-encoded proteins Y3IP1 (Albus et al., 2010), not characterized in cyanobacteria, and Pyg7-1 (Stöckel et al., 2006), that is essential for PSI accumulation in plants, in contrast to the cyanobacterial homolog Ycf37 that has only an accessory function in PSI biogenesis (Wilde et al., 2001). Additional plant nuclear-encoded proteins that are required for the assembly of PSI cofactors have been identified. Among these, Hcf101 is involved in the association of the 4Fe-4S clusters with the PSI apoproteins (Lezhneva et al., 2004), while in mutants lacking the Apo1 protein all the chloroplast iron-sulphur proteins are strongly affected (Amann et al., 2004).

The PSI of higher plants occurs as a monomer surrounded by the LHCI antennas at the PsaF/PsaG side (Amunts et al., 2007), whereas in cyanobacteria no antenna system is present and the PSI reaction centres are organized in trimeric supercomplexes (Jordan et al., 2001). PsaL is responsible for trimerization in cyanobacteria, while the plant-specific PsaH protein prevents oligomerization and it has been proposed to be important for the PSI-LHCII interaction during state transition (Lunde et al., 2000; Kouril et al., 2005). The switch of the mobile LHCII pool between the two photosystems serves to balance their respective excitations and it can be considered as a vital adaptation of plant photosynthesis to the fluctuating light conditions of their environment (Kargul and Barber, 2008). The trimeric state of cyanobacterial PSI can be seen, on the opposite, as a way to optimize harvesting of the dim light in aqueous environments by providing a larger intrinsic antenna system (Amunts and Nelson, 2009). Besides adaptive differences with respect to the prokaryotic ancestor, the plant PSI displays an extreme conservation of all the cofactors of the electron transport chain and of the protein structures they are associated with.

During the Linear Electron Flow (LEF, see Figure 1.1), PSI acts downstream of PSII in transferring electrons from water molecules to the terminal acceptor NADP<sup>+</sup>, with the final overall production of NADPH and ATP. For effective photosynthesis, though, the Cyclic Electron Flow (CEF, for reviews see Shikanai, 2007; Joliot and Johnson, 2011) pathway is also required and this solely depends on the PSI photochemical reactions. In CEF (Figure 1.3) electrons are recycled from the photoreduced ferredoxin to the PQ pool and, through Cyt *b<sub>6</sub>f*, back to PSI. During this process no net reducing power is produced, but the Q-cycle still generates the proton motive force to drive the synthesis of ATP. The electron transport in thylakoids is therefore subjected to a photosynthetic control (Foyer et al., 2012) that balances the ratios of produced reductants and ATP, in order to meet the metabolic needs of the cell. Another important role of CEF is to induce the acidification of the lumen necessary to regulate the quenching of high energy states in fluctuating light conditions (Niyogi et al., 2005). Two partially redundant pathways of cyclic electron flow around PSI are present in higher plants, the one discovered by Arnon and co-workers (Arnon et al., 1954) and a second one that depends on the chloroplast NAD(P)H dehydrogenase complex (NDH, Burrows et al., 1998).

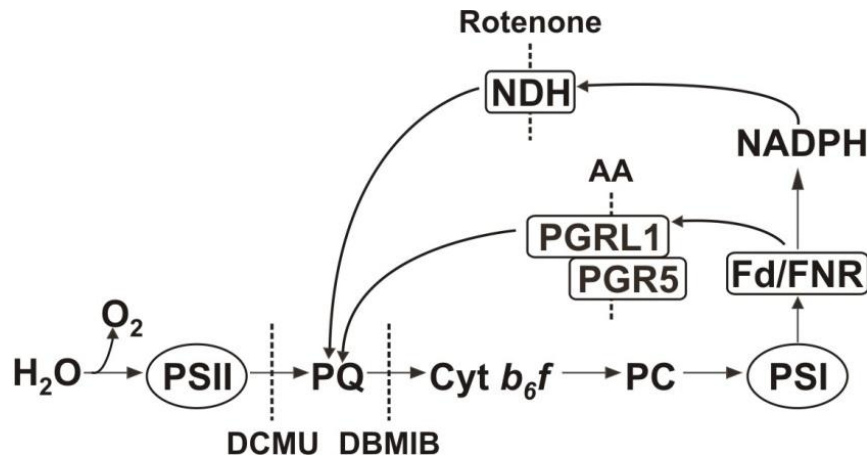


Figure 1.3 Scheme of cyclic electron flow (CEF) in higher plants. Photosystem II (PSII); plastoquinone (PQ); cytochrome *b*<sub>6</sub>*f* complex (Cyt *b*<sub>6</sub>*f*); plastocyanin (PC); photosystem I (PSI); ferredoxin (Fd); ferredoxin-NADPH oxidoreductase (FNR); NADPH dehydrogenase complex (NDH); PROTON GRADIENT REGULATION 5 (PGR5); PROTON GRADIENT REGULATION 5-LIKE 1 (PGRL1). Inhibitors of the different electron transport steps are also indicated: 3-(3,4-dichlorophenyl)-1,1-dimethylurea (DCMU); 2,5-dibromo-3-methyl-5-isopropyl-7-benzoquinone (DBMIB); Antimycin A (AA); Rotenone.

This NDH-dependent CEF is present also in cyanobacteria, where it was shown to be important at limiting CO<sub>2</sub> concentrations (Ogawa, 1991), and the evolutionary conservation of this pathway is also testified by the fact that the NDH subunits are encoded, in plants, by plastidial genes. The NDH-dependent cyclic transport is not inhibited by antimycin A (AA, (Endo et al., 1997), whereas the pathway discovered by Arnon is sensitive to this compound (Tagawa et al., 1963). In the plant AA-sensitive cyclic transport, electrons from reduced ferredoxin are directly transferred to PQ (Bendall and Manasse, 1995) by the action of a “ferredoxin-plastoquinone reductase” (FQR). In *Arabidopsis thaliana*, the two nuclear-encoded thylakoid proteins involved in this pathway have been identified, PROTON GRADIENT REGULATION 5 (PGR5, Munekage et al., 2002) and PROTON GRADIENT REGULATION 5-LIKE 1 (PGRL1, DalCorso et al., 2008). PGRL1 can form homodimers and PGRL1-PGR5 heterodimers and has *in vitro* an AA-sensitive FQR activity, whereas the molecular function of PGR5 is so far not clear but it is necessary for the reduction of PGRL1 (Hertle et al., 2013). In the current model of the AA-sensitive CEF of higher plants, though, open questions still remain, as for example the way in which PGRL1 and PGR5 interact with ferredoxin and where on PSI this interaction takes place.

PSI is a stable and efficient enzyme and has a central role in the physiology of plant photosynthesis but still little is known about the mechanisms involved in its assembly and regulation (Schöttler et al., 2011).

#### 1.4. Evolution of the membrane architecture

Cyanobacteria are Gram-negative eubacteria and have a cell envelope composed of an outer and a plasma membrane that surround a peptidoglycan layer and the cytoplasmic aqueous compartment. Embedded in the cytosol they have a distinct intracellular system of membranes, the thylakoids, where the light-dependent reactions of photosynthesis take place. In most cases, cyanobacterial thylakoids form flattened layers of lipid-bilayer membranes organized in stacks that encircle the cell and cover much of the cytoplasmic space (for a review, see Murat et al., 2012). The number and spacing of the layers in a single stack are species-specific but, in general, they seem not to be fused to the plasma membrane, even if this is still under debate (Liberton et al., 2006). In *Synechocystis sp.* PCC 6803, a well-studied unicellular cyanobacterium, the three to eight thylakoid layers of a single stack converge to sites close to the plasma membranes that have been proposed to connect the two membrane systems in a dynamic way (Nickelsen et al., 2010). Indeed, cyanobacterial thylakoids form a complex network that includes perforations and internal membrane bridges between the layers and large vesicles often close or fused to them. The highly networked structure of cyanobacterial thylakoids ensures communication and flow of cellular components in between the layer stacks (Nevo et al., 2007).

Chloroplasts of land plants are enclosed by a system of two membranes, the outer and inner envelope, that derive from the plasma and outer membranes of the progenitor prokaryote and delimit an aqueous matrix called stroma. The thylakoid membranes, embedded in the stroma, house the photosynthetic protein complexes as in the case on cyanobacteria but they show striking differences in architecture. Chloroplasts thylakoids form grana, cylindrical stacks of 300 to 600 nm in diameter composed of a number of membrane layer that varies from 5 to 20, approximately (Mustárdy and Garab, 2003; Mullineaux, 2005). Each granum consists of superimposed discs connected to each other in a central core of appressed membranes, with the two discs at the top and bottom of the structure having one face exposed to the stroma. The margins of a single disc are highly curved and constitute the merging point of two neighbouring grana membranes at their periphery. The distinct grana stacks of a single chloroplast are interconnected by the stroma lamellae, membrane pairs of few micrometers in length that depart from the grana cylinder and are exposed to the stroma at their external surfaces. The grana stacks and stroma lamellae within one chloroplast form a single continuous network of thylakoid membranes that delimit a single internal aqueous phase, the lumen (Shimoni et al., 2005). This thylakoid network therefore shows a complex architecture



whose precise topography is still debated (Allen and Forsberg, 2001; Shimoni et al., 2005; Mustárdy et al., 2008; Daum and Kühlbrandt, 2011).

Despite the remarkable differences in their architecture, both the bacterial and the plant photosynthetic membranes exhibit similar features, such as bifurcation, bending and folding, that once again demonstrate their tight evolutionary link. Although the mechanism underneath the curvature of thylakoids is not yet known, a protein family has recently been shown to control bending of the photosynthetic membranes and grana formation in *Arabidopsis thaliana* (Armbruster et al., 2013). The family of proteins named CURVATURE THYLAKOID 1 (CURT1) is composed of four members (CURT1A, B, C and D) that are specifically located to the grana margins of *Arabidopsis* thylakoids. They are integral membrane proteins spanning the thylakoid membranes with two transmembrane helices, with their N- and C-termini facing the stroma. They form oligomers, either homo- or hetero-complexes, and their levels within the chloroplast strongly determine the thylakoid architecture. Indeed, in mutant plants lacking the major CURT1 isoform, CURT1A, alone or in combination with the depletion also of the other family members, transmission electron microscopy (TEM) analysis revealed marked alterations of the thylakoid structure. The mutant thylakoids formed disorganized stretches of unstacked membranes and grana stacks much broader and formed by fewer layers than in wild type chloroplasts. In the multiple mutants further modifications involved the presence of curved instead of flat membrane layers as well as of vesicular structures. On the contrary, *Arabidopsis* mutants overexpressing CURT1A have chloroplasts containing grana stacks that are slimmer and reduced in diameter but higher and more abundant than in the wild type, thus confirming the correlation between the CURT1 protein levels and the architecture of the thylakoid membranes. The negative correlation between grana diameter and height is related to the fact that only a fixed proportion of the thylakoid membrane is incorporated in the grana stacks (Albertsson and Andreasson, 2004). The intrinsic ability of the CURT1 proteins to bend membranes was also confirmed by in vitro studies, using liposomes with thylakoid-like lipid composition.

In the absence of CURT1 proteins, pleiotropic effects on the photosynthesis were observed. Indeed, the photosynthetic electron flow resulted to be impaired, especially at high light intensities, and the chloroplast ability of reversibly re-distributing excitation between the two photosystems was also reduced. These effects on photosynthesis can be attributed to the fact that plants adopted several mechanisms to adapt to varying light conditions and that one of them is to modulate in a dynamic manner the degree of thylakoid stacking within their chloroplasts. Indeed, plants adapted to shade and low-light conditions display grana composed

of many more layers of thylakoid membranes than those that prefer bright sunlight (Andersson, 1986).

The photosynthetic membrane topology of land plants reveals a further evolutionary adaptation, with respect to the cyanobacterial counterpart, that depends on a non-homogeneous distribution of the photosystems which are, instead, spatially separated. There is no evidence for an extensive domain organization in cyanobacterial thylakoid membranes, except for row-like associations of PSII dimers (Folea et al., 2008), while in higher plant thylakoids PSI and PSII are spatially separated in order to optimize the photosynthetic efficiency. This spatial separation, called „lateral heterogeneity“ (Andersson, 1986), is just one of the mechanisms with which plants adapt to changing light conditions. PSII and its main antenna proteins, LHCII, are mainly located in grana thylakoids that are, on the opposite, deficient in PSI and LHCI, which are instead predominantly confined to the stroma membranes. This lateral heterogeneity prevents the unregulated transfer of excitation energy between the two pigment systems: electron flow through PSI is much faster than the one through PSII, given the higher quantum efficiency of the first, and therefore spatial separation can help to balance the energy distribution in order to optimize the photosynthetic efficiency (Mustárdy and Garab, 2003). The structure of the thylakoid grana is flexible and the degree of stacking is regulated by the phosphorylation of the LHCII and other phosphoproteins (Fristedt et al., 2009) as well as by the amount of CURT1 proteins (Armbruster et al., 2013). Modifications of the grana structure, in turn, facilitate the mobility of the antenna complexes during state transitions and the switch between linear and cyclic electron flow. Therefore, grana appear to be evolved by higher plants to enhance light harvesting in fluctuating light conditions (Trissl and Wilhelm, 1993; Mustárdy and Garab, 2003; Dekker and Boekema, 2005; Mullineaux, 2005; Daum and Kühlbrandt, 2011).

#### 1.5. Limitations of plant photosynthesis research

Higher plant photosynthesis exhibits an increased complexity with respect to the ancestral counterpart represented by cyanobacteria, despite the conservation of the basic structures and physiology. Many assembly and regulatory mechanisms that specifically evolved in eukaryotic photosynthesis still have to be identified or clarified. Moreover, besides playing the central role in the energy metabolism of plants, the photosynthetic process has been recently shown to be closely related to a variety of other physiological processes that go beyond the chloroplast and influence the physiology of the whole cell, like control of the redox-state (Buchanan and Balmer, 2005), the generation of regulatory reacting oxygen

species (Wagner et al., 2004) and the regulation of the cell cycle (Fukushima et al., 2009). Despite its central role in plant biology, photosynthesis research has been so far challenged by several limiting aspects that are either due to technical shortcomings or are intrinsic to the model species used. Plants are multicellular eukaryotic organisms with specialized organs and a complex physiology and a life-span varying from few weeks to centuries. *Arabidopsis thaliana* is one of the most used model plants for the study of photosynthesis, because of the ease to manipulate it and its relatively short life cycle (about six weeks). Analysis of the function of photosynthesis-related nuclear genes in *Arabidopsis* traditionally relies on the screening of mutants' sets deriving from chemical mutagenesis (EMS, Maple and Møller, 2007) or by the *Agrobacterium*-mediated T-DNA insertion into the genome (Krysan et al., 1999), which can also be used to introduce exogenous sequences into the plant. Both techniques, though, generate mutation in random loci and do not allow targeted mutagenesis because plants usually do not undergo homologous recombination in the nuclear genome. In addition to this, segregation of the generated mutations and screening for the desired phenotype - supposing to have suitable selection conditions - requires quite long time periods and a considerable amount of work. To generate mutants for multiple genes, classical plant crossing techniques have to be employed, together with the subsequent segregation and screening phases. Targeted manipulation is possible in the case of chloroplast genes, because the organellar genetic machinery is prokaryote-like and homologous recombination is therefore taking place. Generation of transplastomic plants is normally done by transforming plastids via particle bombardment of embryos or young plant cells and leads to the integration of the desired DNA into the homologous sequence of the plastidial genome (Gan, 1989). Integration of the exogenous DNA into the target genome can be selected using selectable markers, therefore reducing the screening process (Day and Goldschmidt-Clermont, 2011) and techniques to remove the marker after isolation of the desired mutants have also been developed (Klaus et al., 2004; Day and Goldschmidt-Clermont, 2011). Besides the presented advantages, this technique has so far been limited to a few species, mostly tobacco in the case of photosynthesis research, and is restricted to the few genes still retained by the plastidial genome.

Irrespectively of the genomic compartment where a photosynthesis-related gene is located, studying its function presents an additional level of complexity represented by the fact that a gene mutation quite often results in pleiotropic effects, thus rendering it difficult to identify the primary function of the gene product. Moreover, the quest for new photosynthesis-related candidates is currently based on forward genetics approaches, done by screening sets of

randomly mutated plants for a photosynthetic phenotype. Although successfully used to identify many new players in the photosynthetic process, this approach is limited by the viability of the gene mutations and, on the opposite, by the lack of phenotype in the case of genetic redundancy. Moreover, setting up the appropriate screening procedure for a certain biological process can be often challenging. The increasing number of sequenced genomes recently led to new screenings based on a bioinformatics approach, as in the case of the GreenCut project (Grossman et al., 2010). Although very promising, these methods could still be biased by the limited information and limited understanding they are based on.

#### 1.6. Designing a cyanobacterial platform to study higher plant photosynthesis

Cyanobacteria are the evolutionary ancestors of higher plant chloroplasts and, as such, they harbour a complete photosynthetic apparatus, but they lack all those protein functions and adaptive mechanisms that evolved in the eukaryotic photosynthetic organisms and are therefore plant-specific. Being prokaryotes, they present some advantages with respect to plants. First of all, they contain a single genomic unit in varying number of copies per cell; therefore, there is no need for the co-regulation of genes encoded by two different genomes, like in plants. Cyanobacteria have a shorter life cycle than plants and, being unicellular, a physiology with less levels of complexity. When working with cyanobacteria, an enormous advantage derives from their ability to undergo homologous DNA recombination, which makes it possible to perform targeted gene and genome manipulations. When considering the cyanobacterial qualities in the perspective of research on higher plant photosynthesis, these organisms appear to be potential tools to investigate the function of plant photosynthetic proteins. Indeed, the function of a plant-specific protein expressed in cyanobacteria could be studied in a simpler physiological environment and in the absence of other eukaryotic regulatory components that, if necessary for the function, could be subsequently added. Moreover, it could be possible to replace the photosynthetic machinery of cyanobacteria with the one from higher plants via targeted genomic manipulation in order to identify all the components required for its correct functioning. To this end, libraries of plant transcripts could be used to fish new photosynthesis-related genes by complementing cyanobacterial chimeras containing the plant-type minimal photosynthetic machinery.

#### 1.7. *Synechocystis* as a model organism

One of the most used genetic models for higher plant photosynthesis is *Arabidopsis thaliana*. To generate the proposed cyanobacterial platform, the cyanobacterium *Synechocystis* sp. PCC

6803 (in the following designated *Synechocystis*) is the organism of choice. *Synechocystis* is an excellent cyanobacterial model organism, because it is unicellular and, not forming filamentous structures, it does not fix nitrogen. It has a small, sequenced genome (3.6 Mb) (Kaneko et al., 1996), is able to take up spontaneously exogenous DNA and to integrate it via homologous recombination into the genome. In addition, a spontaneous glucose-tolerant mutant strain is available (Williams, 1988) which can grow heterotrophically in the presence of sugar even in complete darkness (Anderson and McIntosh, 1991), thus making it a convenient organism to study oxygenic photosynthesis. Photosynthetic *Synechocystis* mutants have been extensively used to study PSI (Dühring et al., 2007; Xu et al., 2011) and PSII (Vermaas et al., 1986; Vermaas et al., 1987) and also to investigate the functionality of photosynthesis-related proteins from higher plants in cyanobacteria (Nixon et al., 1991; He et al., 1999). All these studies relied on the employment of gene deletions or replacements.

The classical strategy to delete a target gene or to insert exogenous genetic material into the *Synechocystis* genome via homologous recombination involves the use of a resistance marker (Labarre et al., 1989; Vermaas, 1996). In this approach, the marker, exogenous DNA and two homologous genomic sequences flanking the insertion cassette are cloned into a suicide vector, which is not able to replicate itself in the host cell. After integration of the insertion cassette into the host genome, the resistance-mediating marker allows positive selection of those mutant organisms, in which the integration has occurred. However, to perform additional genomic modifications, the use of different resistance markers is necessary. Consequently, the number of available markers restricts the number of genetic manipulations. To overcome this limitation, so called marker-less strategies have been developed, allowing the removal of the integrated marker. The first marker-less method was established in Gram-negative bacteria using the *nptI-sacB* double selection cassette (Ried and Collmer, 1987): the *nptI* gene confers resistance to the antibiotic kanamycin, while the *sacB* gene from *Bacillus subtilis* (Fouet et al., 1984; Steinmetz et al., 1985) is conditionally lethal for Gram-negative bacteria when grown in the presence of 5 % sucrose. It encodes the enzyme levansucrase that hydrolyzes sucrose leading to the final production of levans (Gay et al., 1983) polymers that are lethal for Gram-negative bacteria. Thus, cells harbouring the *sacB* gene die when grown in presence of 5 % sucrose, although the underlying mechanism is not fully understood. In cyanobacteria, the *nptI-sacB* cartridge was first used to establish marker-less gene replacement in *Anabaena sp.* PCC 7120 (Cai and Wolk, 1990).

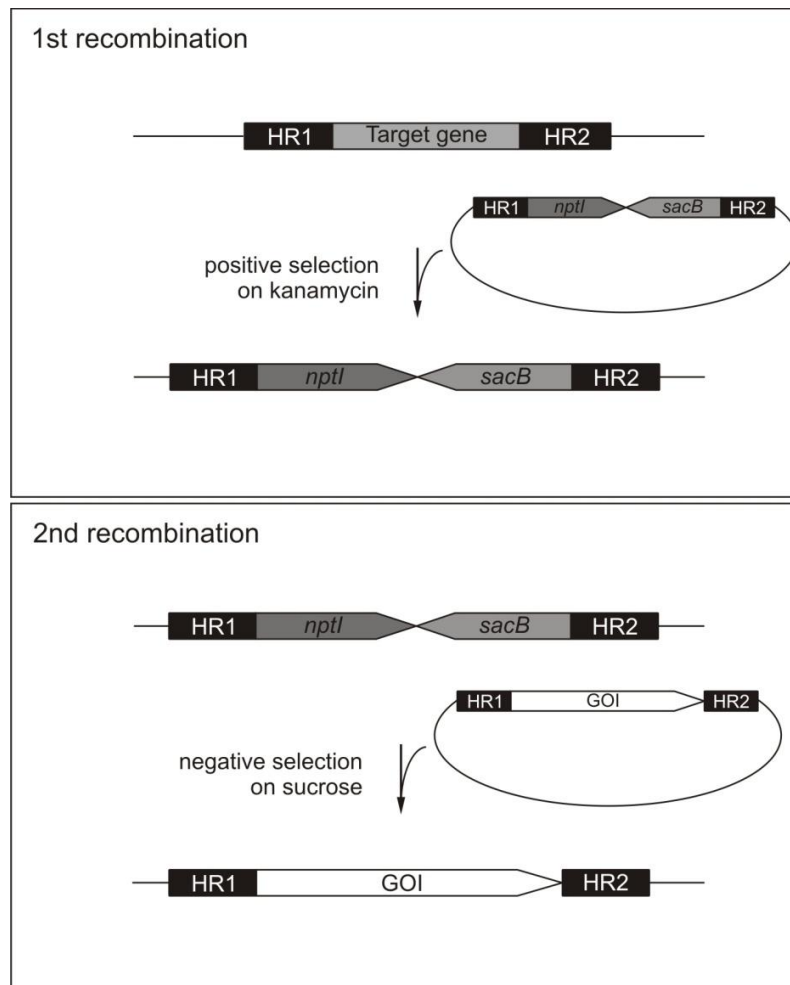


Figure 1.4 Schematic depiction of the classical double recombination strategy. The first recombination step (upper panel), involving a double crossover between the homologous regions HR1 and HR2 of the vector and the genomic target sequence, leads to integration of the *nptI-sacB* cassette in the target gene. After complete segregation of the knockout under positive selection in the presence of kanamycin, a second recombination step (lower panel) takes place. A double crossover between the homologous regions HR1 and HR2 of the vector and the genomic target sequence, leads to replacement of the double selection cassette by the gene of interest (GOI) to introduce. Negative selection on sucrose yields colonies that have lost the entire *sacB* marker and carry the GOI in place of the endogenous target gene.

This replacement is based on two homologous recombination events, each of them requiring a DNA suicide vector and a bacterial transformation step (see Figure 1.4). 1) The target genomic sequence is replaced by the double-selection cassette and the mutants in which the homologous recombination took place are positively selected by their ability to grow in the presence of the antibiotic. 2) A second transformation and homologous recombination event leads to the excision of the *nptI-sacB* selection cartridge by its replacement with the exogenous sequence. The desired mutants can be selected by their resistance to sucrose and kanamycin sensitivity.

An alternative version of double selection was developed for gene replacement in *Synechococcus elongatus* PCC 7942 (Matsuoka et al., 2001). In this approach, the background

strain carries a mutated form of the *rps12* gene (which encodes for the 30S ribosomal subunit S12) conferring resistance to spectinomycin (Funatsu and Wittmann, 1972; Timms et al., 1992). Since the mutation is recessive, the double selection cassette is composed of the kanamycin resistance gene and - as an alternative negative selection marker - of an *rps12* wild type copy, which confers a dominant spectinomycin-sensitive phenotype. Limiting aspects of the *rps12* marker system are the availability of spectinomycin-resistant mutants in other cyanobacterial species and the need to perform all multiple replacements in the *rps12* mutant background.

#### 1.8. Aim of the work

The goal of the presented project was the establishment of a cyanobacterial platform to study novel photosynthesis-related protein functions from higher plants. As a starting point, the PSI core subunits from *Synechocystis* were replaced with the *Arabidopsis* homologs.

In a second approach, the effects of the *Arabidopsis* CURT1A protein on the structure of the *Synechocystis* thylakoids were tested by expressing it in addition to, or in replacement of, the cyanobacterial homolog.

In order to facilitate further extensive manipulations of the *Synechocystis* genome, an alternative marker-less gene replacement strategy was developed which relies on the use of a single plasmid vector and a single transformation step in order to obtain both knockout and replacement bacterial strains. The developed strategy was used to test the function of the *Arabidopsis* PGRL1 and PGR5 proteins in *Synechocystis* and to replace the cyanobacterial PSI PsaA core subunit with the plant homolog.

## 2. MATERIALS AND METHODS

### 2.1. Chemicals, enzymes and radioactive substances

Standard chemicals were purchased from Roth (Karlsruhe, Germany), Duchefa (Haarlem, Netherlands), Applichem (Darmstadt, Germany), Serva (Heidelberg, German), Invitrogen (Darmstadt, Germany) and Sigma-Aldrich (Steinheim, Germany).

Restriction enzymes were purchased from New England Biolabs (Ipswich, MA, USA) and Fermentas (Thermo Scientific, Rockford, USA), Taq DNA polymerase from QIAGEN (Venlo, Netherlands) and Phusion High-Fidelity DNA polymerase from Fermentas.

Radiochemicals ( $^{32}\text{P}$ -dCTP,  $^{35}\text{S}$ -Met,) were from Hartmann Analytic (Braunschweig, Germany).

#### Molecular weight markers

GeneRuler™ 1 kb Plus DNA ladder (Thermo Scientific, Rockford, USA), was used as DNA length standard.

The apparent molecular weight of proteins in SDS-polyacrylamide gel electrophoresis was determined according to PageRuler pre-stained molecular weight marker (10 to 170 kDa) from Pierce (Thermo Scientific).

#### DNA Primers

All the primers used in this study were purchased from Metabion GmbH (Martinsried, Germany).

#### Antibodies

Immuno-decoration of Western blot membranes was done with the following antibodies:  $\alpha$ -CURT1A (Agrisera, Vännäs, Sweden);  $\alpha$ -synCURT1 peptide (BioGenes GmbH, Berlin, Germany),  $\alpha$ -APC  $\alpha/\beta$ , (Agrisera),  $\alpha$ -PGRL1 (Roberto Barbato, Dipartimento di Scienze dell'Ambiente e della Vita, Università del Piemonte Orientale, Alessandria, Italy; Paolo Pesaresi, Dipartimento di Bioscienze, Università degli Studi di Milano, Milano, Italy),  $\alpha$ -PGR5 (Toshiharu Shikanai, Department of Botany, Graduate School of Science, Kyoto University, Sakyo-ku, Kyoto, Japan).



## 2.2. Bacterial strains and vectors

The bacterial strains and plasmids used are described in Table 2.1. *E. coli DH5α* cultures were grown in Luria Broth (LB) medium at 37 °C and shaking at 225 rpm.

Unless otherwise indicated, *Synechocystis* sp. PCC 6803 glucose-tolerant wild type (GT, Himadri Pakrasi, Department of Biology, Washington University, St. Louis) and mutant strains were grown at 30 °C in BG11 medium containing 5 mM glucose (Rippka et al., 1979), under continuous illumination at 30 μmol photons m<sup>-2</sup> s<sup>-1</sup>. Liquid cultures were shaken at 120 rpm. For growth on plates, 1.5 % (w/v) agar and 0.3 % (w/v) sodium thiosulfate were added to the BG11 medium. The PSI-defective mutant strains were grown in LAHG conditions (Light Activated Heterotrophic Growth: darkness, unless 5 min of light per day, as described by Anderson and McIntosh, 1991), in the presence of glucose.

For positive selection of the mutants, increasing concentrations of kanamycin (10 to 100 μg/ml) were added to the medium. For negative selection, BG11 containing 5 % (w/v) sucrose was used.

Table 2.1 Strains used in this study

Strain	Characteristics	Selection markers	Source
<i>E. coli</i> <i>DH5α</i>	Competent cells		
<i>Synechocystis</i>			
WT	WT <i>Synechocystis</i> sp PCC 6803, glucose tolerant	kan <sup>S</sup> , suc <sup>R</sup>	H. Pakrasi (Washington University, St. Louis)
<i>ΔpsaA</i>	<i>nptI-sacB</i> cassette replacing endogenous <i>psaA</i> gene	kan <sup>R</sup> , suc <sup>S</sup>	This study
<i>B_opt<sup>kan</sup></i>	<i>At psaB_opt</i> gene and downstream <i>nptI-sacB</i> cassette replacing endogenous <i>psaB</i>	kan <sup>R</sup> , suc <sup>S</sup>	This study
<i>B_opt</i>	<i>B_opt<sup>kan</sup></i> without <i>nptI-sacB</i> cassette	kan <sup>S</sup> , suc <sup>R</sup>	This study
<i>AB_opt<sup>kan</sup></i>	<i>At psaA/B_opt</i> operon and upstream <i>nptI-sacB</i> cassette replacing endogenous <i>psaA/B</i>	kan <sup>R</sup> , suc <sup>S</sup>	This study
<i>AB_opt</i>	<i>AB_opt<sup>kan</sup></i> without <i>nptI-sacB</i> cassette	kan <sup>S</sup> , suc <sup>R</sup>	This study
<i>CURTIA</i>	<i>CURTIA</i> gene and downstream <i>nptI-sacB</i> cassette replacing <i>slr0168</i> ORF	kan <sup>R</sup> , suc <sup>S</sup>	This study
<i>CURTIA syncurt1</i>	<i>CURTIA</i> gene and upstream <i>nptI-sacB</i> cassette replacing endogenous <i>Syn CURTI</i>	kan <sup>R</sup> , suc <sup>S</sup>	This study
<i>Δapc</i>	<i>SpecR</i> cassette replacing endogenous <i>apcA/B</i> operon	kan <sup>R</sup> , suc <sup>S</sup> , Sm <sup>R</sup>	This study
<i>CURTIA syncurt1Δapc</i>	<i>Δapc</i> in <i>CURTIA syncurt1</i> background	Sm <sup>R</sup>	This study
<i>lux<sup>prim</sup></i>	<i>luxAB</i> operon, interrupted by <i>nptI-sacB</i> cassette, replacing <i>slr0168</i> ORF	kan <sup>R</sup> , suc <sup>S</sup>	This study

<i>lux<sup>sec</sup></i>	Intact <i>luxAB</i> operon replacing <i>slr0168</i> ORF	kan <sup>S</sup> , suc <sup>R</sup>	This study
<i>PGR5</i>	<i>PRGLI-PGR5</i> synthetic operon, interrupted by <i>nptI-sacB</i> cassette, replacing <i>slr0168</i> ORF	kan <sup>R</sup> , suc <sup>S</sup>	This study
<i>PGR5+PGRL1</i>	Intact <i>PRGLI-PGR5</i> synthetic operon replacing <i>slr0168</i> ORF	kan <sup>S</sup> , suc <sup>R</sup>	This study
<i>psaA<sup>prim</sup></i>	<i>At psaA</i> gene, interrupted by <i>nptI-sacB</i> cassette, replacing endogenous <i>psaA</i>	kan <sup>R</sup> , suc <sup>S</sup> , heterotroph	This study
<i>psaA<sup>sec</sup></i>	Intact <i>At psaA</i> gene replacing endogenous <i>psaA</i>	kan <sup>S</sup> , suc <sup>R</sup> , photoautotroph	This study

Table 2.2 Plasmid vectors used in this study

Plasmid	Characteristics	Selection markers	Source
pGEM-T Easy	Backbone for pDSpsaA	amp <sup>R</sup>	Promega, Madison, WI
pRL250	<i>nptI-sacB</i> double selection cassette, <i>sacB</i> gene from <i>Bacillus subtilis</i> <i>SpecR</i> selection cassette, gene from	kan <sup>R</sup> , suc <sup>S</sup> Sm <sup>R</sup>	P. Wolk (Michigan State University)
pICH69822	Destination vector for Golden Gate cloning	kan <sup>R</sup>	E. Weber (Icon Genetics GmbH, Halle)
pRL1063a	<i>luxAB</i> operon from <i>Vibrio fischeri</i>	Sm <sup>R</sup>	P. Wolk (Michigan State University)
pUC57+ <i>psaA<sub>opt</sub></i>	Codon-optimized <i>At psaA</i> gene	amp <sup>R</sup>	GenScript
pUC57+ <i>psaB<sub>opt</sub></i>	Codon-optimized <i>At psaB</i> gene	amp <sup>R</sup>	GenScript
pUC57+ <i>PSI<sub>opt</sub></i>	Codon-optimized <i>PSI</i> synthetic operon	amp <sup>R</sup>	GenScript
pCURT1AOI	pICH69822 with <i>Syn psbA2</i> promoter, <i>CURTIA</i> gene, upstream <i>nptI-sacB</i> cassette from pRL250 and <i>slr0168</i> flanking regions	kan <sup>R</sup> , suc <sup>S</sup>	This study
pCURT1AO	pICH69822 with <i>Syn psbA2</i> promoter, <i>CURTIA</i> gene, downstream <i>nptI-sacB</i> cassette from pRL250 and <i>Syn CURTI</i> flanking regions	kan <sup>R</sup> , suc <sup>S</sup>	This study
pSMapc	pICH69822 with <i>SpecR</i> cassette from and endogenous <i>apcA/B</i> operon flanking regions	kan <sup>R</sup> , Sm <sup>R</sup>	This study
pDSAK1	pGEM-T Easy with <i>nptI-sacB</i> cassette from pRL250 and <i>Syn psaA</i> flanking regions	kan <sup>R</sup> , suc <sup>S</sup>	This study
pDSAB <sub>opt</sub>	pICH69822 with <i>At psaA/B<sub>opt</sub></i> operon with endogenous flanking regions and downstream <i>nptI-sacB</i> cassette from pRL250	kan <sup>R</sup> , suc <sup>S</sup>	This study
pAB1	pGEM-T Easy with <i>At psaB<sub>opt</sub></i> downstream region from <i>B<sub>opt</sub></i> strain	kan <sup>R</sup>	This study
pDSA <sub>opt</sub>	pICH69822 with <i>At psaA<sub>opt</sub></i> gene with flanking regions from <i>B<sub>opt</sub></i> strain and upstream <i>nptI-sacB</i> cassette from pRL250	kan <sup>R</sup> , suc <sup>S</sup>	This study
pAB2	pGEM-T Easy with <i>At psaA<sub>opt</sub></i> upstream region from <i>AB<sub>opt</sub></i> strain	kan <sup>R</sup>	This study
pDSlux	pICH69822 with <i>nptI-sacB</i> cassette from pRL250, <i>luxAB</i> operon from pRL1063a and <i>Syn psbA2</i> promoter and <i>slr0168</i> flanking regions	kan <sup>R</sup> , suc <sup>S</sup>	This study
pDSpgrl1	pICH69822 with <i>nptI-sacB</i> cassette from pRL250, <i>Arabidopsis PGRL1</i> and <i>PGR5</i> coding sequences, <i>Syn psbA2</i> promoter and <i>slr0168</i> flanking regions	kan <sup>R</sup> , suc <sup>S</sup>	This study
pDSpsaA	pGEM-T Easy with <i>nptI-sacB</i> cassette from pRL250, <i>At psaA</i> gene and <i>Syn psaA</i> flanking regions	kan <sup>R</sup> , suc <sup>S</sup>	This study

### 2.3. Generation of recombinant plasmids

All DNA techniques such as plasmid isolation, restriction and ligation were performed according to standard protocols (Sambrook et al., 1989). *Synechocystis* sequences were obtained from Cyanobase (<http://genome.kazusa.or.jp/cyanobase/Synechocystis>). All the plasmids used are listed in Table 2.2. To generate all the fragments used for plasmid constructions, sequences of interest were PCR amplified and then purified from 1 % agarose gel with the QIAgen (Venlo, Netherlands) gel extraction kit following the producer's instructions.

For all vectors, except pDSAK1 and pDSpsaA, the amplified fragments were assembled into the final construct using the one-step Golden Gate Shuffling cloning strategy (Engler et al., 2009) and the plasmid pICH69822 as destination vector. The *nptI-sacB* double-selection cassette was amplified from the pRL250 plasmid, the *SpecR* cassette from a pUR plasmid backbone. The *Synechocystis slr0168* ORF (Kunert et al., 2000) was used as neutral genomic site for the stable integration of the pDSLux and pCURT1A vectors, using the upstream and downstream genomic regions of *slr0168* (~1 kb each) as flanking regions for homologous recombination. The sequences of the *Arabidopsis thaliana* *psaA* and *psaB* genes with a codon usage optimized for expression into *Synechocystis* sp. PCC6803 (*At psaA\_opt* and *At psaB\_opt*) were purchased, cloned into the *EcoRV* restriction site of pUC57, from GenScript (Hong Kong).

The pDSAK1 plasmid was constructed by standard cloning and the *Synechocystis* *psaA* gene was chosen as insertion site, using its upstream and downstream genomic regions (~500 bp each) as flanking regions for homologous recombination. To generate the vector, the *nptI-sacB* cassette was excised from the pRL250 plasmid with *BamHI* and then cloned into the pGEM-T Easy vector (Promega, Madison, Wisconsin) according to the manufacturer's instructions. The *Syn psaA* downstream region was cloned at the 3' of the *nptI-sacB* cassette between the *SpeI* and *SacI* restriction sites, then the upstream region was inserted upstream of the cassette between the *ApaI* and *NcoI* restriction sites. For pDSAB\_opt generation, the *At psaA\_opt* and *At psaB\_opt* sequences were amplified from the pUC57+*psaA\_opt* and pUC57+*psaB\_opt* vectors (GenScript). The two artificial genes were then assembled into a synthetic operon using the *Synechocystis* *psaA* upstream region (~500 bp), *psaA/psaB* intergenic region (*A/B IR*, 245 bp) and *psaB* downstream region (~500 bp). The *nptI-sacB* double selection cassette was placed at the 3' of the *Syn psaB* downstream region and was then followed by a second copy of the same flanking sequences. The pAB1 vector was

generated by cloning the *Syn psaB* downstream region used for the pDSAB\_opt vector assembly into the pGEM-T Easy vector. The pDSA\_opt vector was constructed using the *Syn psaA* upstream region (~500 bp) and the A/B IR fused to the initial region of *At psaB\_opt* (positions +1 → +665) were used for integration of the construct into the genome. Upstream of A/B IR was placed the *At psaA\_opt* gene under the regulation of the endogenous *psaA* promoter ( $P_{psaA}$ , 206 bp). The *nptI-sacB* double selection cassette was cloned between the *Syn psaA* upstream region and the  $P_{psaA}$ -*At psaA\_opt* fusion. The entire  $P_{psaA}$  sequence was included also in the *Syn psaA* upstream region and therefore repeated at both the 5' and 3' of the selection cassette. The pAB2 vector was generated by cloning the *Syn psaA* upstream region used for the pDSA\_opt vector assembly into the pGEM-T Easy vector. All primers used are listed in Table 2.3.

Table 2.3 Primers used in the PSI project. The restriction sites are indicated in bold characters and the *BsaI*-generated overhangs are underlined.

<b>pDSAK1</b>			
<b>Primer Name</b>	<b>Sequence (5'→3')</b>	<b>Purpose</b>	<b>Restriction site</b>
A1 FW	GGCCGCGGGCCCGATTTCCTTGC GGACT CTGAGCCAATTTG	PCR of <i>Syn psaA</i> upstream region	<i>ApaI</i>
A1K RV	TTCAGAACCATGGGCAGGGTTCCTCGCTC G		<i>NcoI</i>
A4K FW	TTCGATCACTAGTACTTTGAGCTGAAG	PCR of <i>Syn psaA</i> downstream region	<i>SpeI</i>
A4 RV	GGCCGCGAGCTCCGATCGGGCGAATGTTTA AAGGATCTTTAATC		<i>SacI</i>
<b>pDSAB_opt</b>			
<b>Primer Name</b>	<b>Sequence (5'→3')</b>	<b>Purpose</b>	<b>Restriction site</b>
A/B UR FW	TTTGGTCTCTAGGTTTCCACCCGCAATAAT CC	PCR of <i>Syn psaA</i> upstream region	<i>BsaI</i>
A/B UR RV	TTTGGTCTCTTCATGCAGGGTTCCTCGCT CGAC		<i>BsaI</i>
A_opt FW	TTTGGTCTCTATGATTATTCG TAGTCCCGAA C	PCR of <i>At psaA_opt</i>	<i>BsaI</i>
A_opt RV	TTTGGTCTCTAAGTCTAACCACAGCAATA ATACG		<i>BsaI</i>
A/B IR FW (P3)	TTTGGTCTCTACTTTGAGCTGAAGTTGGGTT TTC	PCR of <i>Syn psaA/B</i> intergenic region	<i>BsaI</i>
A/B IR RV (P2)	TTTGGTCTCTCCATAGCTTTTCGGAAATTC TCCTCG		<i>BsaI</i>
B_opt FW	TTTGGTCTCTATGGCTTTACGCTTCCCGT TTTTC	PCR of <i>At psaB_opt</i>	<i>BsaI</i>
B_opt2 RV	TTTGGTCTCTAACGTTAGCCAAATTTCCAG AAGTAGAG		<i>BsaI</i>
selection cassette FW	TTTGGTCTCACGTTGGAATTCGATTGATCCG TCGAC	PCR of <i>nptI-sacB</i> double selection cassette	<i>BsaI</i>
selection cassette RV	TTTGGTCTCCATACTTTAGGCCCGTAGTCT GCA		<i>BsaI</i>

A/B DR repl. FW	TTTGGTCTCTTATGCGAATTCCTCTGTTAGG TAATTAAG	PCR of <i>Syn psaB</i> downstream region	<i>Bsal</i>
A/B DR RV	TTTGGTCTCTAAGCTAGCCACCAGCAACCTC AGTG		

<b>pDSA_opt</b>			
<b>Primer Name</b>	<b>Sequence (5'→3')</b>	<b>Purpose</b>	<b>Restriction site</b>
A2 UR FW	TTTGGTCTCTAGGTTTATTTCCGGCAATGGCA TG	PCR of <i>Syn psaA</i> upstream region	<i>Bsal</i>
A2 UR RV	TTTGGTCTCTAACGGCAGGGTTCTCCTCGCT CG		
selection cassette FW	TTTGGTCTCACGTTGGAATTCGATTGATCCG TCGAC	PCR of <i>nptI_sacB</i> double selection cassette	<i>Bsal</i>
selection cassette RV	TTTGGTCTCCCATACTTTAGGCCCGTAGTCT GCA		
A2 prom. FW	TTTGGTCTCTTATGATTTTAAATTATTGTTAC GCAGGTCTTG	PCR of <i>Syn psaA</i> promoter	<i>Bsal</i>
A/B UR RV	TTTGGTCTCTTCATGCAGGGTTCTCCTCGCT CGAC		
A_opt FW	TTTGGTCTCTATGATTATTCGTAGTCCCGAA C	PCR of <i>At psaA_opt</i>	<i>Bsal</i>
A_opt RV	TTTGGTCTCTAAGTCTAACCACAGCAATA ATACG		
A/B IR FW	TTTGGTCTCTACTTTGAGCTGAAGTTGGGTT TTC	PCR of <i>Syn psaA</i> downstream region from <i>B_opt</i>	<i>Bsal</i>
A2 DR RV	TTTGGTCTCTAAGCAGCCCTTGGGGATGGG GTAAC		

<b>Others</b>			
<b>Primer Name</b>	<b>Sequence (5'→3')</b>	<b>Purpose</b>	
kan_S1 (P5)	GGTCTTGACAAAAAGAACCGGGC	Primers used to check presence of <i>nptI_sacB</i>	
<i>sacB</i> _S1 (P6)	ATTCTTCCGTCAAGAAAGTC		
AB seq 1 (P11)	TGTGAGGGAACCTGGAACCTC	Primers used for genotyping	
AB seq 2 (P8)	CATAATCTGCAGTTGGCGATC		
AB seq 4 (P1)	CACAAAGGACTTTATGAAATC		
AB seq 5 (P4)	GGACAAAGAAGATGGCACCCG		
AB seq 7 (P12)	TCCAGTAAATCGTTGTAACG		
AB seq 8 (P9)	TCTGAATTTTGGACCTTTCGC		
AB seq 9 (P10)	AGCACATTATCTTCGTTCTG		
AB seq 10 (P7)	GCTGGGACGTGGTCATAAAG		

For pCURT1AOI generation, the *CURT1A* coding sequence lacking the predicted cTP was amplified from *Arabidopsis* cDNA and placed under control of the *Synechocystis* strong *psbA2* promoter ( $P_{psbA2}$ , Eriksson et al., 2000). The promoter-gene fusion and the downstream *nptI-sacB* double selection cassette were placed between the *slr0168* flanking regions. The pCURT1AO vector was generated using the same  $P_{psbA2}$ -*CURT1A* fusion as for pCURT1AOI, but the *nptI-sacB* cassette was placed upstream of it and the upstream and downstream genomic regions of the *Synechocystis slr0168* gene (*Syn CURT1*, ~500 bp each) were used as flanking regions for homologous recombination. The pSMMapc vector was

constructed by cloning the *SpecR* cassette between the upstream and downstream regions (~1 kb each) of the *Synechocystis apcAB* dicistronic operon (*slr067*, *slr1986*). All primers used are listed in Table 2.4.

Table 2.4 Primers used in the CURT1 project. The restriction sites are indicated in bold characters and the *Bsal*-generated overhangs are underlined.

<b>pCURT1AOI</b>			
<b>Primer Name</b>	<b>Sequence (5'→3')</b>	<b>Purpose</b>	<b>Restriction site</b>
PG UR FW	TTTGGTCTCT <u>AGGT</u> TGCTCAGCAGTGACCTATTC	PCR of <i>slr0168</i> upstream region	<i>Bsal</i>
PG UR RV	TTTGGTCTCT <u>TGGG</u> GCCACTGTTATTTTGATTG		<i>Bsal</i>
psbA2P (C3) FW	TTTGGTCTCT <u>CCCA</u> TGGAAAAACGACAATTAC	PCR of <i>psabA2</i> promoter	<i>Bsal</i>
COE_P RV	TTTGGTCTCT <u>TTGG</u> TTATAATTCCTTATGTATTTG		<i>Bsal</i>
CURT1A FW	TTTGGTCTCT <u>CCAA</u> ATGGCTTCTTCAGAAGAGAC CTC	PCR of <i>At CURT1A</i> CDS	<i>Bsal</i>
CURT1A2 (C4) RV	TTTGGTCTCT <u>AACG</u> CTATTCGCTTCCTGCGATCTT C	without cTP	<i>Bsal</i>
selection cassette FW	TTTGGTCTC <u>ACGT</u> TGGAATTCGATTGATCCGTCG AC	PCR of <i>nptI_sacB</i> double selection cassette	<i>Bsal</i>
selection cassette RV	TTTGGTCTC <u>CCATA</u> CTTTAGGCCCGTAGTCTGCA		<i>Bsal</i>
PG DR2 FW	TTTGGTCTCT <u>TATG</u> CAATTTTCGTTTGCGAATTTAC	PCR of <i>slr0168</i> downstream region	<i>Bsal</i>
PG DR2 RV	TTTGGTCTCT <u>AAGC</u> ATAAAAATACCTTCCCATC		<i>Bsal</i>
<b>pCURT1AO</b>			
<b>Primer Name</b>	<b>Sequence (5'→3')</b>	<b>Purpose</b>	<b>Restriction site</b>
CURT UR FW	TTTGGTCTCT <u>AGGT</u> TTTTTGACCTATCTGGGTGA AG	PCR of <i>slr0483</i> upstream region	<i>Bsal</i>
CURT UR RV	TTTGGTCTCT <u>AACG</u> AGCTTCCCATATTGGGGC		<i>Bsal</i>
selection cassette FW	TTTGGTCTC <u>ACGT</u> TGGAATTCGATTGATCCGTCG AC	PCR of <i>nptI_sacB</i> double selection cassette	<i>Bsal</i>
selection cassette RV	TTTGGTCTC <u>CCATA</u> CTTTAGGCCCGTAGTCTGCA		<i>Bsal</i>
COE_P FW	TTTGGTCTCT <u>TATG</u> CCCATGGAAAAACGACAAT TAC	PCR of <i>psabA2</i> promoter	<i>Bsal</i>
COE_P RV	TTTGGTCTCT <u>TTGG</u> TTATAATTCCTTATGTATTTG		<i>Bsal</i>
CURT1A FW	TTTGGTCTCT <u>CCAA</u> ATGGCTTCTTCAGAAGAGAC CTC	PCR of <i>At CURT1A</i> CDS	<i>Bsal</i>
CURT1A RV	TTTGGTCTCT <u>GACA</u> CTATTCGCTTCCTGCGATCTT C	without cTP	<i>Bsal</i>
CURT DR FW	TTTGGTCTC <u>ATGT</u> CTCCAGACCGCCCCAG	PCR of <i>slr0483</i> downstream region	<i>Bsal</i>
CURT DR RV	TTTGGTCTCT <u>AAGC</u> CAAATGCCATTCTGGGCG		<i>Bsal</i>
<b>pSM<sub>apc</sub></b>			
<b>Primer Name</b>	<b>Sequence (5'→3')</b>	<b>Purpose</b>	<b>Restriction site</b>
APC UR FW	TTTGGTCTCT <u>AGGT</u> ICGGCAATACTGGCGGTGTAA G	PCR of <i>Syn apcA/B</i> operon upstream region	<i>Bsal</i>
APC UR RV	TTTGGTCTCT <u>GTTT</u> GGATGGATTCCCTCCGTAAAG		<i>Bsal</i>
SM cass (C7) FW	TTTGGTCTCT <u>AAAC</u> CTTGCGCTCGTTTCG	PCR of <i>SpecR</i> selection cassette	<i>Bsal</i>
SM cass RV	TTTGGTCTCT <u>TTAT</u> TTTGCCGACTACCTTGGTGATC		<i>Bsal</i>

APC DR FW	TTTGGTCTCTATAATCCTGGATTCCCCTGGGTG	PCR of <i>Syn</i> <i>BsaI</i> <i>apcA/B</i> operon downstream region <i>BsaI</i>
APC DR RV (C8)	TTTGGTCTCTAAGCGGATCTAGGTTGTGGTTCCG	

**Others**

Primer Name	Sequence (5'→3')	Purpose
synCURT1 FW (C1)	TTTGGTCTCTCAAATGGTGGGCCGTAAACATTC	Primers used to check presence of <i>Syn CURT1</i>
synCURT1 RV (C2)	TTTGGTCTCTGACACTAACCGCCAAAAATTGCT C	
apcAB FW (C5)	GAAATCAATCGTGAATGCTG	Primers used to check presence of <i>Syn apcA/B operon</i>
apcAB RV (C6)	CGGTAACCTCTTTGATGGCT	

To generate the pDSlux vector, the *luxAB* dicistronic operon from *Vibrio fischeri* was derived from the pRL1063a plasmid (Wolk et al., 1991). The operon was placed under control of  $P_{psbA2}$ , by fusing it upstream of *luxA*. Two amplicons of the *luxAB* operon were generated, the first starting at position +1 of *luxA* and ending at position +460 of *luxB* and the second starting at position +856 of *luxA* and ending at the 3' end of *luxB*. Thus, the sequences of the two fragments overlap for 1055 base pairs. The two amplicons were separated by the *nptI-sacB* double selection cassette. The promoter-operon fusion and the interrupting *nptI-sacB* double selection cassette were placed between the *slr0168* flanking regions. To generate the pDSpgrl1 vector, the sequences encoding the *Arabidopsis thaliana* PGRL1 and PGR5 mature proteins were amplified from cDNA and placed each under control of one copy of  $P_{psbA2}$ . Two amplicons of the PGRL1 coding sequence were generated, the first (5' *PGRL1*) covering the +1 → +503 region and the second (*PGRL1*) the entire sequence. Thus, the sequences of the two fragments overlap for 503 base pairs. The  $P_{psbA2}$ -5' *PGRL1* fusion was placed upstream of the *nptI-sacB* cassette. The *PGRL1* amplicon was placed downstream of the cassette, followed by the  $P_{psbA2}$ -*PGR5* fusion. The *PGRL1-PGR5* synthetic operon, interrupted by the *nptI-sacB* double selection cassette, was placed between the *slr0168* flanking regions. The pDSpsaA plasmid was constructed by overlapping PCR and subsequent standard cloning steps and the *Synechocystis psA* gene was used as insertion site, using its upstream and downstream genomic regions (~500 bp each) as flanking regions for homologous recombination. To generate the vector, the *nptI-sacB* cassette was excised from the pRL250 plasmid with *BamHI* and then cloned into the pGEM-T Easy vector (Promega, Madison, Wisconsin) according to the manufacturer's instructions. The *At psA* (*AtCG00350*) coding sequence was thus placed under control of the endogenous *Synechocystis psA* promoter (contained in HR1). Two fragments of *At psA* were amplified from plant cDNA, the first (5' *At psA*) covering the +1

→ +1430 and the second (3' *At psaA*) the +922 → 3' end positions. The two amplicons, overlapping for 509 base pairs, were assembled with the upstream and downstream flanking regions via overlapping PCR. The downstream amplicon was cloned at the 3' of the *nptI-sacB* cassette between the *SpeI* and *SacI* restriction sites, then the other amplicon upstream of the cassette between the *ApaI* and *NotI* restriction sites. All primers used are listed in Table 2.5.

Table 2.5 Primers used in the marker-less gene replacement project. The restriction sites are indicated in bold characters and the *Bsal*-generated overhangs are underlined.

<b>pDSlux</b>				
<b>Primer Name</b>		<b>Sequence (5'→3')</b>	<b>Purpose</b>	<b>Restriction site</b>
<i>slr0168</i> FW	UR	TTTGGTCTCT <u>AGGT</u> ACAGGCCCTCAAGGCCCTG	PCR of <i>slr0168</i> upstream region	<i>Bsal</i>
<i>slr0168</i> RV	UR	TTTGGTCTCT <u>GCCACT</u> GTTATTTTGATTGGTGGC		
<i>slr0168</i> FW (R5)	DR	TTTGGTCTCT <u>TTTCG</u> TTTGCGAATTTACACCAG	PCR of <i>slr0168</i> downstream region	<i>Bsal</i>
<i>slr0168</i> RV (R6)	DR	TTTGGTCTCT <u>AAGCT</u> AGGGTGGAGCCAGTGGC		
selection cassette FW		TTTGGTCTC <u>ACGTT</u> GGAATTCGATTGATCCGTCGAC	PCR of <i>nptI_sacB</i> double selection cassette	<i>Bsal</i>
selection cassette RV		TTTGGTCTC <u>CCATACT</u> TTAGGCCCGTAGTCTGCA		
Lux1 (R1)	FW	TTTGGTCTCT <u>CCAAAT</u> GAAAGTTTGAAATATTTGTTTTC	PCR of <i>luxAB</i> first amplicon	<i>Bsal</i>
Lux1	RV	TTTGGTCTCT <u>AACGC</u> CATAAAAGTCGTTTTGGGGATG		
Lux2	FW	TTTGGTCTCT <u>TATGG</u> TATGACTGCTGAGTCCGCAAG	PCR of <i>luxAB</i> second amplicon	<i>Bsal</i>
Lux2 (R4)	RV	TTTGGTCTCT <u>CGAA</u> TGTTGAATAAATCGAACTTTTG C		
DS prom	FW	TTTGGTCTCT <u>TGGCCC</u> CATGGAAAAACGACAATTAC	PCR of <i>psabA2</i> promoter	<i>Bsal</i>
DS prom	RV	TTTGGTCTCT <u>TTGGT</u> TATAATTCCTTATGTATTTGTGCG		
<b>pDSpgrl1</b>				
<b>Primer Name</b>		<b>Sequence (5'→3')</b>	<b>Purpose</b>	<b>Restriction site</b>
<i>slr0168</i> FW (R7)	UR	TTTGGTCTCT <u>AGGT</u> ACAGGCCCTCAAGGCCCTG	PCR of <i>slr0168</i> upstream region	<i>Bsal</i>
<i>slr0168</i> RV	UR	TTTGGTCTCT <u>GCCACT</u> GTTATTTTGATTGGTGGC		
<i>slr0168</i> FW	DR	TTTGGTCTCT <u>TTTCG</u> TTTGCGAATTTACACCAG	PCR of <i>slr0168</i> downstream region	<i>Bsal</i>
<i>slr0168</i> RV	DR	TTTGGTCTCT <u>AAGCT</u> AGGGTGGAGCCAGTGGC		
selection cassette	FW	TTTGGTCTC <u>ACGTT</u> GGAATTCGATTGATCCGTCGAC	PCR of <i>nptI_sacB</i>	<i>Bsal</i>



selection cassette RV	TTTGGTCTCC <u>CATA</u> CTTTAGGCCCGTAGTCTGCA	double selection cassette	<i>BsaI</i>
DS prom FW	TTTGGTCTCTTGGCCCCATGGAAAAACGACAATTAC	PCR of <i>psabA2</i> promoter, first copy	<i>BsaI</i>
DS prom RV	TTTGGTCTCTTTGGTTATAATTCCTTATGTATTTGTGCG		<i>BsaI</i>
DS pgr1 FW	TTTGGTCTCTCCAAATGGCCACAACAGAGCAATC	PCR of 5' <i>PGRL1</i> amplicon	<i>BsaI</i>
DS pgr1 RV	TTTGGTCTCTA <u>ACG</u> ATCTCAAAACCTGTAATGTGCGTC		<i>BsaI</i>
DS pgr2 FW	TTTGGTCTCTTATGATGGCCACAACAGAGCAATC	PCR of <i>PGRL1</i> entire amplicon	<i>BsaI</i>
DS pgr2 RV	TTTGGTCTCTTGGGTTAAGCTTGGCTTCCTTCTGGC		<i>BsaI</i>
DS prom <sup>2</sup> FW	TTTGGTCTCTCCCATGGAAAAACGACAATTAC	PCR of <i>psabA2</i> promoter, second copy	<i>BsaI</i>
DS prom <sup>2</sup> RV	TTTGGTCTCTCCATTTGGTTATAATTCCTTATGTATTTGTCG		<i>BsaI</i>
DS pgr5 FW	TTTGGTCTCTATGGCTGCTGCTTCGATTTC	PCR of <i>PGR5</i> amplicon	<i>BsaI</i>
DS pgr5 RV (R8)	TTTGGTCTCTCGAACTAAGCAAGGAAACCAAGCCTC		<i>BsaI</i>

<b>pDSpsaA</b>			
<b>Primer Name</b>	<b>Sequence (5'→3')</b>	<b>Purpose</b>	<b>Restriction site</b>
A1 FW (R11)	GGCCGCGGGCCCGATTCCCCTTGCGGACTCTGAGCC AATTG	PCR of <i>Syn psaA</i> upstream region	<i>ApaI</i>
A1 RV	TGGTTCCGGCGAACGAATAATCATGCAGGGTTCTCCTC GCTCGACAATG		
A2 FW	CATTGTCGAGCGAGGAGAACCCTGCATGATTATTCGTT CGCCGGAACCAG	PCR <i>At psaA</i> first amplicon	<i>NotI</i>
A1DS RV	TTCGAATGCGGCCGCTGTAATTGTATAGC		
A4DS FW	TCAATCACTAGTATGTATAGGAC	PCR <i>At psaA</i> second amplicon	<i>SpeI</i>
A3 RV (R12)	GGAAAACCCAACTTCAGCTCAAAGTTTATCCTACTGCAA TAATTCTTGC		
A4 FW	GCAAGAATTATTGCAGTAGGATAAACTTTGAGCTGAA GTTGGGTTTTCC	PCR of <i>Syn psaA</i> downstream region	<i>SacI</i>
A4 RV	GGCCGCGAGCTCCGATCGGGCGAATGTTTAAAGGAT CTTTAATC		

<b>Others</b>			
<b>Primer Name</b>	<b>Sequence (5'→3')</b>	<b>Purpose</b>	
<i>psaA</i> <sup>gUR</sup> FW (R9)	TGTGAGGGAACCTTGGAACCTC	Primers used to check presence of <i>Syn psaA</i>	
<i>psaA_syn</i> RV (R10)	GATCATAATCACGCACCATG		
DS <sub><i>nptI</i></sub> RV (P2)	AAGATGCGTGATCTGATCCTTC	Primers used to check presence of <i>nptI_sacB</i>	
<i>sac_S2</i> (P3)	AGCATATCATGGCGTGTAATATGGG		

#### 2.4. Synechocystis transformation

*Synechocystis* WT or mutant strains were transformed with plasmid vectors purified with the QIAgen (Venlo, Netherlands) Midiprep kit.

For each transformation, 10 ml of growing cells at an OD<sub>730</sub> of 0.4 were harvested by centrifugation and resuspended in 1/20 volume of BG11. The cell number per ml was calculated from OD<sub>730</sub> with the formula: 1 OD<sub>730</sub> = 7×10<sup>7</sup> cells. 2 µg of plasmid DNA per transformation were added to the cells. Transformations were incubated in light for 5 hours, the last 3 hours with shaking. For recovery, fresh BG11 was added and the transformations were incubated overnight in the dark with shaking at 30 °C. On the next day, cells were collected by centrifugation at 4500xg for 10 min, resuspended in a small volume of fresh BG11 medium and plated on BG11 agar plates containing the correct antibiotic. Mutants that integrated the *nptI-sacB* cassette in their genome were positively selected on BG11 agar plates containing 10 µg/ml kanamycin, whereas those that integrated the *SpecR* cassette were selected on BG11 agar plates containing 5 µg/ml spectinomycin. Unless otherwise indicated, plates of transformed cells transformed were incubated in light at 30 °C. To calculate the transformation efficiencies, the number of obtained transformants was counted and then the following equation was used: Transformation frequency = ‘number of transformants’ / ‘total number of cells before transformation’. For complete segregation of the mutants, increasing kanamycin (up to 100 µg/ml) and spectinomycin (up to 50 µg/ml) concentrations were used.

#### 2.5. Synechocystis counter-selection and frequency calculation of second recombinants

For second recombination, with consequent removal of the *nptI-sacB* cassette and counter selection, completely segregated strains harbouring the double selection cartridge were used. Cells were grown in BG11 liquid medium containing 100 µg/ml kanamycin to an OD<sub>730</sub> of 0.4, then 10 ml were harvested by centrifugation and resuspended in 1/20 volume of fresh BG11 and the cell number per ml was calculated as described before. 2 µg of plasmid DNA per transformation were added to the cells and transformations were incubated in light for 5 hours, the last 3 hours with shaking. As *Synechocystis* cells contain multiple copies of the genome, liquid cultures were then allowed to recover for 5 days in fresh BG11 medium without selection in order to allow them to lose all the copies of *sacB*. After the incubation period, 2 ml of each liquid culture were plated on BG11 solid medium containing 5 % sucrose. Unless otherwise specified, plates were incubated in light at 30°C. To calculate the frequency of second recombination, the number of recombinants was counted and the

following equation was used: ‘Recombination frequency’ = ‘number of recombinants’ / ‘total number of cells’ before recombination. Genomic PCR was used to confirm the complete segregation of first and second recombinants.

For second recombination and counter selection in the case of the “single-step” double recombination strategy, completely segregated first recombinant strains were grown in liquid BG11 containing 100 µg/ml kanamycin to an OD<sub>730</sub> of 1. For each of these cultures 500 µl were pelleted, washed and resuspended in 10 volumes of BG11 without antibiotic and the cell number per ml was calculated as described before. The liquid cultures were then grown for 5 days without selection and subsequently 2 ml of each liquid culture were plated on BG11 solid medium containing 5 % sucrose.

## 2.6. Plant cultivation and growth conditions

*Arabidopsis thaliana* WT (ecotype Col-0) seeds were incubated in the dark on wet Whatman paper for two days at 4 °C, then transferred to soil under controlled climate chamber conditions (PFD: 80 µmol m<sup>-2</sup> s<sup>-1</sup> 16h/8h dark/light).

## 2.7. Nucleic acid manipulation

### 2.7.1. Standard and high-fidelity PCR

For genotyping of bacterial strains, PCR analysis was performed using 0.5 µl of genomic DNA as template in a total reaction volume of 20 µl. The reaction mix contained 1x PCR-buffer (QIAGEN), 100 µM dNTPs, 200 µM primers, 0.5 units of Taq DNA polymerase. The PCR products were then loaded on a 1% agarose TAE (150 mM Tris-HCl, 1.74 M Acetic acid, 1 mM EDTA) gel and visualized by Ethidium bromide staining.

DNA fragments were amplified from *Synechocystis* genomic DNA or *Arabidopsis* Col-0 cDNA with the Phusion High-Fidelity DNA Polymerase (Thermo Scientific, Rockford, USA). Reactions were performed in a total volume of 20 µl each containing 1x Phusion HF reaction buffer, 200 µM dNTPs, 200 µM of each primer and 0.4 units Phusion HF DNA Polymerase. The PCR-products were loaded on a 1% agarose gel and then cut from the gel and purified with the QIAGEN gel extraction kit following the producer’s instructions.

### 2.7.2. Genomic DNA isolation

Small-scale isolation of *Synechocystis* genomic DNA for genotyping and cloning was performed using the xanthogenate method, according to Tillett and Neilan (2000). Two ml of

exponentially growing liquid cultures were pelleted and resuspended in 50 µl of TE buffer (10 mM Tris/HCl pH 7.4, 1 mM EDTA pH 8.0) containing 100 µg/ml RNase A (DNase-free). 750 µl XS buffer (1 % calciumethylxanthogenate, 100 mM Tris/HCl pH 7.4, 20 mM EDTA pH 8.0, 1% SDS, 800 mM NH<sub>4</sub>OAc) was added to each sample and, after inverting them 4-6 times, the tubes were incubated at 70 °C for 2 hours to dissolve membranes. The suspensions were then vortexed for 10 sec, incubated in ice for 30 min and centrifuged for 10 min at 13000xg. The supernatant was transferred in a new tube and DNA was precipitated by adding 0.7 volumes of isopropanol and by centrifuging for 10 min at 12000xg. The DNA pellet was washed with 70 % ethanol, dried and resuspended in 100 µl of ddH<sub>2</sub>O.

For Southern blot analysis, high-quality genomic DNA was isolated as follows. 50 ml of liquid culture in the late exponential phase were centrifuged at 4000xg for 10 min at 4 °C and washed twice in 10 ml of TE buffer. The pellet was resuspended in 1 ml of TES buffer (25 % w/v sucrose, 50 mM Tris/HCl, 1 mM EDTA pH 8.0), frozen in liquid N<sub>2</sub>, thawed at 60°C and frozen again. After thawing again, 5 mg/ml lysozyme, 0.1 µg/ml RNaseA and 100 mM EDTA (pH 8.0) were added and the suspension was incubated at 37 °C for 1 hour. Then, 3 units of proteinase K and 2 % SDS were added and the sample was incubated at 60 °C for an additional hour. The genomic DNA was extracted twice by adding an equal volume of phenol-chloroform (1:1 w/v) and the obtained aqueous phase was cleaned from traces of phenol with one volume of chloroform. The DNA in the aqueous phase was then precipitated with 0.7 volumes of isopropanol and washed with 70 % ethanol. The DNA pellet was air-dried for 1 hour and resuspended overnight at 4 °C in 50 µl of H<sub>2</sub>O. All centrifugation steps were performed at 4 °C.

### 2.7.3. RNA isolation

The total RNA from *Arabidopsis thaliana* was extracted from leaf ground tissue using one volume of extraction buffer (300 mM NaCl, 50 mM Tris-HCl pH 7.5, 20 mM EDTA, 0.5 % SDS) and one volume of phenol-chloroform-isoamylalcohol (PCI) followed by solubilization at 65 °C for 5 minutes. After a centrifugation step (10 minutes at 7000 g), the supernatant was mixed with one volume of 8 M LiCl, incubated for two hours at -20 °C and centrifuged for 30 minutes at 4 °C at 7000xg. The pellet was then washed with 75 % ethanol and resuspended in 80 µl of DEPC-treated water.

The total RNA from *Synechocystis* sp. PCC 6803 was extracted with the PGTX 95 method, according to Pinto et al. (2009). Cells from 50 ml of exponentially liquid cultures were pelleted, resuspended in 1 ml of PGTX (phenol 39.6 % w/v, glycerol 6.9 % w/v, 8-

hydroxyquinoline 0.1 % w/v, EDTA 0.58 % w/v, sodium acetate 0.8 % w/v, guanidine thiocyanate 9.5 % w/v, guanidine hydrochloride 4.6 % w/v and Triton X-100 2 % w/v) and incubated at 95 °C for 5 min. After cooling on ice for 5 min, samples were vigorously mixed with 1/10 volume of chloroform, incubated 5 min at room temperature and centrifuged for 15 min at 12000xg, 4 °C. The aqueous phase was then further extracted with one volume of phenol-chloroform-isoamylalcohol (PCI), and the RNA in the supernatant was precipitated with 0.7 volumes of isopropanol. The RNA pellet was washed with 75 % ethanol, air-dried and resuspended in 80 µl of DEPC-treated water.

#### 2.7.4. Plant cDNA synthesis

Synthesis of *Arabidopsis thaliana* cDNA was performed using the iScript reverse transcriptase kit (Bio-Rad, Hercules, CA, USA). During the whole procedure, DEPC-treated water was used. For digestion of DNA contaminations, DNase treatment of 1 µg of RNA was performed in a total reaction volume of 10 µl, containing 1x PCR buffer (Qiagen, Venlo, Netherlands) + MgCl<sub>2</sub> and 0.5 units of DNase I. The reaction mix was incubated at room temperature for 30 minutes and the enzyme was then inactivated by adding 2.5 mM EDTA and further incubating for 15 min at 65 °C. Each RNA sample was then used in a total reverse transcription reaction volume of 20 µl, containing 1x iScript reaction mix buffer and 1 µl of iScript reverse transcriptase. The first-strand cDNA synthesis was performed according to the following protocol by using a thermocycler (BioRad): 5 minutes at 25 °C, 40 minutes at 42 °C and 5 minutes at 85 °C.

#### 2.7.5. Southern analyses

Southern blot analyses were performed according to Sambrook et al. (1989). For Southern blot analysis, 5 µg of genomic DNA were digested, in 100 µl of total reaction volume, with 5 units of the appropriate restriction enzyme, according to the manufacturer's instructions. Reactions were incubated overnight at 37 °C. The obtained digestion products were purified with phenol-chloroform extraction, precipitated with isopropanol and resuspended overnight at 4°C in 20 µl ddH<sub>2</sub>O each. After 5 min denaturation at 65 °C, the samples were mixed with 4 µl of 6x loading dye and electrophoretically separated on a 0.8 % agarose gel in 0.5x TBE (40 mM Tris-HCl, pH 8.3, 45 mM boric acid, 1 mM EDTA) at 80 V for 6 hours. After the separation, the DNA fragments in the gel were visualized with Ethidium bromide staining and then they were depurinated by incubating the gel in 0.2 M HCl for 10 min. After careful rinsing, the gel was denatured by gently shaking it in 1.5 M NaCl, 0.5 M NaOH for 45 min

and then neutralized for further 45 min in 3 M NaCl, 0.5 M Tris, pH 7.0. The gel was then blotted on a positively-charged nylon membrane (Hybond N+; GE Healthcare, Freiburg, Germany) by using the capillary transfer technique. A glass plate was placed on top of a glass basin filled with 20x SSC buffer (2 M NaCl, 0.2 M Na-citrate; pH 7.0). A paper bridge was placed on top of this plate, consisting of 1 piece of Whatman paper (3 MM) slightly larger than the gel and long, in order to reach into the 20x SSC buffer in the basin. The bridge was wetted with 10xSSC and, on top of that, 2 pieces of Whatman paper of the same size of the gel and also wetted with 10xSSC were placed. Air bubbles were carefully removed and the gel was placed upside down on the paper and then, on its back side, the positively charged nylon membrane upfront pre-incubated in 2x SSC buffer. On top of the membrane 2 further sheets of Whatman paper were added, also pre-wetted in 2x SSC buffer and a stack of paper towels about 10 cm tall. A weight of about 400 g was placed on top of the sandwich, to drive the flux of the blotting buffer via capillary force. The capillary transfer was allowed to run over night for approximately 16 hours. The membrane was UV-crosslinked. For the pre-hybridization-step, the membrane was placed into a glass tube containing 20 ml of hybridization buffer preheated to 60 °C. 160 µl of previously denatured (100 °C, 5 minutes) herring sperm DNA (10 ng/µl) were added and the tube was then incubated in a rotating oven at 67 °C for at least 5 hours. For probe preparation, approximately 100 ng of PCR-product were filled up to 12 µl with ddH<sub>2</sub>O, denatured at 100 °C for 5 minutes and cooled on ice for 5 minutes. Afterwards, 4 µl of 1xOLB Buffer (50 mM Tris pH 6.8, 10 mM MgOAc, 50 mM DTT, 0.5 mg/ml BSA, 33 µM each of dATP, dTTP and dGTP), 1 µl of Klenow DNA polymerase and 3 µl of radioactive <sup>32</sup>P-dCTP were added to the probe and the reaction was incubated at 37 °C for 1 hour. The probe was purified with the Illustra MicroSpin™ G-25 Columns (Freiburg, Germany) according to the producer's instructions and eluted in 100 µl ddH<sub>2</sub>O. The probe was then denatured (100 °C for 5 min) together with 60 µl of herring sperm DNA (10 ng/µl) and added to the filter. Hybridization was carried on overnight at 67 °C in the rotating oven. For the washing step, the probe was discarded and 10 ml of washing buffer (0.1 % SDS, 0.2 M NaCl, 20 mM NaH<sub>2</sub>PO<sub>4</sub>, 5 mM EDTA; pH7.4) pre-warmed to 60 °C were added in the tube that was further incubated at 67 °C. After 30 minutes the washing buffer was exchanged and the tubes were put back in the oven for 15 minutes. The washing buffer was discarded and the membrane was washed again at room temperature in RT buffer (6 mM NaH<sub>2</sub>PO<sub>4</sub>, 1 mM EDTA, 0.2 % SDS; pH 7.0) for one hour on a shaker. The membrane was then exposed on a radioactive-sensitive phosphor-screen overnight. Primers used to amplify the probes are listed in Table 2.

Signals were detected with a phosphor imager and IMAGEQUANT (Typhoon, GE Healthcare, <http://www.gehealthcare.com/>).

#### 2.7.6. Northern analyses

Northern blot analyses were performed according to Sambrook et al. (1989) loading 15 µg of total RNA. To 15 µl of RNA 15 µl of formamide, 4 µl of formaldehyde and 3 µl of 10x MEN (0.2 M MOPS, 50 mM Na acetate, 10 mM EDTA; pH 7.0) buffer were added. The samples were incubated at 65 °C for 15 minutes and afterwards put on ice for 5 minutes. Then 8 µl of 6x loading dye were added, the samples were loaded on an agarose gel (2 % agarose, 6 % formaldehyde, 1x MEN buffer) and then ran at 40 V for 3 hours. The gel was then blotted on a positively-charged nylon membrane (Hybond N+; GE Healthcare, Freiburg, Germany) by using the capillary transfer technique as previously described for the southern blot. The blotting assembly was allowed to run over night for approximately 16 hours and the membrane was afterwards UV-crosslinked. For the pre-hybridization-step the hybridization buffer was preheated to 60 °C. 20 ml of hybridization buffer and 160 µl of previously denaturated (100 °C, 5minutes) herring sperm DNA (10 ng/µl) were added. The tube was incubated in a rotating oven at 60 °C overnight. For probe preparation approximately 100 ng of PCR-product were filled up to 12 µl with ddH<sub>2</sub>O, denaturated at 100 °C for 5 minutes and cooled down on ice for 5 minutes. Afterwards, 4 µl of 1x NEBuffer 2, 1 µl of Klenow DNA polymerase, 33 µM dNTPs (without CTP) and 3 µl of radioactive <sup>32</sup>P-dCTP were added to the probe followed by incubation over night at room temperature. For probe purification, Illustra MicroSpin™ G-25 Columns were used according to the producer's instructions. For the washing step the washing buffer (0.1 % SDS, 0.2 M NaCl, 20 mM NaH<sub>2</sub>PO<sub>4</sub>, 5 mM EDTA; pH7.4) was pre-warmed in a water bath to 60 °C. The probe was discarded and 10 ml of washing buffer were added and further incubated at 65 °C. The washing buffer was kept at 60 °C. After 30 minutes the washing buffer was exchanged and the tubes were put back to 60 °C for 15 minutes. The membrane was then exposed to a radioactive sensitive screen overnight. Primers used to amplify the probes are listed in Table 2.3. Signals were acquired and quantified with a phosphor imager and IMAGEQUANT (Typhoon, GE Healthcare, [www3.gehealthcare.com](http://www3.gehealthcare.com)).

## 2.8. Protein manipulation

### 2.8.1. Protein preparation and immuno-blot analyses

For total protein extraction, *Synechocystis* cultures in the exponential growth phase were collected by centrifugation and resuspended in 1 volume of thylakoid buffer (50 mM HEPES/NaOH pH 7.0, 5 mM MgCl<sub>2</sub>, 25 mM CaCl<sub>2</sub>, 10 % glycerin). Cell suspensions were transferred into a 2 ml tube together with 0.5 volumes of glass beads (0.25-0.5 mm diameter), and vortexed 5 times for 20 sec. Samples were placed on ice for 1 min between each vortexing step. Beads and unbroken cells were pelleted by centrifuging at 16000xg for 3 min and then the supernatant, corresponding to the total protein fraction, was transferred into a new tube. For preparation of thylakoid fractions, the crude extract was diluted in 2 volumes of thylakoid buffer and membranes were pelleted at 16000xg, 4 °C, for 30 min. The thylakoid pellet was washed once more in thylakoid buffer and resuspended in a small volume of it. Proteins from both total and membrane fractions were solubilized with 2 % LDS and 100 mM DTT at room temperature for 1 hour and subsequently denatured at 80°C for 1 min. Non soluble material was removed by centrifugation at 16000xg for 10 min. Total protein concentration in the samples was measured with Amido Black staining (Schaffner and Weissmann, 1973).

The protein samples were loaded on a Tris-tricine SDS-Polyacrylamide gel (Schagger and von Jagow, 1987) with the desired acrylamide concentration and, afterwards, proteins were transferred to PVDF membranes (Ihnatowicz et al., 2004). After blotting, membranes were saturated with 5 % milk proteins dissolved in 1x TBS-T (150 mM NaCl, 10 mM Tris pH 8.0, 0.1 % v/v Tween20) and saturated membranes were incubated overnight at 4°C with the specific primary antibody diluted in TBS-T containing 5 % milk proteins. After removal of the primary antibody and 3 washing steps in TBS-T (10 min each), membranes were incubated for 1 hour with the corresponding secondary antibody, diluted in TBS-T containing 5 % milk proteins, conjugated with horseradish peroxidase. Detection of the horseradish peroxidase signal was performed using the Pierce ECL Western Blotting Substrate kit (Thermo Scientific, Rockford, USA).

### 2.8.2. Blue-Native analyses of thylakoid protein complexes

For native electrophoretical separation of thylakoid complexes, *Synechocystis* thylakoid fractions were prepared as described above but all steps were performed on ice and protease inhibitors (1 mM ACA, 1 mM PMSF, 4 mM benzamidin) were added to the thylakoid buffer.



Chlorophyll concentration of thylakoid suspensions was then measured as follows: 5  $\mu\text{l}$  of each sample were diluted 1:200 in 80 % acetone and incubated in the dark at  $-20\text{ }^{\circ}\text{C}$  for 30 min. Membrane debris were pelleted at  $16000\times g$  for 10 min. Absorbance at 663 nm was measured and the chlorophyll concentration was calculated with the formula:  $C = A_{663} \times \text{dil. factor} / 86.86$ .

50  $\mu\text{g}$  of chlorophyll for each sample were washed and resuspended to a final concentration of 0.5  $\mu\text{g}/\mu\text{l}$  in thylakoid buffer containing 1 % n-Dodecyl- $\beta$ -D-Maltoside. Solubilisation was performed on ice at  $4\text{ }^{\circ}\text{C}$  with gentle shaking for 50 min, followed by 10 more min at room temperature. Insoluble material was pelleted by centrifugation at  $16000\times g$ ,  $4\text{ }^{\circ}\text{C}$ , for 30 min and supernatant was then mixed with 0.1 volumes of Coomassie loading solution (750 mM aminocaproic acid, 5 % Coomassie-G). Thylakoid protein complexes were separated on a Blue-Native PAGE (gradient gel, 4-12 % polyacrylamide) (Schagger et al., 1988). After 12 hours of run, the blue cathode buffer (50 mM Tricine, 15 mM Bis-Tris pH 7.0, 0.02 % Coomassie-G) was replaced with fresh buffer without Coomassie-G. Anode buffer (50 mM Bis-Tris pH 7.0) was replaced as well with fresh one. After the run, gel stripes corresponding to single samples were incubated for 20 s in a denaturing buffer (6 % SDS, 200 mM  $\text{Na}_2\text{CO}_3$ , 3 %  $\beta$ -mercaptoethanol) and proteins separated in the second dimension by SDS-PAGE (15 % polyacrylamide gel (Shapiro et al., 1967)). 2D gel was stained with Colloidal Coomassie staining (10 % ammonium sulfate, 0.1 % Coomassie G-250, 3 % orthophosphoric acid, 20 % Ethanol) and destained with water.

### 2.8.3. *In vivo* translation assay

For *in vivo* radioactive labelling of thylakoid proteins, *Synechocystis* liquid cultures in the exponential growth phase were used. Equal amount of cells, based on the  $\text{OD}_{730}$ , were harvested by centrifugation at  $4500\times g$  for 10 min and then resuspended in BG11 supplemented with 5 mM glucose to a final  $\text{OD}_{730}$  corresponding to 300  $\text{ng}/\mu\text{l}$  of chlorophyll *a* in the wild type sample. The same volume of the wild type was used for the other samples. The samples were incubated for 1 hour under normal growth conditions ( $30\text{ }\mu\text{mol m}^{-2}\text{ s}^{-1}$  light intensities,  $30\text{ }^{\circ}\text{C}$ ), with shaking, then supplemented with 500  $\mu\text{Ci}/\text{ml}$  of  $^{35}\text{S}$ -Met and incubated for additional 30 min, in order to radiolabel newly translated proteins. Protein radiolabelling was terminated by 1 mM of non-radioactive Methionine and cells were then collected by centrifugation at  $4000\times g$ , for 10 min, in a centrifuge pre-cooled to  $4\text{ }^{\circ}\text{C}$ . Thylakoids fractions were prepared as described before, resuspended to a final concentration corresponding - in the wild type - to 0.5  $\mu\text{g}/\mu\text{l}$  of chlorophyll *a* and solubilised for 1 hour at

room temperature with 2 % LDS and 100 mM DTT. The same volume of the wild type was used for the other samples. The soluble fraction was obtained by centrifugation at 16000xg for 10 min at room temperature. Samples corresponding, in the wild type, to 15 µg of chlorophyll were loaded and separated on an SDS-PAGE gel with 12 % polyacrylamide. The gel was then stained with Colloidal Coomassie staining, dried and exposed to Storage Phosphor Screen (Fuji) and radioactive labelled proteins were detected with the Typhoon PhosphorImager (GE Healthcare, Munich, Germany).

## 2.9. Spectroscopic and fluorimetric analyses

### 2.9.1. P700 oxidation-reduction kinetics measurements

The photo-oxidation and dark-reduction kinetics of P700 were measured in intact cells using the  $A_{820}$  change, as described (Herbert et al., 1995). The  $A_{820}$  was monitored using the modulated Dual-PAM 100 detection system (Walz, Effeltrich, Germany). The instrument operated with a time constant of 20 ms. Samples for  $A_{820}$  measurements were prepared at room temperature by washing exponentially growing cultures with BG11 not supplemented with glucose and resuspending them to a final  $OD_{730}$  of 1. After 10 min of dark-adaption, the samples were placed in a quartz cuvette with 1 cm of path length into the Optical Unit ED-101US/MD mounted to Mounting Stand ST-101 with attached Measuring Heads DUAL-E and DUAL-DB. Inhibitors of electron transport were added to the samples prior to measurements to block different inputs of electrons to PSI, as has been done previously (Maxwell and Biggins, 1976; Herbert et al., 1992; Yu et al., 1993). Input from PSII was blocked with 25 µM DCMU. Input from the plastoquinone pool was blocked with 25 µM DBMIB. Stock solutions of the inhibitors were prepared to 1 mM in 1 % ethanol and then diluted 40x in the final samples. Mock treatment of the samples was performed, as a control, adding 1/40 of their final volume of 1 % ethanol prior to measurements. For the P700 measurements, modulated far red measuring light was used and samples were excited with white actinic light ( $100 \mu\text{mol m}^{-2} \text{s}^{-1}$  light intensities) for 3 sec, followed by a dark period of 5 sec. The P700 traces shown are representative of three independent experiments.

### 2.9.2. Bacterial whole-cell absorbance spectra

Absorbance spectra of whole *Synechocystis* cells were recorded using a spectrophotometer. Cells were harvested, washed and resuspended in BG11 liquid medium to a final  $OD_{730}$  of 0.5.

Their absorbance spectra were recorded between 350 and 750 nm and normalized to the light scattering at 730 nm.

### 2.9.3. Low temperature (77 K) fluorescence emission spectra

77K fluorescence was recorded using an in-house built spectrofluorometer. *Synechocystis* samples grown under different light intensities were used. Cells were harvested, washed and resuspended in BG11 liquid medium to a final OD<sub>730</sub> of 0.5, dark-adapted for 10 min and then rapidly frozen in liquid nitrogen. To investigate the stoichiometry of the PSI and PSII complexes, their fluorescence emission spectra under the Chl *a* excitation at 435 nm were recorded between 600 and 800 nm. Fluorescence emission peaks of PSI (720 nm) of the different strains were compared by normalizing the PSII emission peak (695 nm) to the one from WT.

### 2.10. Luciferase assay

Luciferase activity was induced by the addition of decanal, an analogue of the luciferase substrate luciferin, to the cyanobacterial suspension to a final concentration of 1 mM (from 50 mM decanal in methanol/water 50 %, v/v stock). The reaction was incubated for 15 min with mild shaking and then luminescence was measured with a microplate reader (Safire<sup>2</sup>; Tecan, <http://www.tecan.com/>) at room temperature. Luminescence values were related to the suspension optical density at 730 nm, also measured with the microplate reader. Each suspension was measured in duplicates and the assay was repeated twice with independently grown cultures.

For luciferase activity from agar plates, cells grown on solid medium were spread with the decanal solution and luminescence was detected with the FUSION FXT imaging system (Peqlab Biotechnologie GmbH, Erlangen, Germany).

### 2.11. TEM analyses

Transmission electron microscopy analysis of *Synechocystis* cells was performed in collaboration with Prof. Dr. Gerhard Wanner, Biozentrum der LMU, Planegg-Martinsried, Germany.

### 2.12. Database analyses and software tools

Gene models, mRNAs and gene sequences have been obtained from the NCBI (<http://ncbi.nlm.nih.gov/>), Cyanobase (<http://genome.kazusa.or.jp/cyanobase/>) and TAIR

(<http://arabidopsis.org>) databases. Nucleic acid sequence analysis and *in silico* manipulation was performed using the VectorNTI Advance 9.1 (Invitrogen) and BioEdit Sequence Alignment Editor ([www.mbio.ncsu.edu/bioedit/bioedit.html](http://www.mbio.ncsu.edu/bioedit/bioedit.html)) software. Chloroplast transit peptides of *Arabidopsis* proteins were predicted by consulting the TargetP database ([www.cbs.dtu.dk/services/TargetP](http://www.cbs.dtu.dk/services/TargetP)). Protein multi-alignments were performed using ClustalW (Thompson et al., 2002) and Boxshade ([http://ch.embnet.org/software/BOX\\_form.html](http://ch.embnet.org/software/BOX_form.html)).

### 3. RESULTS AND DISCUSSIONS

#### 3.1. Replacement of the *Synechocystis* PSI complex

The introduction of *Arabidopsis* PSI in replacement of the *Synechocystis* endogenous one was chosen as starting point for the project because of its high degree of conservation between the two organisms and, in general, along the green lineage. As already shown in Table 1.1, 11 genes must be replaced and 4 introduced *de novo* in order to introduce the *Arabidopsis* PSI in *Synechocystis*. The two largest PSI proteins PsaA and PsaB were exchanged in the first place. The PsaA and PsaB subunits originated through gene duplication (Kirsch et al., 1986) and are highly conserved even in organisms separated by a billion years of evolution, which is underlined by the high sequence similarity (about 80 %) in pairwise alignments with the *Arabidopsis* and *Synechocystis* proteins. Strongly conserved regions include the four cysteines (two each provided by *psaA* and *psaB*) that organize the iron-sulphur cluster (4Fe-4S) Fx, which is essential for functional electron transfer (Heathcote et al., 2003).

PsaA and PsaB are encoded by the plastidial tri-cistronic operon *psaA-psaB-rps14* in *Arabidopsis* and in all the higher plants and are under the transcriptional regulation of the light-responsive *psaA* promoter  $P_{psaA}$  (Chen et al., 1993; Lezhneva and Meurer, 2004). Accumulation of the *psaA/B* transcript is regulated in all higher plants and the amounts of PSI and PSII are transcriptionally modulated in a complementary manner according to changes in light quantity and quality (Allen and Pfannschmidt, 2000). The structure of the *psaA-psaB* operon in *Synechocystis* is similar to the *Arabidopsis* counterpart, but is di-cistronic as it lacks the *rps14* gene at its 3' end. The chloroplastic and the bacterial operon possess a number of common genetic regulatory elements since they are both transcribed and translated by a prokaryotic machinery. The *Synechocystis*  $P_{psaA}$  promoter also displays a light-dependent functional regulation that probably involves regulatory components mediating the signalling from photoreceptors (Herranen et al., 2005). Moreover, the *psaA* and *psaB* genes are separated in both organisms by an intergenic region (A/B IR) whose low divergence throughout the photoautotrophs lineage suggests the retention of cis-acting elements similar to those involved in prokaryotic translation initiation (Peredo et al., 2012). Indeed, the two intergenic regions have slightly different sizes (26 bp in *Arabidopsis*, 246 bp in *Synechocystis*) but both contain a Shine-Dalgarno sequence that promotes translation in prokaryotes.

Although the *psaA-psaB* regulatory elements are partially conserved between *Synechocystis* and *Arabidopsis*, they diverged during evolution in order to adapt to the different cellular and

external environments of higher plants. Therefore, in order to avoid perturbing the transcription and mRNA processing of the operon, only the PsaA and PsaB coding sequences of *Synechocystis* were replaced with the plant counterparts, maintaining the surrounding genetic elements (Figure 3.1A).

To prevent an inefficient translation of the introduced *Arabidopsis* genes, their coding sequences were optimized for heterologous expression in *Synechocystis* (OptimimGene™ algorithm, GenScript, Piscataway, U.S.A.). Different organisms show a different selective use of synonymous codons in encoding their proteins, called “codon usage”. Moreover, codon usage is different for each genome type and the main difference is the choice between codons ending in cytidine/guanosine or in adenosine/uridine. When comparing higher plants and cyanobacteria, chloroplastic genes preferentially contain codons ending in A/U, while most cyanobacteria contain C/G-endings (Campbell and Gowri, 1990). Besides codon usage bias, the algorithm used for *psaA-psaB* replacement also optimized the GC and GpC content and removed mRNA secondary structure, cryptic splicing sites, repeats and other undesirable transcript processing sites. In the obtained *Arabidopsis* synthetic genes, named *At psaA\_opt* and *At psaB\_opt*, the Codon Adaptation Index (CAI) was increased, respectively, from 0.42 to 0.94 and from 0.43 to 0.95.

### 3.1.1. Generation of the PSI core subunits PsaA and PsaB mutants

To generate a *Synechocystis* strain with a complete knockout of the PSI reaction core, glucose-tolerant wild type cells were transformed with the pDSAK1 vector, which led to the integration of the *nptI-sacB* double selection cassette in replacement of the endogenous *psaA* gene. Since absence of the PsaA protein prevents the assembly and accumulation of functional PSI complexes and causes a severe light-sensitivity and the inability to grow photoautotrophically, selection of the transformants was performed in Light Activated Heterotrophic Growth (LAHG) conditions as previously described by Anderson and McIntosh (1991). Selection of the transformants on agar medium supplemented with kanamycin yielded colonies with the integrated *nptI-sacB* cassette and the deleted *psaA* gene. The obtained *ΔpsaA* mutant was sequentially re-streaked on increasing antibiotic concentrations to achieve the complete segregation. This strain was used as a reference to investigate the effects of replacing the *Synechocystis* PsaA and PsaB proteins with the respective homologs from *Arabidopsis thaliana* and, more specifically, to determine whether the plant proteins could lead to the assembly of a functional PSI. A mutant was generated in which both the *Syn psaA* and *psaB* coding sequences were replaced by the *At psaA\_opt* and *At psaB\_opt* synthetic

genes. In this mutant, called *AB\_opt*, the synthetic coding sequences replaced the endogenous ones.

The *AB\_opt* mutant was generated stepwise. The glucose-tolerant wild type *Synechocystis* strain was initially transformed with the pDSAB\_opt vector in order to substitute the entire *psaA/B* operon. Selection of the transformants on kanamycin was performed in normal light, in order to select for a light-tolerant phenotype, but still on BG11 medium containing glucose. In the obtained transformants the *nptI-sacB* double selection cassette downstream of the operon and the *At psaB\_opt* gene could be detected, but not *At psaA\_opt* (data not shown). PCR on genomic DNA and sequencing of the obtained amplified fragments revealed that the first homologous recombination occurred through the *psaA/B* intergenic region and the *psaB* downstream region, thus leading only to the replacement of the *Syn psaB* gene. The reason why the *At psaA\_opt* gene was not integrated properly can be explained by the length of the entire synthetic operon (~5 kb) and by the presence of the homologous intergenic region (*A/B IR*) separating the desired recombination site and the *nptI* positive marker. The obtained mutant (*B\_opt<sup>kanR</sup>*) was used as background for the subsequent replacement of *Syn psaA*. *B\_opt<sup>kanR</sup>* was transformed with the plasmid pAB1 in order to excise the *nptI-sacB* cassette and to obtain a marker-less strain. After a recovery of 5 days, transformants lost all *sacB* copies and selection on 5 % sucrose yielded markerless mutants, called *B\_opt*. Transformation of *B\_opt* was performed using the pDSA\_opt vector in order to replace *Syn psaA* with the artificial homolog *At psaA\_opt*, this time introducing the *nptI-sacB* cassette upstream of the operon. The endogenous *psaA* promoter, placed between the cassette and the recombinant gene, could have caused an undesired recombination as *A/B IR* did in the case of pDSAB\_opt, even if its smaller size would correlate with a lower probability of recombination. Anyway,  $P_{psaA}$  was kept in order to allow expression of the introduced *At psaA\_opt* also before removal of the double selection cassette. Indeed, selection on kanamycin yielded colonies still able to grow in full light and harbouring the entire *At psaA/B\_opt* synthetic operon. Complete segregation of the mutant, *AB\_opt<sup>kanR</sup>*, was confirmed by PCR and subsequent removal of the double selection cassette was performed via transformation with the pAB2 vector. Cells that still contained *nptI-sacB* were negatively selected on 5 % sucrose while the surviving transformants constituted the *AB\_opt* mutant strain. These mutants were, as those of all the previous recombination steps, still bluish, but not light sensitive like the  $\Delta psmA$  knockout strain and they could grow under normal light conditions (Figure 3.1C). To confirm correct segregation of the genotypes in the  $\Delta psmA$ , *AB\_opt<sup>kanR</sup>* and *AB\_opt* mutants, genomic PCR was performed using six primer pairs (Figure

3.1B). In the wild type strain, the primer pairs P1+P2 and P3+P4 generated amplicons spanning the *Syn psaA-psaB* intergenic region and the *Syn psaA* and *Syn psaB* genes, respectively. None of these PCR products were detectable in the two replacement strains, confirming that they had lost both the endogenous genes, while only primers P3+P4 generated an amplicon in  $\Delta$ *psaA* that still retained *Syn psaB*. Primer pair P5+P6 amplified the *nptI-sacB* selection cassette from the  $\Delta$ *psaA* and *AB\_opt*<sup>kanR</sup>, but not *AB\_opt*, genomes. The region spanning the *At psaB\_opt* gene and its downstream region could be amplified, combining primers P7 and P8, in the *AB\_opt*<sup>kanR</sup> and *AB\_opt* mutants, as well as the amplicon spanning the *At psaA\_opt* and *At psaB\_opt* recombinant genes (primer pair P9+P10). The primers P11 and P12 generated a PCR product covering the *At psaA\_opt* 5' end and its upstream genomic region in the *AB\_opt* mutant strain, confirming the complete excision of the *nptI-sacB* cassette. In the case of *AB\_opt*, partially overlapping amplicons covering the whole integrated synthetic operon, including the upstream and downstream flanking sequences, were also sequenced to confirm its accuracy.

### 3.1.2. Molecular analysis of the PSI core mutants

The growth phenotypes of the  $\Delta$ *psaA*, *AB\_opt*<sup>kanR</sup> and *AB\_opt* mutant strains were analyzed by spotting them on BG11-agar plates under different selective and trophic conditions (Figure 3.1C). The  $\Delta$ *psaA* mutant displayed resistance to kanamycin, deriving from the integrated *nptI* resistance gene, but, being PSI-deficient, it only grew under LAHG conditions. In LAHG, bacteria are grown heterotrophically in presence of 5 mM glucose, in the dark except for a single short exposure to dim light every 24 h, which is necessary to maintain the circadian rhythm and ensure normal progression through the cell cycle. Being an obligate heterotroph and light-sensitive,  $\Delta$ *psaA* was unable to grow neither in continuous bright light nor without glucose. The *AB\_opt*<sup>kanR</sup> mutant was also resistant to kanamycin while *AB\_opt* was sensitive to the presence of the antibiotic. Interestingly, both the mutants containing the *psaA* and *psaB* optimized genes from *Arabidopsis* were not light sensitive and were partially able to grow photoautotrophically on BG11 agar plates containing no sugar. Although in these conditions they could grow only at a much slower rate (see Figure 3.1C) than the wild type, this suggested that the *At PsaA* and *At PsaB* proteins could partially replace the function of the *Synechocystis* homologs, at least to the extent of restoring light tolerance and the ability to grow photoautotrophically. Moreover, the presence of the same phenotype in both replacement mutants indicated that the *nptI-sacB* cassette upstream of the *P<sub>psaA</sub>* promoter in *AB\_opt*<sup>kanR</sup> did not influence the operon function.



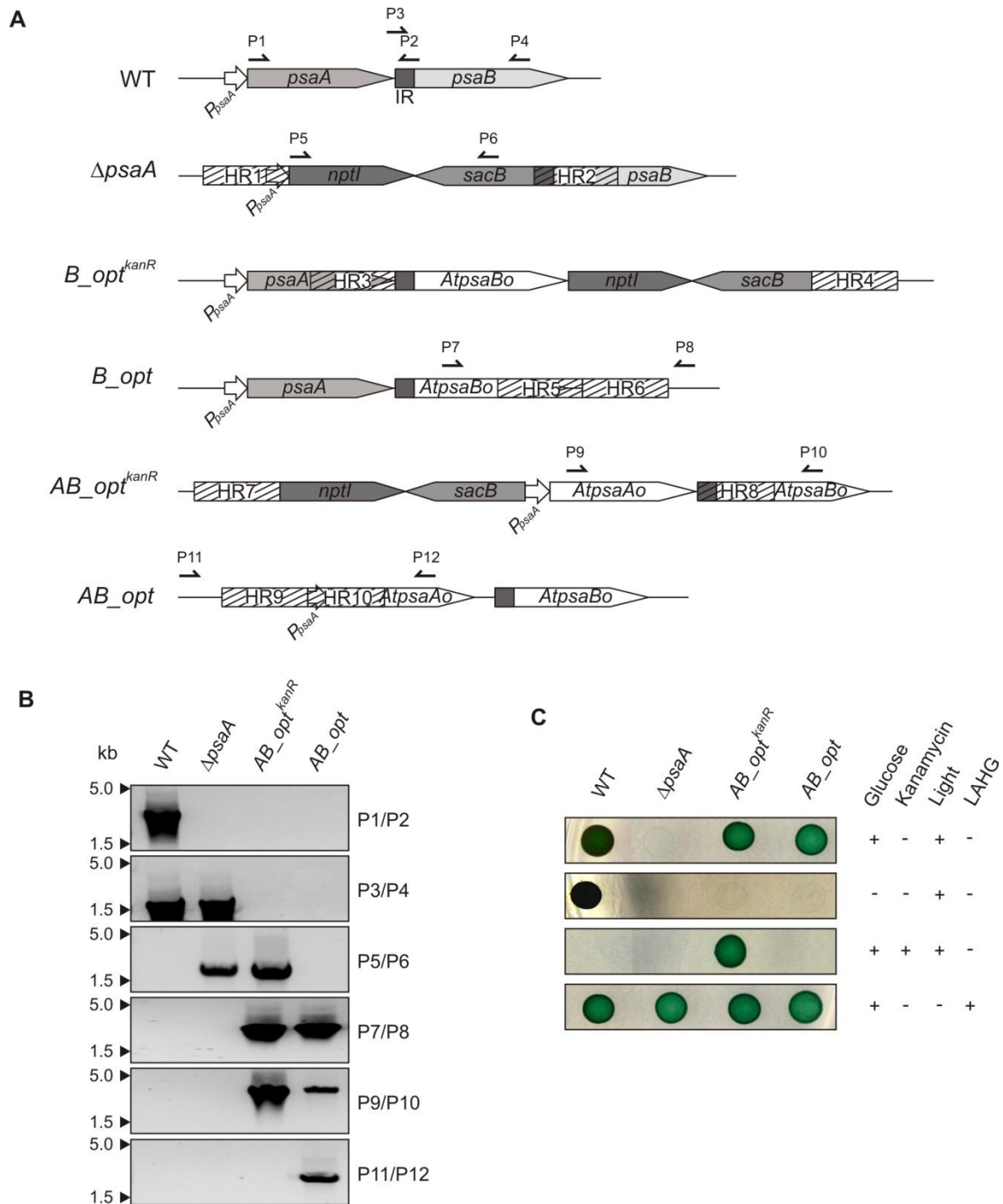


Figure 3.1 Analysis of the *psaA-psaB* mutant strains

(A) Schematic depiction of the mutant strains after the subsequent transformation steps. The genomic regions used for targeted homologous recombination are highlighted at each step (HR1-10). Annealing sites of the primers used for genotyping (P1-12) are indicated.

(B) Complete segregation of the *Synechocystis*  $\Delta$ *psaA*,  $AB\_opt^{kanR}$  and  $AB\_opt$  strains generated by the genetic manipulations represented in (A). Note that  $B\_opt^{kanR}$  and  $B\_opt$  are not shown because they already constituted the background genotypes of the  $AB\_opt^{kanR}$  and  $AB\_opt$  mutants shown here.

(D) Drop test of  $\Delta$ *psaA*,  $AB\_opt^{kanR}$  and  $AB\_opt$  mutants on selective media. Liquid cultures at an  $OD_{730}$  of 0.4 were washed with BG11 without glucose and spotted (15  $\mu$ l each) onto BG11 medium containing either 100  $\mu$ g/ml kanamycin or no selection. When tested for light sensitivity, cells were grown mixotrophically, in

continuous light at  $30 \mu\text{mol photons m}^{-2} \text{ s}^{-1}$  on BG11 supplemented with 5mM glucose. When tested for autotrophic growth, cells were grown in continuous light at  $30 \mu\text{mol photons m}^{-2} \text{ s}^{-1}$  on BG11 without glucose. When grown in Light Activated Heterotrophic Growth (LAHG) conditions, the cells were incubated in the dark on BG11 supplemented with 5 mM glucose, and exposed to light for 5 min every 24 hours.

The growth phenotype of the *Synechocystis* mutants with the *At psaA* and *At psaB* optimized genes replacing the endogenous counterparts suggested that the introduced recombinant genes were functional at least to some extent, because their presence was sufficient to partially rescue the PSI-deficient phenotype of  $\Delta\textit{psaA}$ . Expression of the cyanobacterial and plant PSI core genes was analyzed by Northern blot in the wild type,  $\Delta\textit{psaA}$  and *AB\_opt* strains (Figure 3.2A). When hybridizing the filters with the *Syn psaA* and *Syn psaB* radiolabelled probes, the target transcripts were detected only in WT. In both cases, a 5 kb and a 2.2 kb band, corresponding to the unprocessed *Syn psaA-psaB* and to the processed *Syn psaA* or *Syn psaB* transcripts, respectively, were present, as already reported in literature (Herranen et al., 2005). The probes hybridized neither to the *AB\_opt* nor to the  $\Delta\textit{psaA}$  RNA sample, which confirms that disruption of the *psaA* gene prevents also transcription of *psaB*. On the contrary, the *At psaAo* and *At psaBo* probes hybridized to the *AB\_opt* RNA sample, thus confirming that the two plant genes were transcribed in this mutant strain. Moreover, two bands (of 5 and 2.2 kb, respectively) were present in both cases as it was shown for the endogenous counterparts, demonstrating that the replacement operon could be transcribed and the mRNA was correctly processed. The abundance of the *At psaA\_opt* and *At psaB\_opt* transcripts could not be quantified and compared with that of the endogenous ones in WT, because of the different hybridization efficiencies of the probes.

Although the plant genes were transcribed in the *AB\_opt* strain, it was not possible to detect the corresponding proteins when performing immunoblot analysis on total or thylakoid protein fractions. Failure to detect At PsaA and At PsaB proteins could either be explained by a drastically lowered translation rate or by an increased instability of the synthesized polypeptides.

In order to identify the cause for the absence of At PsaA and At PsaB, *in vivo* pulse labelling of proteins from WT,  $\Delta\textit{psaA}$  and *AB\_opt* strains was performed. Cells were incubated for 30 min in light in the presence of  $^{35}\text{S}$ -Methionine that was incorporated into newly translated proteins. After the incubation period, *de novo* synthesized thylakoid proteins were isolated and separated on a denaturing polyacrylamide gel. Prior to loading, samples were adjusted according to the  $\text{OD}_{730}$  of the initial cell suspensions. Equal loading was confirmed by Coomassie staining of the gel and, in the wild type, positions of the PsaA and PsaB proteins

were assigned according to previous immunodecoration results (data not shown), while D1 and D2 core subunits of PSII were annotated referring to Ossenbühl et al. (2006).

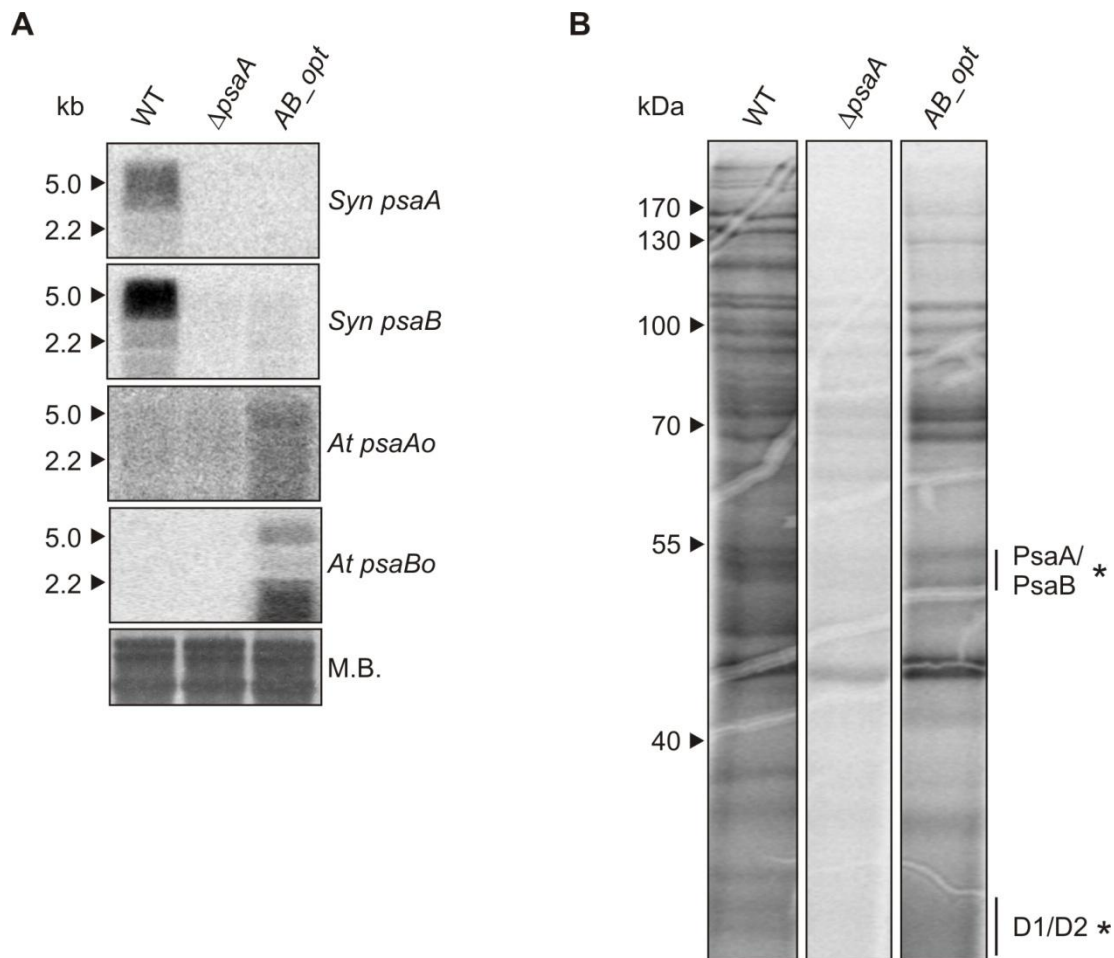


Figure 3.2 Expression and translation analysis in the *psaA-psaB* strains

(A) Northern blot analysis of *Synechocystis* *psaA* and *psaB* genes and of the recombinant *Arabidopsis* optimized homologs (*At psaAo* and *At psaBo*, respectively) in the WT,  $\Delta$ *psaA* and *AB\_opt* strains. 20  $\mu$ g of RNA were loaded for each lane and equal loading was verified by methylene blue staining of the membrane. The probes covered the entire sequences of the target genes. Hybridization was performed at 60 °C, according to the Materials and Methods.

(B) Protein synthesis in the WT,  $\Delta$ *psaA* and *AB\_opt* strains. Newly synthesized thylakoid proteins were isolated from cell suspensions after 30 min incubation with  $^{35}$ S-Met under 30  $\mu$ mol m $^{-2}$  s $^{-1}$  light intensities. First, proteins were fractionated by SDS-PAGE. Then, the gel was stained with coomassie and dried. Signals of *de novo* synthesized proteins were detected by autoradiography. Expected sizes of the PsaA/PsaB and D1/D2 proteins are indicated with asterisks (\*).

The autoradiogram of the gel (Figure 3.2B) showed a drastic reduction of the protein synthesis rate in the  $\Delta$ *psaA* knockout mutant with respect to the WT, although the amount of proteins loaded on the gel was equal for all three genotypes. The overall protein translation rate of membrane proteins in the *AB\_opt* mutant was higher than in the PsaA knockout strain but lower than in the wild type. The presence of newly translated PsaA and PsaB *Arabidopsis*

proteins could not be unambiguously determined due to a lack of precise information about electrophoretic mobility of the different membrane proteins.

Although it could not be clarified that synthesis and accumulation of the *Arabidopsis* PSI core proteins took place in the replacement mutant, the presence of *At psaA\_opt* and *At psaB\_opt* transcripts lead to a partial rescue of the drastic *ΔpsaA* translational impairment shown in Figure 3.2B. These preliminary results were consistent with the growth phenotypes of the analyzed strains.

To investigate the effects of the genetic manipulations in *ΔpsaA* and *AB\_opt* on the assembly and accumulation of the membrane protein complexes, BN-PAGE analysis was performed. Thylakoid membranes were solubilised with  $\beta$ -DM and photosynthetic complexes were fractionated by Blue Native PAGE. Six major bands, representing the PSI supercomplexes, trimeric PSI, dimeric PSI, dimeric PSII/ATPase, monomeric PSI, and monomeric PSII, were detected in the WT (Figure 3.3A, left panel) and annotated according to available literature (Herranen et al., 2004; Yao et al., 2011). It has to be noted that the bands representing PSI complexes are the only green ones, as chlorophyll *a* is mainly associated to photosystem I in *Synechocystis* (Fujita et al., 1988). Blue Native gels were stained with Coomassie in order to visualize pigment-less and low-abundant complexes (Figure 3.3A, right panel). The unstained and the Coomassie-stained BN PAGES revealed that all PSI complexes and supercomplexes were absent in *ΔpsaA*, while PSII and ATPase complexes were still present in wild type-like amounts. Instead, two additional chlorophyll-containing complexes could be identified in the *AB\_opt* mutant strains (indicated by the asterisks). The two additional complexes migrated similarly into the BN PAGE compared to the PSI dimer and the PSI supercomplexes of the wild type sample. No PSI trimer - the most abundant PSI supercomplex in the wild type - , could be identified in the PSI-core replacement mutant. The observed differences in the photosynthetic complexes corresponded to changes in the *in vivo* absorption spectra of the analyzed strains (Figure 3.3B). In *ΔpsaA* the absorption peaks of Chl *a*, at 438 and 681 nm, were essentially absent and also the peak corresponding to phycocyanin (PC) was reduced with respect to the wild type. In the *AB\_opt* strain, the PC peak was higher than in *ΔpsaA*, although it was still lower than in WT. Notably, the replacement mutant accumulated to a certain extent also chlorophyll, thus confirming that the additional complexes observed in the BN-PAGE were associated with the pigment. The markedly reduced Chl *a*/PC ratios accounted for the blue colour of both mutant strains.

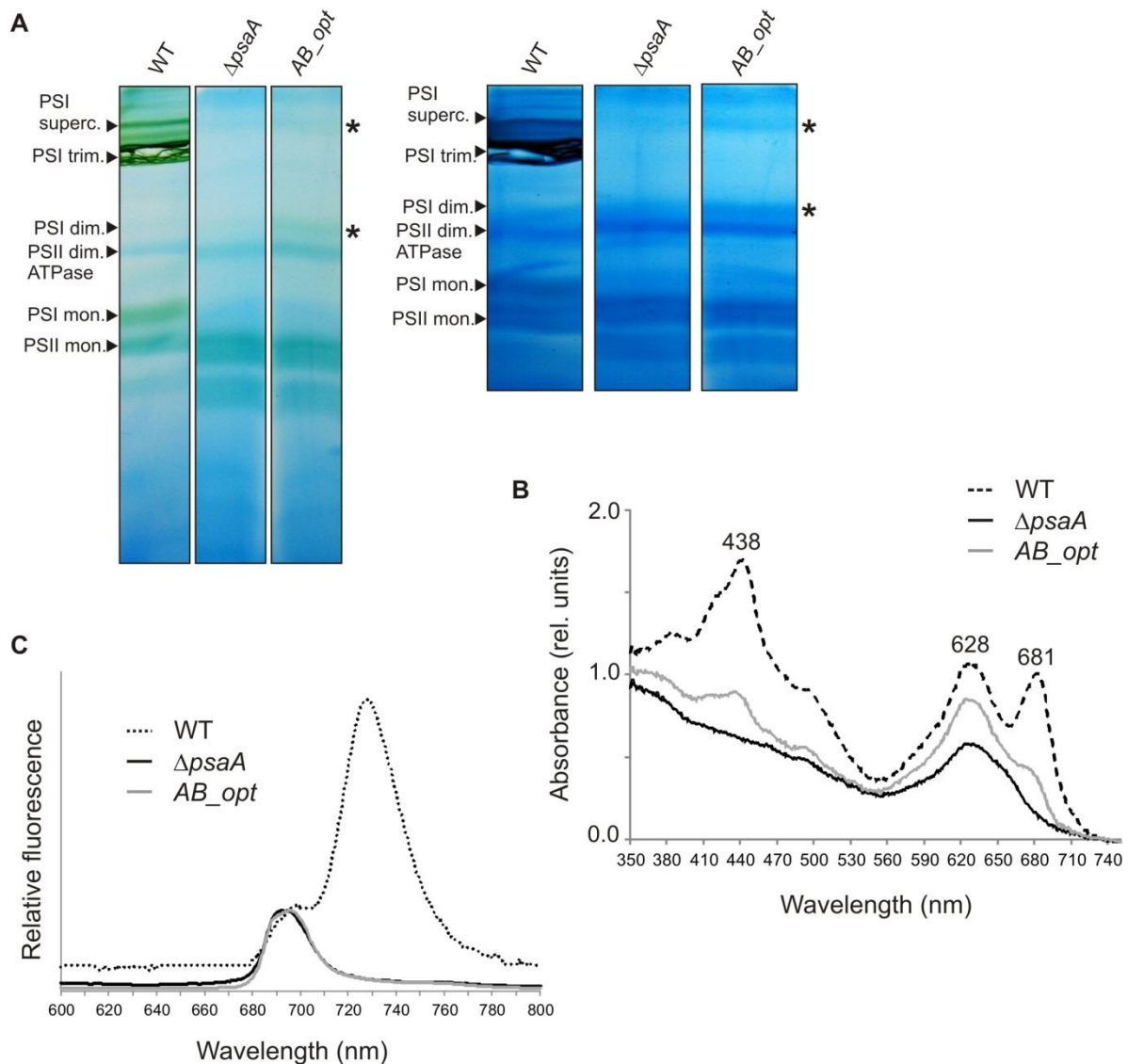


Figure 3.3 Analyses of photosynthetic complexes in the WT,  $\Delta psaA$  and  $AB\_opt$  strains

(A) Blue native analyses of thylakoid membranes. Thylakoid membranes were isolated and then solubilised with  $\beta$ -DM (1 %). Protein preparations corresponding to 50  $\mu$ g chlorophyll *a* were fractionated on BN gels (4-12% gradient). Blue Native gels were stained with coomassie (R250) to visualize complexes containing no chlorophyll-binding proteins.

(B) *In vivo* absorption spectra of *Synechocystis* WT,  $\Delta psaA$  and  $AB\_opt$  strains. The peaks at 438 and 681 nm correspond to the maxima of Chl *a* absorption, the peak at 628 nm corresponds to the absorption maximum of PC. The spectra were normalized to the absorbances at 730 nm.

(C) Steady-state fluorescence emission spectra at 77 K. Cell suspensions were adjusted to an  $OD_{730}$  of 0.5 and dark-adapted for 10 min prior to freezing. Fluorescence emission spectra were measured by exciting cells at 435 nm and were normalized to the PSII emission peak at 695 nm. The curves are representative of two repetitions.

In the attempt to detect the presence of PSI with an independent experiment, fluorescence emission spectra of the two photosystems at low temperature (77 K) were measured in cell suspensions of the WT,  $\Delta psaA$  and  $AB\_opt$  *Synechocystis* strains (Figure 3.3C). Chlorophyll *a* was excited with light at 435 nm and the recorded fluorescence emission was normalized to the PSII emission peak at 695 nm. Three main peaks were present in the WT sample; two

originating from PSII, at 685 and 695 nm, and one at 725 nm which corresponds to PSI (Murakami, 1997). As expected, PSI fluorescence at 725 nm was higher than PSII fluorescence at 695 nm, because the PSI/PSII ratio varies from about 1 to almost 4 in *Synechocystis* depending on the growth light conditions. Despite the observed differences in their photosynthetic complex composition (Figure 3.3A), the *ΔpsaA* and *AB\_opt* mutants showed comparable fluorescence emission spectra. Both displayed the 685 and 695 nm emission peaks deriving from the PSII-associated chlorophyll *a* molecules but no PSI fluorescence emission could be observed. Based on the absence of PSI fluorescence emission, the *Synechocystis AB\_opt* mutants appear not to accumulate any functional PSI reaction centre.

### 3.1.3. Discussion: *Arabidopsis* PsaA and PsaB can partially complement the function of the *Synechocystis* homologs

Among the two photosystems characterizing all the photo-oxygenic organisms, PSI is more conserved between cyanobacteria and higher plants. PSI is responsible of transferring electrons from plastocyanin, located on the luminal side of thylakoids, to ferredoxin on the stromal side. Although core components and structures of the cyanobacterial and chloroplast PSI complexes are similar, some differences exist between them. In cyanobacteria, PSI is normally trimeric and each monomer consists of 12 protein subunits, whereas that of plants is composed of at least 15 subunits and mainly exists as a monomer associated with thylakoid-embedded light-harvesting proteins. Four out of 15 subunits (PsaG, PsaH, PsaN and PsaO) are newly evolved in chloroplasts, whereas one cyanobacterial subunit (PsaM) was lost in higher plants. PSI complex assembly is only poorly understood presumably because assembly intermediates cannot be readily identified. In recent years, forward and reverse genetic approaches provided a starting point for the study of PSI assembly, but the analysis of mutants with impaired accumulation of the complex is difficult in plants, where a complete PSI depletion is lethal. This aspect could be responsible for the failure to identify fundamental regulatory proteins required for the assembly and function of PSI. For this reason, together with the high homology level, photosystem I was chosen as the starting point to generate the *Synechocystis* platform having the photosynthetic machinery replaced by that of the flowering plant *Arabidopsis thaliana*.

As already reported in previous studies, knockout of the *psaA* and *psaB* genes prevents the assembly of any functional PSI complex in *Synechocystis*. Although these mutants are PSI-deficient, they can grow in Light Activated Heterotrophic Growth conditions, whereas the

mutation is lethal in both photoautotrophic and mixotrophic conditions. Indeed, PSI depletion was found to correlate with an extreme light sensitivity of the resulting mutants; this is observed both in *Anabaena variabilis* ATCC 29413 (Mannan et al., 1991) and *Synechocystis* sp. PCC 6803 (Smart et al., 1991; Smart and McIntosh, 1993). The same phenotype can be observed in the *ΔpsaA* mutant generated in the present study, where the *Syn psaA* gene is completely replaced by the *nptI-sacB* double selection cassette. This strain is characterized by a turquoise-blue colour, since most of chlorophyll *a* is associated with PSI in cyanobacteria. As expected, the *psaA* knockout causes a severe light sensitivity and the mutant's inability to grow in absence of glucose as energy supply.

The replacement of the *Synechocystis psaA* and *psaB* coding sequences with the optimized homologs from *Arabidopsis thaliana*, in the generated *AB\_opt* strain, results in a partial rescue of the described phenotype, at least regarding the light sensitivity. Indeed, *AB\_opt* cells are capable of growing under both LAHG and mixotrophic conditions, even if their colour still resembled that of *ΔpsaA*. The double replacement mutant is also able to grow photoautotrophically, but with slower growth rates under mixotrophic conditions. The fact that the mutant shows only partial complementation could not be traced back to a lack of transcription, because both plant genes were proven to be transcribed (Figure 3.2A). *At psaA\_opt* and *At psaB\_opt* transcripts accumulate in the mutant cells, with a wild type-like processing pattern which consists of a 5 kb *psaA-psaB* transcript and of the mature 2.2 kb transcripts, respectively.

Several attempts to express photosynthetic genes from higher plants in *Synechocystis* were carried out in former studies. The *psbA* gene from *Poa annua* was introduced into a *Synechocystis* mutant background strain missing all three *psbA* genes (*psbA1/2/3*). It could be shown that the corresponding plant PSII core protein accumulated in the *Synechocystis* mutant strain (Nixon et al., 1991). Instead, CP43 from spinach accumulated in cyanobacterial cells only when fused with the C-terminus of the endogenous *Synechocystis* counterpart, which is apparently necessary for its stability (Carpenter et al., 1993). In another study an Lhcb gene from pea was introduced into *Synechocystis* but the protein did not accumulate, because it was degraded (He et al., 1999). However, the full-length translated recombinant protein could be detected in low amounts by pulse labelling experiments.

In this study it cannot be unambiguously determined if the plant PsaA and PsaB full-length proteins are translated in *AB\_opt*, because annotation of protein bands in *in vivo* pulse labelling experiments (Figure 3.2B) was uncertain. Irrespectively of this, major changes in the general translation profiles of the analyzed strains are present. When comparing equal steady-

state amounts of thylakoid proteins, *de novo* synthesis is drastically reduced in the *ΔpsaA* knockout with respect with wild type, whereas in the *AB\_opt* replacement strain the overall translational rate is partially increased, but lower than in WT. Therefore, although the presence of the recombinant PsaA and PsaB proteins could not be demonstrated, several phenotypic differences were observed after introducing the two plant genes in *AB\_opt* which cannot be explained by their gene transcription alone (Figure 3.1C). The extreme sensitivity to photoinhibition of *Synechocystis* mutants depleted of PSI and of the associated chlorophylls has been proposed to originate from their inability to efficiently quench the electrons coming from PSII (Smart et al., 1991). Indeed, functional PSII and phycobilisome complexes assemble in unmodified amounts in the PSI-less strains (Figure 3.3A), suggesting that syntheses of these three complexes are independently regulated (Shen et al., 1993). Three possible electron acceptors for PSII have been proposed to act in strains lacking PSI: i) ferredoxin, which reduces NADP<sup>+</sup> (Arnon et al., 1981) ii) cytochrome oxidase, via the Cyt *b<sub>6</sub>f* complex, which is shared between photosynthesis and respiration in cyanobacteria (Sandmann and Malkin, 1984) iii) or a hydrogenase, which would reduce H<sup>+</sup> to hydrogen gas and has been purified from cyanobacteria (Ewart and Smith, 1989). According to these findings, the markedly reduced sensitivity to photoinhibition of the *AB\_opt* mutants (Figure 3.1C → drop test, growth in normal light) can be attributed to the presence of an electron acceptor for PSII not present in *Δpsa*. In the thylakoids of the knockout strain, all various PSI complexes and super complexes are completely missing, while the other complexes of the photosynthetic machinery are still present. In the mutant expressing the *Arabidopsis psaA-psaB* genes, two more complexes can in fact be detected in addition to those present in *Δpsa*. The greenish appearance of these novel complexes suggests their association with chlorophyll molecules and their sizes are comparable with those of the wild type PSI dimer and supercomplexes. Despite these strong suggestions of the presence of some chimeric PSI complex, the generated *Synechocystis* replacement mutant shows the same fluorescence emission spectrum as the PSI-less strain. Absence of the PSI fluorescence emission signal indicates that the additional thylakoid complex detected is not functional and reasons for this have to be investigated in future experiments.

In cyanobacteria, the PSI biogenesis starts with the formation of the large, heterodimeric PsaA/PsaB reaction centre. Subsequently, low molecular mass subunits are added to the core scaffold, beginning with the extrinsic subunits of the stromal ridge (PsaC, PsaD, and PsaE), which is involved in ferredoxin binding (Schöttler et al., 2011). Non-functionality of PSI hybrids could be due to a poor structural interaction of the recombinant plant-type core with



the low molecular mass cyanobacterial subunits, even if it has been shown that the 3D conformation of the conserved PSI subunits is virtually identical in higher plants and cyanobacteria (Amunts and Nelson, 2008). Either way, it is tempting to speculate that introduction of the other 13 *Arabidopsis* subunits in the *AB\_opt Synechocystis* mutant might possibly lead to the accumulation of a functional plant-type PSI. In fact, a synthetic operon encoding for the missing PSI mature plant proteins has already been constructed, to be introduced into the replacement strain (data not shown). A remarkable feature of PSI complex is that it contains an extremely high amount of non-protein components. Indeed, almost one third of its total mass consists of different co-factors, such as chlorophylls, carotenoids, phylloquinones and 4Fe-4S clusters. These co-factors are known to be fundamental for PSI complex function, but also for its structural integrity. One explanation for PSI instability can be that those co-factors are not properly associated with the apoproteins. The higher plant and cyanobacterial PSI complexes show a high homology level also in the coordination sites for the carriers of the electron transport chain chlorophylls and carotenes, that are conserved at nearly identical positions and orientations (Amunts and Nelson, 2009). It can therefore be almost certainly excluded that the observed lack of PSI function in the *AB\_opt Synechocystis* strain is caused by a defect in co-factors assembly. A more likely scenario is the lack of plant-specific factors required for the PSI biogenesis in *Synechocystis*. In plants, indeed, gene products have been identified by mutational analyses that may act as regulatory or scaffold proteins in the assembly of PSI. The conserved chloroplast proteins Ycf3, Ycf4, and Pyg7-1 (Ycf37 in *Synechocystis*) - along with specific cyanobacterial proteins like BtpA and RubA - appear to be involved in posttranslational steps of PSI assembly (Dühring et al., 2007). Although these factors show a remarkable degree of sequence similarity in cyanobacteria and chloroplasts, their inactivation has different consequences in the respective organisms (Chi et al., 2012). Therefore, the lack of functionality of the tentative chimeric PSI accumulating in the *Synechocystis AB\_opt* strain might be due to the absence, in the host organism, of one or more of the plant-specific forms of these factors. In order to investigate this, the first necessary step is to determine the subunit composition of the complex indentified in the *AB\_opt* mutant that could be used as a genetic background to screen for proteins that are needed for PSI functional assembly in *Arabidopsis thaliana*.



(A) Scheme of synCURT1 (149 aa) protein structure. The four predicted  $\alpha$ -helices (H1-4) and two transmembrane domains (TM) are indicated, together with the specific antibody recognition site.

(B) Sequences of *Arabidopsis* CURT1A, B, C and D and of synCURT1 were aligned using ClustalW (Thompson et al., 2002) and Boxshade. Conserved amino acids are highlighted by black boxes, whereas grey ones indicate closely related amino acids. Predicted chloroplast transit peptides of the plant proteins are indicated in lowercase letters and CURT1A and synCURT1 peptide sequences used for antibody generation are indicated in italics. The four predicted  $\alpha$ -helices (H1-4) and the two TMs (~, in bold characters) are also highlighted.

### 3.2.1. Generation of *Synechocystis* mutants with altered CURT1 protein levels

Unlike higher plants, the thylakoid membranes in cyanobacteria do not form grana: in *Synechocystis* they are organised in parallel layers converging in sites close to the plasma membrane. To investigate to which extent the CURT1 proteins have an impact also on cyanobacterial thylakoid architecture, mutants of the cyanobacterium *Synechocystis* with altered levels of the endogenous (synCURT1) or *Arabidopsis* (CURT1A) CURT1 protein were generated (Figure 3.5A). In fact, complete loss of synCURT1 seemed to have severe consequences for cell viability, because the attempt to obtain fully segregating knockout strains for synCURT1 failed. However, it was possible to generate both strains that express CURT1A either in addition (strain: *CURT1A*) or instead of synCURT1 (strain: *CURT1A syncurt1*).

The suicide vectors used to generate the mutants, pCURT1A and pCURT1Asyncurt1 respectively, were assembled using the Golden Gate cloning strategy. In both cases expression of the *Arabidopsis* CURT1A coding sequence, lacking the cTP, was driven by the strong *Synechocystis*  $P_{psbA2}$  promoter. In the *CURT1A* strain, the endogenous gene was introduced into the *slr0168* genomic neutral site, whereas it was used to directly replace the *Synechocystis* endogenous gene in *CURT1A syncurt1*. The fact that it was possible to achieve the complete segregation of *CURT1A syncurt1* indicates that *Arabidopsis* CURT1A can replace the function of the *Synechocystis* homolog to a certain extent.

Genetic backgrounds of the mutants were confirmed by PCR on genomic DNA (Figure 3.5B) and the synCURT1 and CURT1A protein accumulation by immunodecoration using the specific antibodies raised against the two protein homologs. As expected, both proteins were localized in the thylakoid protein fraction. Interestingly, the strain that expressed CURT1A in addition to endogenous synCURT1 expressed less synCURT1 than the wild type and less CURT1A than *CURT1A syncurt1* (Figure 3.5C). These differences suggest that *Synechocystis* might have mechanisms to prevent an excessive accumulation of CURT1 proteins, thus strengthening the hypothesis of their conserved function.

The growth rate of the two mutant strains, and in particular that of *CURT1A syncurt1*, was reduced with respect to wild type cells, indicating that the plant homolog is only partially able to complement *synCURT1* function (Figure 3.5D).

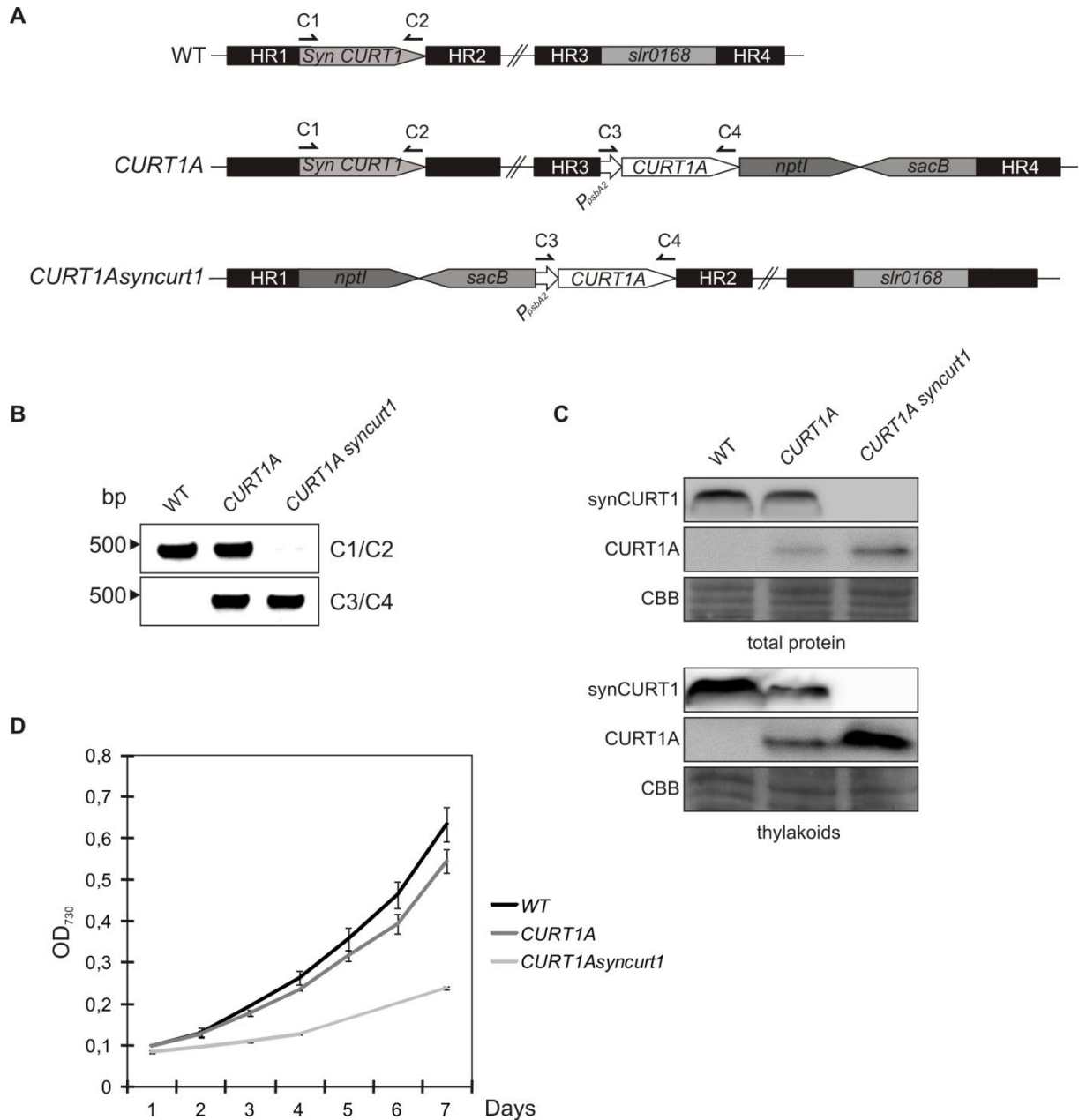


Figure 3.5 Analysis of the *CURT1* strains

(A) Scheme of the *CURT1A* and *CURT1A syncurt1* mutant strains. In *CURT1A* the *Arabidopsis CURT1A* coding sequence, lacking the cTP and placed under regulation of the *psbA2* promoter, is integrated in the neutral site *slr0168* while the endogenous *Syn CURT1* is intact. In *CURT1A syncurt1* the *Arabidopsis CURT1A* coding sequence, lacking the cTP and placed under regulation of the *psbA2* promoter, replaces the endogenous *Syn CURT1*. Annealing sites of the primers used for genotyping (C1-4) are indicated.

(B) Complete segregation of the generated *Synechocystis CURT1* strains, referring to the genetic manipulations represented in (A).

(C) Immunoblot analysis of *synCURT1* and *CURT1A* proteins in total protein and thylakoid fractions of WT and mutant strains. 15  $\mu$ g of protein were loaded for each lane.

(D) Growth rate analysis of WT and *CURT1* mutants grown in photoautotrophic conditions. Optical density at 730 nm was measured every 24 hours for 7 days and three independent cultures for each strain were used.

The thylakoid architecture of the obtained mutant strains was analysed by TEM and it revealed several changes caused by the altered *CURT1* levels (Figure 3.6). The thylakoids of the mutants did not form the typical ordered parallel sheets of the wild type *Synechocystis* cells: on the contrary, the layers were mostly spanning the cytoplasm in an unordered manner and no contact sites with the plasma membrane could be observed.

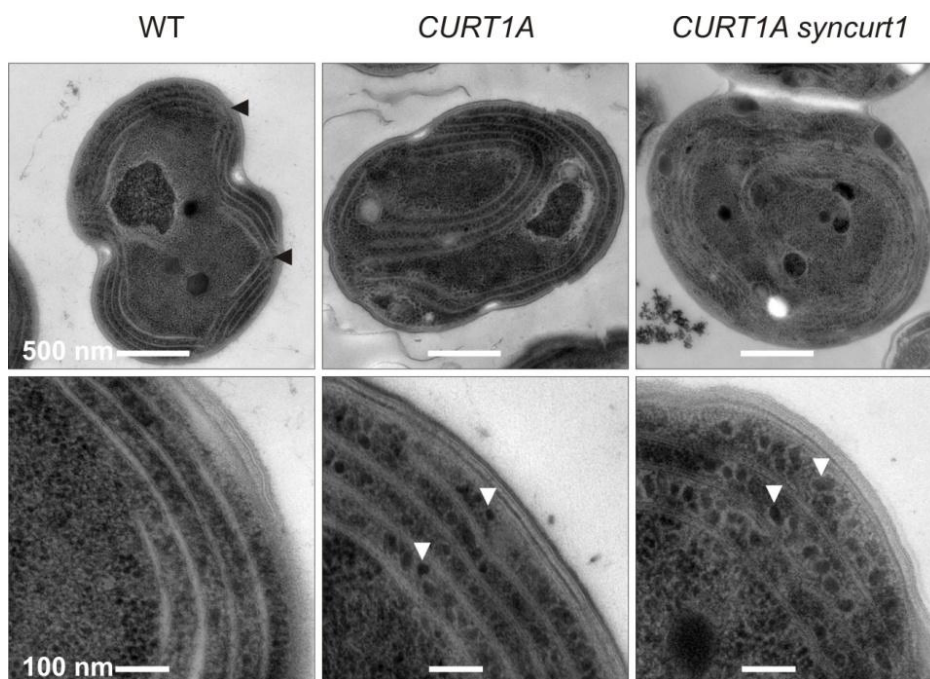


Figure 3.6 Analysis of thylakoid structure of *CURT1* mutants by TEM (Armbruster et al., 2013).

Thylakoid contact sites with the plasma membrane are indicated, in WT, by black arrowheads. Exemplary detached phycobilisomes are indicated by white arrowheads.

Moreover, instead of being smooth, the thylakoids presented a crumpled appearance with a decreased average lumen width (the wild type,  $23.8 \pm 2.9$  nm; *CURT1A*,  $19.5 \pm 1.5$  nm; *CURT1A syncurt1*,  $17.3 \pm 2.9$  nm;  $n > 30$  cells). Probably due to the unevenness of the membrane surface, the phycobilisomes, which in wild type cells are normally associated to the thylakoid membranes, were detached from the mutant thylakoids and could be seen as electron-dense spots in proximity of the membrane layers.

### 3.2.2. Knockout of phycobilisomes in *CURT1A syncurt1*

Given these results, it was tempting to speculate that, because this physical impediment represented by the phycobilisomes does also prevent the direct interaction of thylakoid

membranes, overexpression of CURT1 might actually succeed in inducing grana formation in *Synechocystis* strains without phycobilisomes. To verify this hypothesis, mutants were generated in which the allophycocyanin (AP)  $\alpha$  and  $\beta$  subunits, the main protein components of the phycobilisomes core discs, were knocked out. *ApcA*, *apcB* and *apcC* constitute a tricistronic operon in *Synechocystis* and their interruption was shown to lead to phycobilisome-deficient mutants lacking assembled antenna complexes (Ajilani et al., 1995). To generate the phycobilisome knockout mutants  $\Delta apc$  and *CURT1A syncurt1* $\Delta apc$ , WT and *CURT1A syncurt1* were transformed with the pSMapc vector (Figure 3.6A). Homologous recombination between the vector and the genome led to the replacement of the entire *apcA* and *apcB* coding sequences with the *SpecR* positive selection cassette. Complete segregation of the obtained  $\Delta apc$  and *CURT1A syncurt1* $\Delta apc$  mutants was confirmed by PCR on genomic DNA (Figure 3.6B) and by immunoblot analysis of synCURT1, CURT1A and AP  $\alpha$  and  $\beta$  proteins (Figure 3.6C). As previously reported (Ajilani and Vernotte, 1998), both mutant strains showed a greenish-olive colour and grew at a slower rate with respect to the wild type and these phenotypical traits were even stronger in the *CURT1A syncurt1* genotypical background.

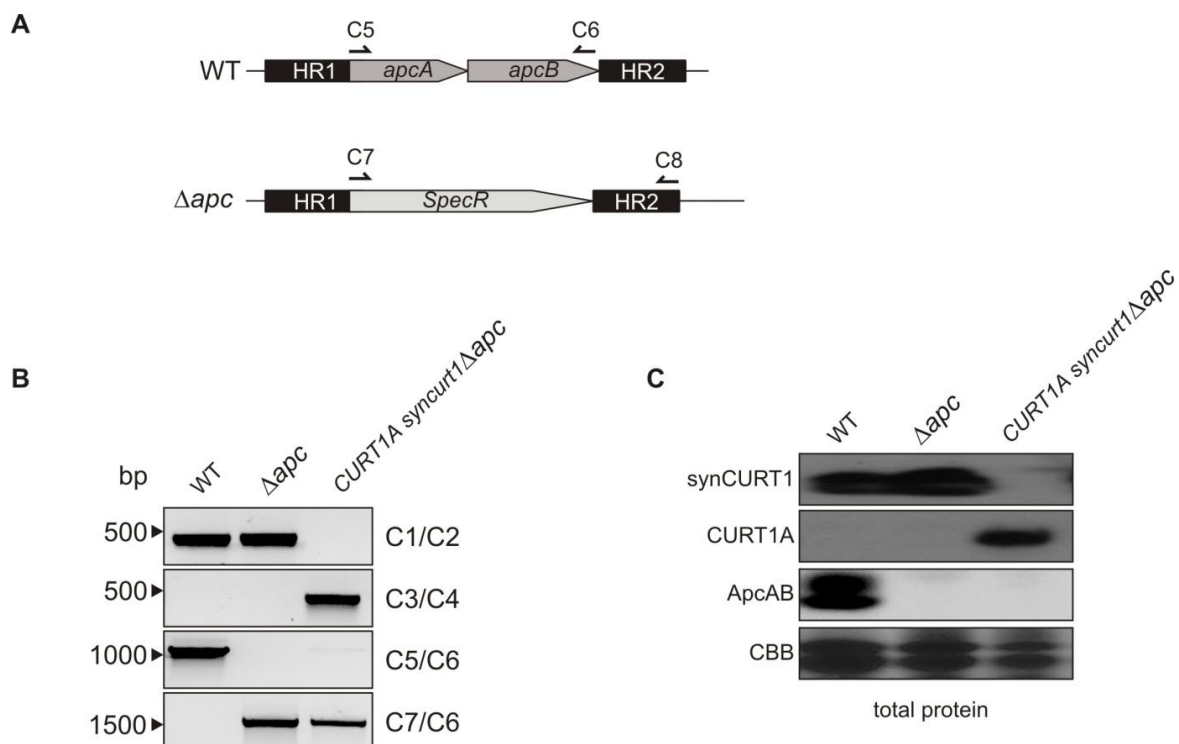


Figure 3.6 Analysis of the phycobilisome mutant strains  
 (A) Scheme of the  $\Delta apc$  gene manipulation. The *Synechocystis apcAB* operon is replaced by the *SpecR* selection cassette in  $\Delta apc$ . In *CURT1A syncurt1* $\Delta apc$ , the *apcAB* knockout is in the *CURT1A syncurt1* mutant background. Annealing sites of the primers used for genotyping (C5-8) are indicated.

(B) Complete segregation of the generated *Synechocystis*  $\Delta apc$  and *CURT1A syncurt1 $\Delta apc$  strains, referring to the genetic manipulations represented in (A).*

(C) Immuno-blot analysis of synCURT1 and CURT1A proteins in total protein fraction of WT and mutant strains. 15  $\mu$ g of protein were loaded for each lane.

The thylakoid architecture of the  $\Delta apc$  mutant strains was analysed by TEM. As previously reported (Collins et al., 2012), absence of phycobilisomes in the  $\Delta apc$  mutant strain caused a decrease in the long-range curvature of the thylakoids that did not necessarily follow the shape of the plasma membrane as they normally do in wild type cells (Figure 3.7). As expected, the electron-dense spots representing phycobilisomes were not present anymore in the mutant and this resulted in a diminished distance between the thylakoid layers, as a consequence of the lack of steric hindrance of the antenna complexes (Olive et al., 1997). The *CURT1A syncurt1* $\Delta apc$  mutant presented the same alterations of the membrane architecture as  $\Delta apc$ , but additional effects caused by altered levels of the CURT1 proteins were also present in this strain. The thylakoids of *CURT1A syncurt1* $\Delta apc$  appeared to be less crumpled than in *CURT1A syncurt1* but, at the same time, the layers were pronouncedly curved in a wavy-shape.

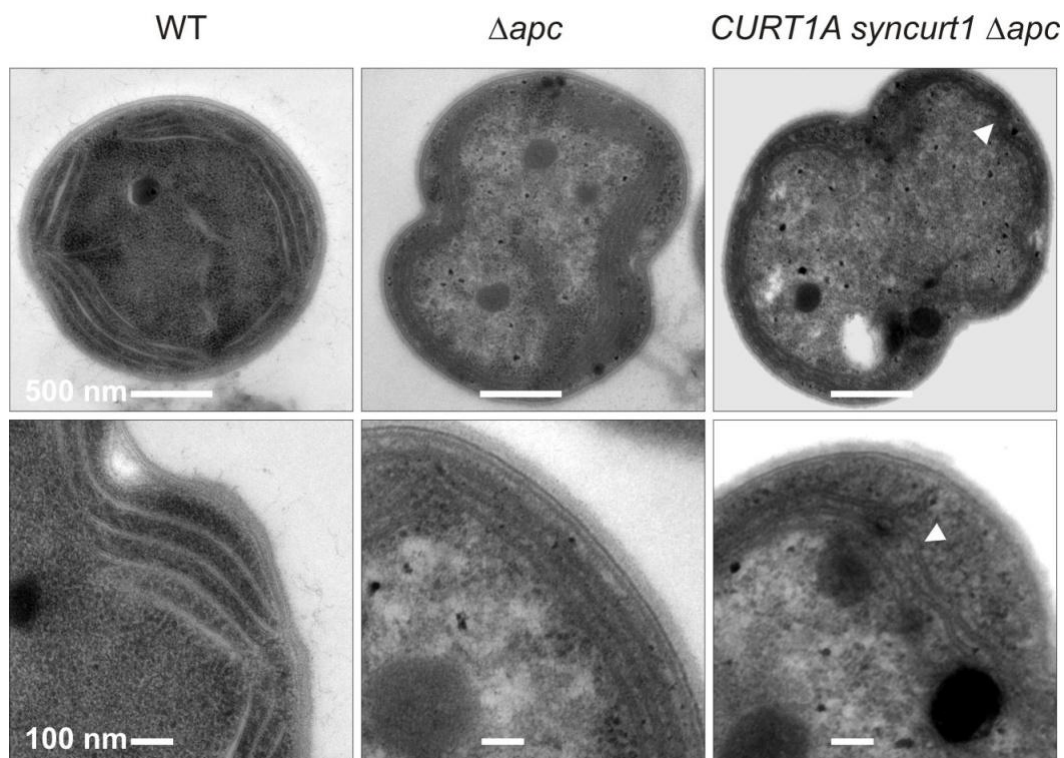


Figure 3.7 Analysis of thylakoid structure of  $\Delta apc$  mutants by TEM. Exemplary curvatures of thylakoid membranes are indicated, in *CURT1A syncurt1* $\Delta apc$ , by white arrowheads.

### 3.2.3. Discussion: *Synechocystis* and *Arabidopsis* CURT1 proteins have a conserved function in determining the thylakoid architecture

Taken together, the results suggest that CURT1 proteins have also a role in determining the architecture of thylakoid membranes in cyanobacteria, the evolutionary ancestors of plant chloroplasts. Conservation of the protein function throughout evolution is also supported by the fact that *Arabidopsis* CURT1A could partially replace *Synechocystis* CURT1.

Expression of *Arabidopsis* CURT1A in *Synechocystis* cells caused modifications in the thylakoid structure, although it was not possible to unequivocally clarify, whether the reduced levels of endogenous synCURT1 or the presence of the *Arabidopsis* protein itself were responsible for them. In either case, the crumpled appearance of thylakoids in the analysed mutants and the decrease in lumen width, determining an increased membrane curvature, led to detachment of phycobilisomes.

When the steric hindrance of phycobilisomes was abolished in the *CURT1A syncurt1Δapc* mutant thylakoid membranes resulted to be wave-shaped, with a smoother surface appearance compared to the background genotype. Although no grana-like structures could be detected, an increased membrane-bending ability could be observed when CURT1A was overexpressed in replacement of synCURT1 in the absence of phycobilisomes.

To better dissect the effects on CURT1A accumulation in *Synechocystis* cells, comparisons with the *syncurt1* knockout mutant should be done, also regarding the phycobilisome depletion.

### 3.3. Development of a single vector-based based strategy for marker-less gene replacement in *Synechocystis*

#### 3.3.1. Design of the strategy

In order to generate *Synechocystis* strains with one or all of the photosynthetic complexes replaced by their higher plant counterparts, many gene manipulations would be needed. As summarized in the introduction and shown in the previous experiments, marker-less gene replacement can be the technique of choice to achieve such results. Irrespective of the selection variant they rely on, marker-less gene replacement methods usually require the use of two subsequent transformation events, each of them with a different vector.

In order to minimize cloning and transformation steps, an alternative strategy was developed for marker-less gene replacement in *Synechocystis*, also using the *nptI-sacB* cartridge, in which, although two subsequent genomic recombination events still occur, a single bacterial



transformation event and a single vector are required (Viola et al., 2014). This is also the case of double recombination strategies that rely on a first integration of the whole vector into the target genomic sequence via single crossing-over, as in the case of allelic exchange (Laloti and Heath, 2001; Clerico et al., 2007). In this case, the second recombination, leading to the excision of the integrated vector, generates two populations of bacteria, one that reverts to wild type and one that keeps the desired mutation. Thus, screening of the population of the second recombinants by PCR needs to be done. The strategy developed in this study overcomes this step by leading to a final bacterial population exclusively composed of mutants.

In this method, schematically depicted in Figure 3.8, two subsequent homologous recombination events take place and two subsequent mutants, with knockout and replacement of the target gene respectively, can be obtained by simply growing the transformed cells under different selective conditions in a stepwise manner, without the need of a second transformation. The first recombination event leads to the integration of the construct, containing the DNA sequence to be introduced interrupted by the selection marker, into the cyanobacterial genome via double crossing-over; the second recombination, a single crossing-over, takes place in between direct repeats present in the integrated construct itself and causes excision of the double selection cassette and reconstitution of the introduced DNA sequence. In this way two subsequent mutants, with knockout and replacement of the target gene respectively, can be obtained by simply growing the transformed cells under different selective conditions in a stepwise manner. A double-recombination vector suited for this strategy includes several essential elements: (1) a replication origin for *E. coli* that is not functional in *Synechocystis*; (2) flanking sequences homologous to *Synechocystis* chromosomal sites to allow stable integration of the construct in the target genome (designated as HR1 and HR2); (3) the *nptI-sacB* double selection cassette, separating the two portions of the sequence to be integrated, that allow both positive and negative selection of the *Synechocystis* recombinants; (4) the exogenous gene of interest (GOI) to introduce, split in two partially overlapping (shaded box) segments divided by the *nptI-sacB* cassette; (5) a *Synechocystis* endogenous promoter to induce the expression of the introduced recombinant gene(s).

When *Synechocystis* cells are transformed with such a vector, the initial recombination event leads to the integration of the construct, containing the exogenous gene(s) to be introduced interrupted by the *nptI-sacB* cassette, into the cyanobacterial genome (Figure 1, upper panel) via double crossing-over between the two flanks of the construct, HR1 and HR2, and the

corresponding homologous sequences present in the cyanobacterial genome. Strains that have integrated the construct in this way contain the *nptI-sacB* cassette in the target locus and therefore can grow in the presence of kanamycin, which is used for their positive selection, but are sensitive to sucrose. Complete segregation of the first-round [“prim(ary)”] recombinants leads to loss of the endogenous target gene and, moreover, the integrated GOI is not functional because the *nptI-sacB* cassette interrupts its sequence.

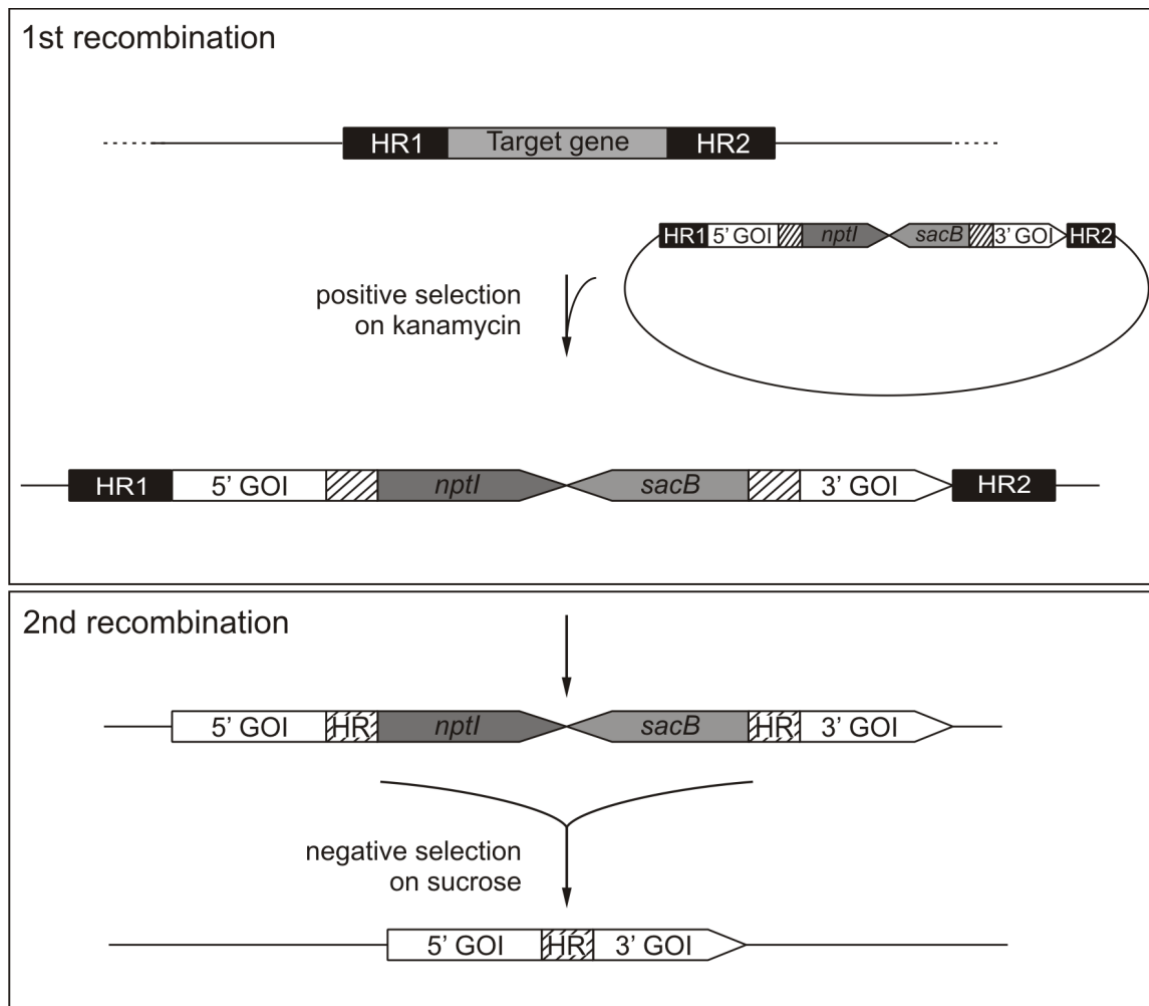


Figure 3.8 Schematic depiction of the single-step double recombination strategy (Viola et al., 2014). The first recombination step (upper panel), involving a double crossover between the homologous regions HR1 and HR2 of the vector and the genomic target sequence, leads to genomic integration of the construct. Note that the integrated gene of interest (GOI) is split into two parts, 5' and 3', the sequences of which partially overlap (shaded box). The 5' and 3' GOI segments are separated from each other by the *nptI-sacB* selection cassette, which renders the first recombinant mutants resistant to kanamycin and sensitive to sucrose. After complete segregation of the replacement under positive selection in the presence of kanamycin, which ensures the total elimination of the endogenous target gene function, release of the selective pressure allows the second recombination to take place (lower panel). In this step, a crossover involving the overlapping regions of the split GOI leads to the excision of the *nptI-sacB* cassette. Negative selection on sucrose yields colonies that have lost the entire *sacB* marker and carry the intact, functional GOI in place of the endogenous target gene.

After complete segregation, the positive selective pressure is released and the mutants are grown without selection in order to allow the second recombination event to occur (Figure 1, lower panel), without any transformation step being required. The second recombination event takes place via a single crossing-over in between direct internal repeated sequences present in the integrated construct itself and causes excision of the double selection cassette, restoring the integrity of the introduced gene(s). Mutants in which the second recombination is incomplete can be efficiently counter-selected on sucrose, because only those recombinants that have lost the whole *nptI-sacB* cassette will survive. As a consequence, in the population generated by the second round of recombination [“sec(ondary) recombinants”], the target gene is replaced by the transgenic DNA of choice and no selection marker remains in the genome.

### 3.3.2. Confirmation of the strategy: introduction of the luciferase reporter system

To test the efficacy of the one-step double recombination strategy, glucose-tolerant WT *Synechocystis* cells were transformed with the vector pDSlux (Figure 3.9A). The mutants obtained after the first round of recombination, *lux<sup>prim</sup>*, harboured an interrupted *luxAB* operon inserted in the *Synechocystis slr0168* ORF. This dicistronic operon is composed of the *luxA* and *luxB* genes, and encodes the heterodimeric luciferase enzyme which, in presence of its substrate analogue decanal, produces a luminescent product. In the mutants obtained after the second recombination round, named *lux<sup>sec</sup>*, excision of the double selection cassette led to the reconstitution of the intact *luxAB* operon under the control of  $P_{psbA2}$ .

The frequencies of the first and second recombination events were calculated for the *lux* mutants. Ten independent *lux<sup>prim</sup>* strains obtained after the first recombination were selected and allowed to undergo a second recombination.

Table 3.1 Frequency of the second recombination event in independent *lux<sup>prim</sup>* strains

	#1	#2	#3	#4	#5	#6	#7	#8	#9	#10
<i>lux<sup>sec</sup></i>	$7 \times 10^{-6}$	$5 \times 10^{-7}$	$7 \times 10^{-6}$	$4 \times 10^{-6}$	$7 \times 10^{-6}$	$1 \times 10^{-7}$	$2 \times 10^{-6}$	$2 \times 10^{-5}$	$2 \times 10^{-5}$	$2 \times 10^{-5}$

The transformation frequency was  $4 \times 10^{-5}$ , which is comparable to the values reported in literature (Zang et al., 2007). The frequency of the second recombination varied between

$2 \times 10^{-5}$  and  $1 \times 10^{-7}$  (Table 3.1), with an average value of  $9 \times 10^{-6}$ , revealing that it occurs with a frequency about ten times lower than the first.

Five of the original ten independent *lux<sup>prim</sup>* first recombinants and two *lux<sup>sec</sup>* second recombinants for each of the five *lux<sup>prim</sup>* clones were selected for further analyses.

To confirm the correct segregation of the expected DNA modifications in the generated mutants, genomic PCR was performed using three primer pairs. In all five *lux<sup>prim</sup>* mutants, but in none of the *lux<sup>sec</sup>* strains, the primer pairs R1+R2 and R3+R4 generated amplicons (respectively, 2.7 and 2.3 kb) spanning the 5' or 3' regions respectively of the *nptI-sacB* cassette and the flanking segment of the interrupted *luxAB* operon. When combined, primers R1 and R3 amplified the reconstituted *luxAB* operon, generating a PCR product of 2.3 kb that was detectable only in the *lux<sup>sec</sup>* second recombinants. The *slr0168* downstream region (HR2, ~1 kb), used as a positive control, could be amplified in all the samples using the primer pair R5+R6 (Figure 3.9B).

Gene replacement via homologous recombination is sometimes prone to error, and may result in non-homologous DNA integration into the genome, thus generating mutants with multiple or non-targeted genomic insertions. However, when Southern blots bearing genomic *XmaI* digests from WT and the selected *lux* mutants were probed with a fragment of the *luxAB* recombinant operon (Figure 3.8C), two labelled bands (F1 and F2, with 7.5 and 8.3 kb respectively) corresponding to the split *luxAB* operon were found in the *lux<sup>prim</sup>* mutants, while the detection of a single band of 11 kb (F3) in the *lux<sup>sec</sup>* recombinants confirmed the presence of the reconstituted intact operon. The absence of any signal of unexpected size indicated that only homologous recombination events at the correct target loci occurred.

In order to characterize the growth phenotype of the *lux* mutants, they were grown on various BG11-based media (Figure 3.9D). When spotted on BG11 plates supplemented with 5 mM glucose and not containing any selection pressure, all *lux<sup>prim</sup>* and *lux<sup>sec</sup>* mutant strains grew normally. The *lux<sup>prim</sup>* first recombinant strains were able to grow in the presence of kanamycin and, furthermore, the presence of 5 % sucrose in the medium was lethal for them, confirming the functionality of both the positive and the negative selection markers. Conversely, all the *lux<sup>sec</sup>* strains were sensitive to kanamycin, as they had lost the *nptI* resistance gene, and grew on BG11 supplemented with 5 % sucrose because they no longer harboured the *sacB* gene. None of the strains could grow on BG11 supplemented with both kanamycin and sucrose, as expected.

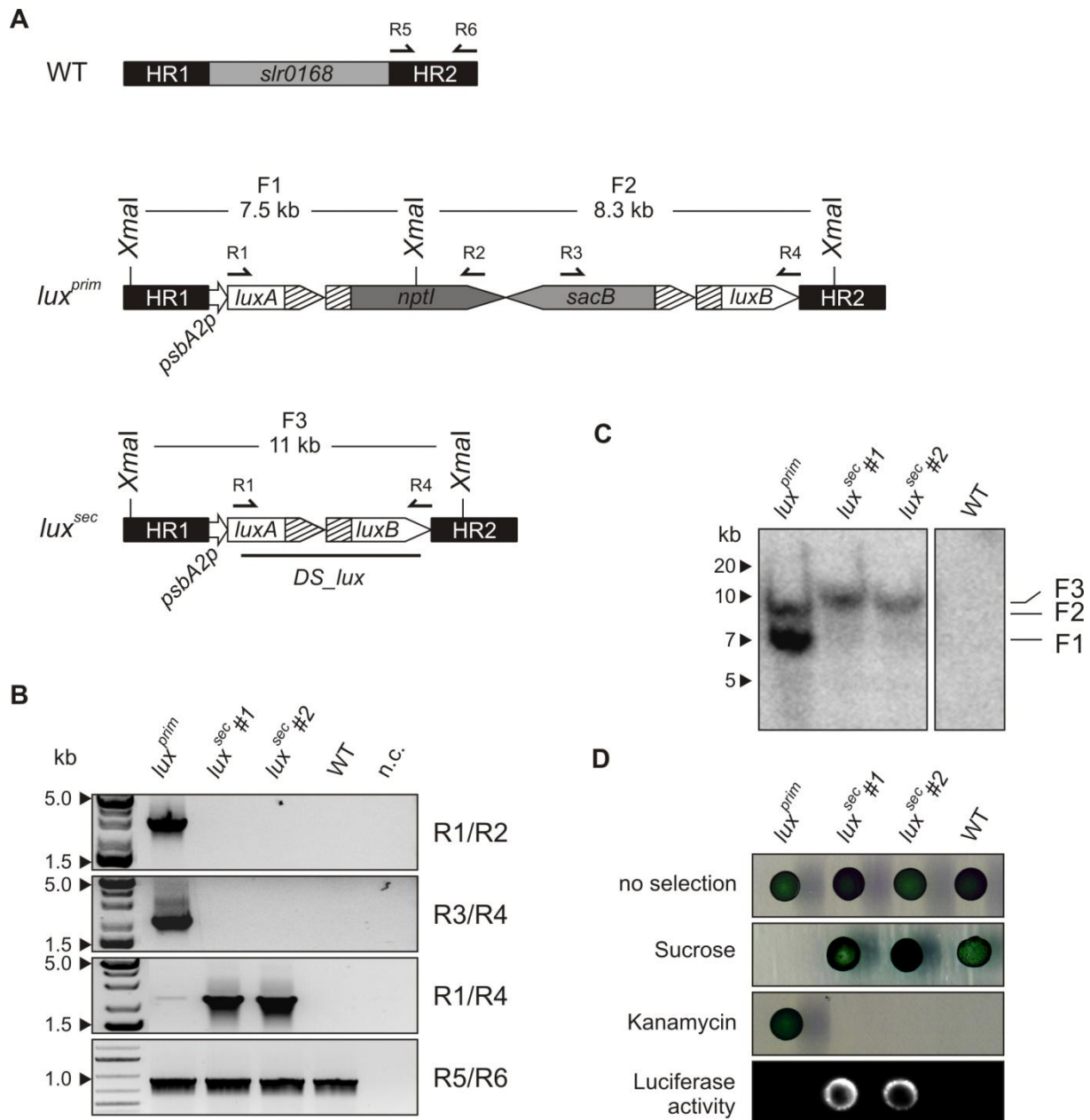


Figure 3.9 Analysis of the *lux* strains (Viola et al., 2014)

(A) Schematic depiction of the mutant strains after the first and second recombination rounds following transformation with the *lux* constructs. The *lux* construct was integrated in the neutral receptor site *slr0168*. In *lux<sup>prim</sup>*, the *nptI-sacB* cassette interrupted the *luxB* gene. In *lux<sup>sec</sup>*, loss of the cassette led to the reconstitution of the entire *luxAB* operon under the regulation of the *psbA2* promoter. Annealing sites of the primers used for genotyping (R1-6) and of the *DS<sub>lux</sub>* probe used for Southern hybridization as well as the positions of the *XmaI* restriction sites are indicated.

(B) Complete segregation of the *Synechocystis lux* strains generated by the genetic manipulations represented in (A) Genotyping PCR was performed on five independent *lux<sup>prim</sup>* first-round recombinants and, for each of them, two second-round recombinants. Note that *lux<sup>prim</sup>*#2-5 behaved like *lux<sup>prim</sup>*#1. Expected sizes of the amplicons generated by the used primer pairs were: R1/R2, 2.7 kb; R3/R4, 2.3 kb; R1/R4, 2.3 kb; R5/R6, 1 kb. Negative control (n.c.) was included. **C.** Southern analysis of genomic DNA from *Synechocystis* WT and *lux* mutants. The *XmaI* restriction map of the *slr0168* genomic region in the analyzed strains and the probe used for hybridization are shown in A. Five  $\mu$ g of DNA were loaded per lane. Genomic fragments F1 (7.5 kb) and F2 (8.3) were detected in *lux<sup>prim</sup>*, the fragment F3 (11 kb) in the *lux<sup>sec</sup>* strains. Note that *lux<sup>prim</sup>*#4-5 behaved like

*lux<sup>prim</sup>*#1. The lane corresponding to WT is also shown. (C) Southern analysis of genomic DNA from *Synechocystis* WT and *lux* mutants. The *Xma*I restriction map of the *slr0168* genomic region in the analysed strains and the probe used for hybridization are shown in (A). Five µg of DNA were loaded per lane. Genomic fragments F1 (7.5 kb) and F2 (8.3 kb) were detected in *lux<sup>prim</sup>*, the fragment F3 (11 kb) in the *lux<sup>sec</sup>* strains. Southern analysis was performed on five independent *lux<sup>prim</sup>* first-round recombinants and, for each of them, two second-round recombinant strains.

(D) Drop test of *lux* mutants on selective media. Liquid cultures at an OD<sub>730</sub> of 0.4 were washed with BG11 without glucose and spotted (15 µl each) onto BG11 medium containing either 100 µg/ml kanamycin or 5% sucrose or no supplement. Colonies from the non-selective plate were incubated with 1 mM decanal and luminescence was determined to quantify luciferase activity.

The *luxAB* operon codes for two proteins that are both required for the expression of luminescence, a gene function not naturally present in *Synechocystis*. In *lux<sup>prim</sup>* mutants the full-length copy of the *luxB* gene is not fused to a functional promoter; therefore, the LuxB subunit of the luciferase cannot be synthesized. The second recombination (in *lux<sup>sec</sup>* mutants) is expected to reconstitute the entire *luxAB* operon under the regulation of *P<sub>psbA2</sub>*, thus allowing the expression and assembly of the functional enzyme. To confirm this, all the spotted strains were tested for luminescence (Figure 3.9D, lower panel). Strong luciferase activity was detectable only in the *lux<sup>sec</sup>* strains, carrying the reconstituted *luxAB* operon, and almost absent in all the *lux<sup>prim</sup>* mutants. A faint luminescent background was always detectable in the first-round recombinants, possibly due to read-through transcription of *luxB* from the *nptI* promoter. To better quantify the luciferase activity, light emission was measured for the ten *lux<sup>prim</sup>* strains used for second recombination and ten *lux<sup>sec</sup>* independent recombinants for each of them (Table 3.2). The luminescence values relative to the untransformed WT *Synechocystis* strain clearly indicated a gain of function in all the *lux<sup>sec</sup>* strains, albeit with a certain inter-strain variability. The level of luciferase activity in the *lux<sup>prim</sup>* transformants ranged between 1.5- and 2.5-fold higher than in the WT, while in the second-round recombinants it was at least ten times higher than in WT.

Table 3.2 Luciferase activity relative to OD<sub>730</sub> in *Synechocystis lux<sup>prim</sup>* and *lux<sup>sec</sup>* mutants. For each strain, the first recombinant and ten independent second recombinants were analyzed. Each suspension was measured in duplicate and the assay was repeated twice with independently grown cultures. Average luminescence values of the mutants are relative to background signal in the untransformed WT *Synechocystis* strain, which value was set to 1.

	#1	#2	#3	#4	#5	#6	#7	#8	#9	#10
<i>lux<sup>prim</sup></i>	2.6±1.4	2.3±0.4	1.8±0.4	2±1.2	2.1±0.7	1.8±0.5	2.2±1.1	1.7±0.6	1.5±0.8	1.5±1
<i>lux<sup>sec</sup></i> (1-10)	17.3±4	61.8±11	16.6±4	24.1±6	15.3±5	23.2±9	22.7±9	10.4±3	10.6±3	13.1±4

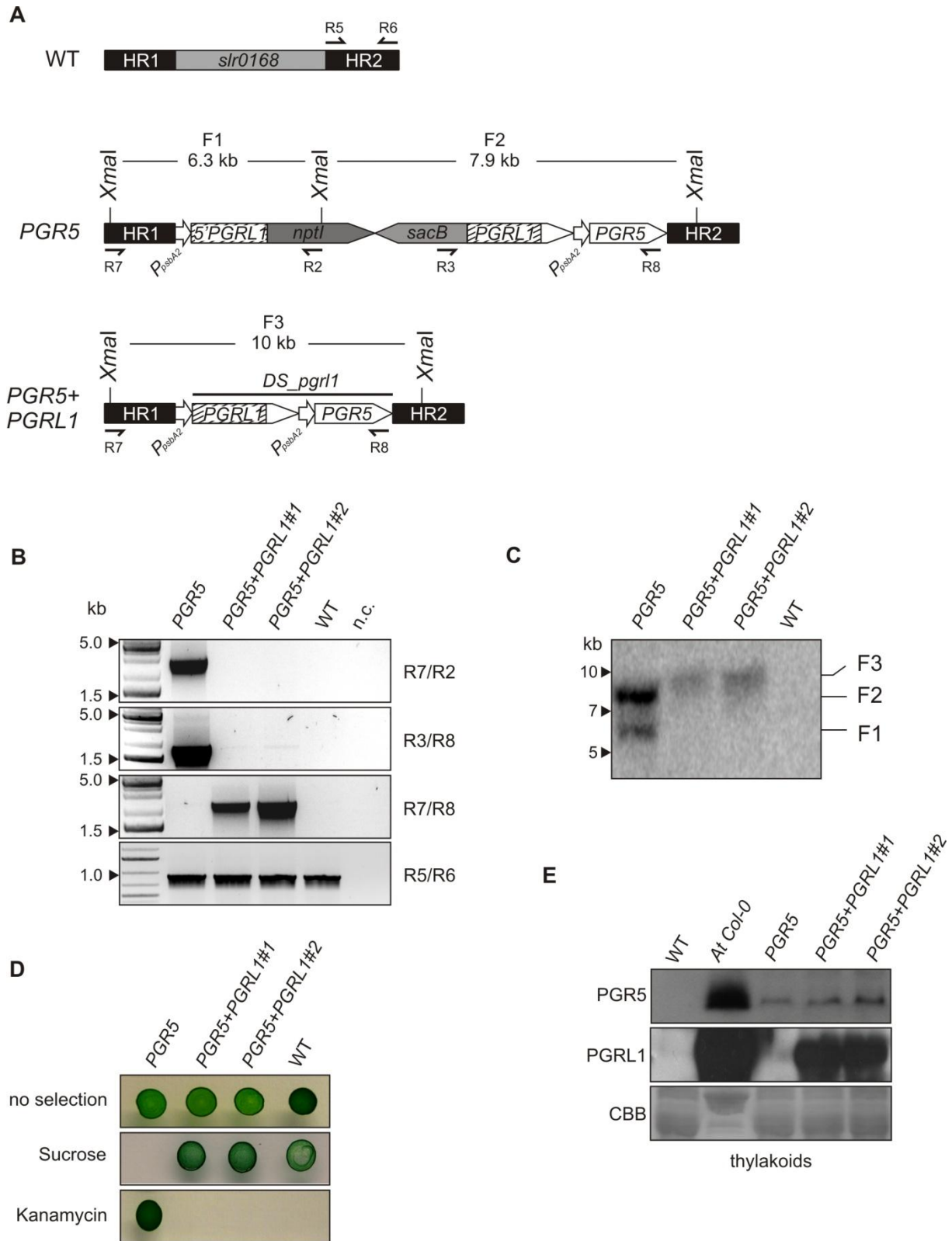
### 3.3.3. Application of the strategy: 1. Introduction of *Arabidopsis* PGRL1 and PGR5 proteins

The same strategy was used to introduce the *Arabidopsis thaliana* PROTON GRADIENT REGULATION 5 (PGR5) and PROTON GRADIENT REGULATION 5-LIKE 1 (PGRL1) proteins into *Synechocystis*. These chloroplast proteins were previously shown to be both necessary and sufficient for the NDH-independent Cyclic Electron Flow (CEF) around Photosystem I during photosynthesis (Hertle et al., 2013), also defined as the Antimycin A (AA)-sensitive pathway. This CEF pathway is present in higher plants but no corresponding mechanism is found in cyanobacteria, in which only the NDH-complex-mediated cyclic transport has been identified.

Glucose-tolerant WT *Synechocystis* cells were transformed with the pDSpgrl1 vector (Figure 3.10A). The *PGR5* mutants positively selected after the first recombination harboured a synthetic construct in the *slr0168* neutral region, in which the sequences coding for the two mature *Arabidopsis* proteins were assembled, each under the regulation of one  $P_{psbA2}$  copy. The *PGRL1* coding sequence was interrupted by the *nptI-sacB* double selection cassette in *PGR5* mutants, whereas the  $P_{psbA2}$ -*PGR5* transcriptional fusion was intact. In the subsequent second recombination round, excision of the double selection cassette led to the reconstitution of the intact  $P_{psbA2}$ -*PGRL1* fusion in the *PGR5*+*PGRL1* mutants.

As in the case of the *lux* mutants, the correct segregation of the *PGRL1* genetic manipulations was confirmed by genomic PCR using three primer pairs. The primer pairs R7+R2 and R3+R8 generated amplicons (of 2.7 and 1.7 kb, respectively) spanning the 5' or 3' regions of the *nptI-sacB* cassette and the flanking segment of the interrupted *PGRL1-PGR5* operon. These two PCR products were present in *PGR5*, but in none of the two selected *PGR5*+*PGRL1* mutants. The reconstituted operon (2.3 kb) could be amplified only in the *PGR5*+*PGRL1* second recombinants combining primers R7 and R8. The *slr0168* downstream region (HR2, ~1 kb), used as a positive control, could be amplified in all the samples using the primer pair R5+R6 (Figure 3.10B).

Accuracy of the targeted homologous DNA integration into the genome was also verified by Southern blot analysis of genomic *XmaI* digests from WT and the selected *PGRL1* mutants. The digested genomes were probed with the entire *PGRL1-PGR5* recombinant operon (Figure 3.10C). Two labelled bands (F1 and F2, with 6.3 and 7.9 kb respectively) corresponding to the split *PGRL1-PGR5* operon were found in *PGR5*, while a single band of 10 kb (F3) was detected in the *PGR5*+*PGRL1* recombinants, corresponding to the intact operon. No signal of unexpected size was present in any of the mutants.

Figure 3.10 Analysis of the *PGRL1* strains

(A) Schematic representation of the mutant strains after the first and second recombination following transformation with the pDS<sub>pgr1</sub> vector. The *PGRL1-PGR5* construct was integrated in the genomic neutral locus *slr0168*. In *PGR5*, the *nptI-sacB* cassette interrupted the *PGRL1* gene. In *PGR5+PGRL1*, loss of the cassette led to the reconstitution of the entire *PGRL1-PGR5* synthetic operon, with each gene under the regulation of one copy of the *psbA2* promoter. Annealing sites of the primers used for genotyping (R2, 3, 5-8)



and of the *DS\_pgrll* probe used for Southern hybridization as well as the positions of the *XmaI* restriction sites are indicated.

(B) Complete segregation of the *Synechocystis* *PGRL1* strains generated by the genetic manipulations represented in (A). Genotyping PCR was performed on one *PGR5* first-round and two *PGR5+PGRL1* second-round recombinants. Expected sizes of the amplicons generated by the used primer pairs were: R7/R2, 2.7 kb; R3/R8, 1.7 kb; R7/R8, 2.3 kb; R5/R6, 1 kb. Negative control (n.c.) was included.

(C) Southern analysis of genomic DNA from *Synechocystis* WT and *PGRL1* mutants. The *XmaI* restriction map of the *slr0168* genomic region in the analysed strains and the probe used for hybridization are shown in (A). Five  $\mu\text{g}$  of DNA were loaded per lane. Genomic fragments F1 (6.3 kb) and F2 (7.9) were detected in *PGR5*, the fragment F3 (10 kb) in the *PGR5+PGRL1* strains.

(D) Drop test of *PGRL1* mutants on selective media. Liquid cultures at an  $\text{OD}_{730}$  of 0.4 were washed with BG11 without glucose and spotted (15  $\mu\text{l}$  each) onto BG11 medium containing either 100  $\mu\text{g/ml}$  kanamycin or 5% sucrose or no supplement.

(E) Immuno-blot analysis of *Arabidopsis* *PGR5* and *PGRL1* proteins in thylakoid fractions of WT and mutant strains. 15  $\mu\text{g}$  of protein were loaded for each lane and thylakoid proteins from *Arabidopsis thaliana* were included as a positive control.

The *PGRL1* strains were also tested by growing them on various BG11-based media (Figure 3.10D). All *PGR5* and *PGR5+PGRL1* mutant strains grew normally in the absence of selective pressure, whereas only the *PGR5* first recombinants survived in the presence of kanamycin and it did not grow when 5 % sucrose was added to the medium. On the contrary, all the *PGR5+PGRL1* strains were sensitive to kanamycin and grew on BG11 supplemented with 5 % sucrose, as they had lost both the *nptI* and the *sacB* marker genes. The combined presence of both kanamycin and sucrose resulted to be lethal for all the strains.

Accumulation of the *PGRL1* and *PGR5* proteins, not naturally present in *Synechocystis*, was probed by immunoblot of isolated membrane proteins using the specific antibodies raised against the two plant proteins. *Arabidopsis* wild type thylakoid proteins were used as a positive control. As expected, the *PGR5* strain expressed only *PGR5* and, conversely, both the *PGR5* and the *PGRL1* proteins accumulated in the two *PGR5+PGRL1* recombinants (Figure 3.10E).

In order to investigate whether the recombinant *PGR5* and *PGRL1* proteins were capable of supporting the NDH-independent CEF pathway in *Synechocystis*, the photooxidation and dark-reduction kinetics of the PSI reaction centre, P700, were measured in the *PGRL1* mutants.

As already reported (Yu et al., 1993; Thomas et al., 1998) the cyclic electron transport pathway in whole cells of cyanobacteria can be studied by measuring the changes in absorbance at 820 nm, to determine the P700 redox state and its re-reduction kinetics. In cyanobacteria the electron flow through the Cyt *b<sub>6</sub>f* complex, which is shared between the photosynthetic and the respiratory electron transport chains (Scherer, 1990), is the limiting step in the re-reduction of the oxidized P700 (P700<sup>+</sup>). Illumination with actinic white light,

exciting both PSII and PSI, causes the reduction of the plastoquinone pool and the depletion of the proximal electron donor of PSI that gets oxidized. In subsequent darkness, P700<sup>+</sup> gets reduced by electrons coming from both the PSII-dependent linear electron flow and the NDH-dependent cyclic electron flow.

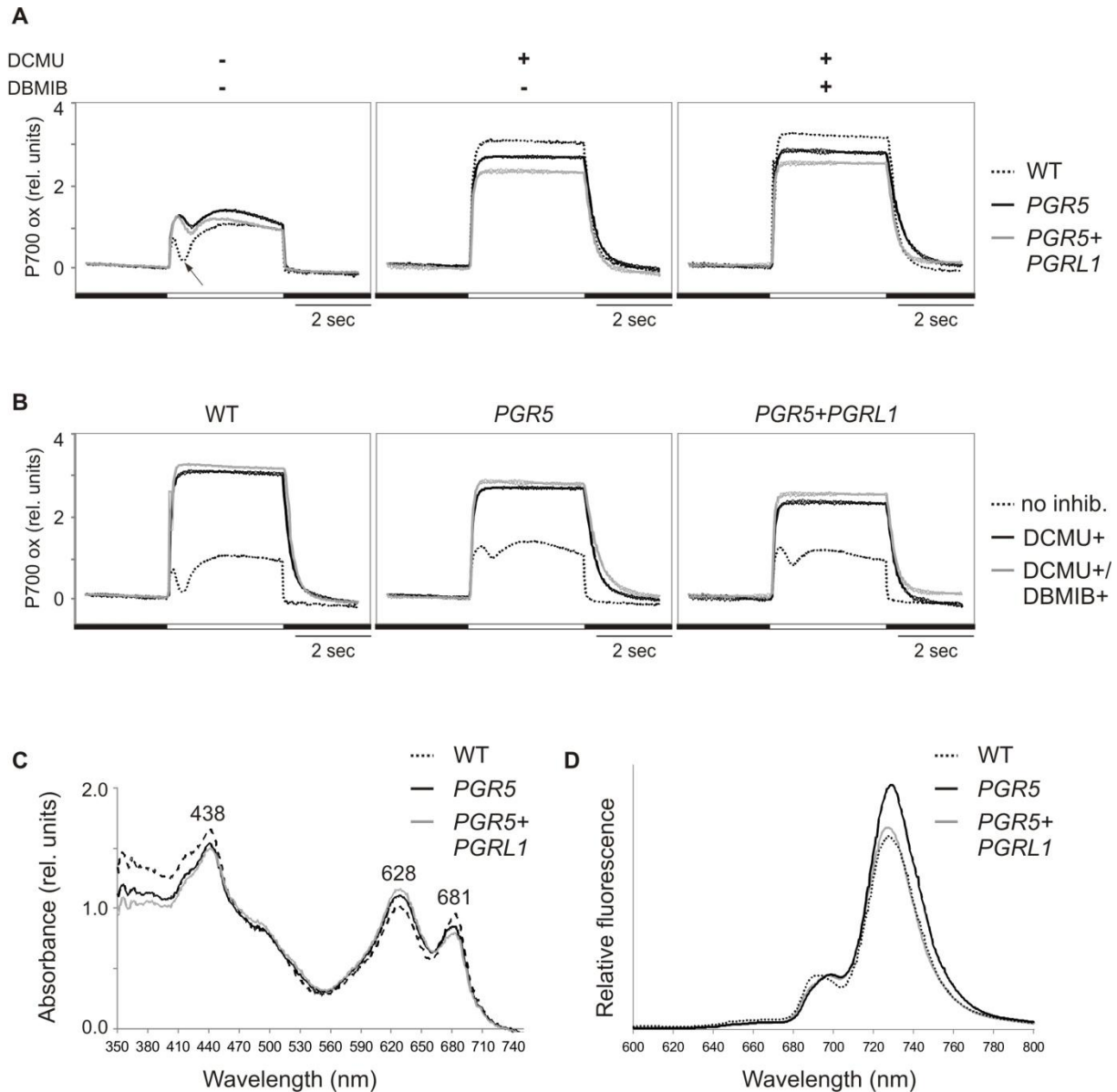


Figure 3.11 Physiological characterization of the *PGR5* strains

(A) and (B) P700 oxidation (P700 ox) traces of *Synechocystis* WT, *PGR5* and *PGR5+PGRL1* strains. The  $A_{820}$  was measured with a Dual-PAM-100 fluorometer, with and without addition of 25  $\mu\text{M}$  DCMU or 25  $\mu\text{M}$  DBMIB. The traces are representative of two repetitions. Cell suspensions were adjusted to an  $\text{OD}_{730}$  (used as indication of an equal amount of biomass) of 10 and dark-adapted for 10 min prior to measurements. Three second after the onset of far red measuring light, white actinic light (30  $\mu\text{mol photons m}^{-2} \text{s}^{-1}$ ) was supplied for 3 sec. The bars under each P700 trace represent the absence (dark bars) and presence (white bars) of actinic illumination. The P700 oxidation signal is relative to the “zero” level at the onset of actinic illumination. In (A) the P700 traces of the three analyzed strains for each inhibitor treatment are compared. The initial oxidation rate is proportional to the efficiency with which excitation energy is delivered to P700. The re-reduction rate is

proportional to the transfer to P700 of electrons deriving both from PSII and from the cyclic electron flow. A re-reduction transient can be seen just after the onset of light when no inhibitors are added to the samples (black arrow). In (B) the P700 traces of the three different inhibitor treatments for each analyzed strain are compared.

(C) *In vivo* absorption spectra of *Synechocystis* WT, *PGR5* and *PGR5+PGRL1* strains. The peaks at 438 and 681 nm correspond to the maxima of Chl *a* absorption, the peak at 628 nm corresponds to the absorption maximum of PC. The spectra were normalized to the absorbance at 730 nm.

(D) Steady-state fluorescence emission spectra at 77 K of cells of *Synechocystis* WT, *PGR5* and *PGR5+PGRL1* strains. Cell suspensions were adjusted to an OD<sub>730</sub> of 0.5 and dark-adapted for 10 min prior to freezing. Fluorescence emission spectra were measured with excitation at 435 nm and normalized to the PSII emission peak at 695 nm. The curves are representative for two repetitions.

The different inputs of electrons to PSI can be selectively blocked using inhibitors (Maxwell and Biggins, 1976; Herbert et al., 1992; Yu et al., 1993): input from PSII can be abolished with the herbicide 3-(3,4-dichlorophenyl)-1,1-dimethylurea (DCMU), input from the plastoquinone pool with the artificial quinone 2,5-dibromo-3-methyl-5-isopropyl-7-benzoquinone (DBMIB).

Absorbance at 820 nm in *Synechocystis* cell suspensions at an OD<sub>730</sub> of 10, previously dark-adapted for 10 min, was measured (Figure 3.11) and used as expression of the relative P700 oxidation level (P700<sup>+</sup>). In the wild type, exposure to white actinic light caused a rapid oxidation of P700 which was then transiently re-reduced by electrons from PSII before reaching the steady-state oxidation level (Figure 3.11A, black arrow). When illumination ceased, the P700<sup>+</sup> signal quickly fell back to the dark level thanks to electron input from PSII and the CEF. In DCMU-treated WT cells the block of electron flow from PSII was testified by the lack of the re-reduction transient after onset of illumination, the higher steady-state level of the P700<sup>+</sup> signal, as well as its slower re-reduction kinetics in the dark. These observations were in accord with fact that, in presence of DCMU, CEF is the only pathway responsible for the PSI reduction. WT treated with both DCMU and DBMIB showed an even higher steady-state level of PSI oxidation. Indeed, DBMIB inhibits the electron transfer from the plastoquinone pool to the cytochrome *b<sub>6</sub>f* complex, therefore blocking the flow of electrons to PSI deriving from both the PSII and the CEF. In the untreated strain expressing *PGR5*, and even more pronouncedly in those expressing both *PGRL1* and *PGR5*, the P700<sup>+</sup> signal was rising faster and to a higher level than in WT and the initial transient re-reduction was greatly reduced. According to this, the electrons extracted from PSI by exciting light appeared to be acquired by downstream acceptors in a more efficient way than in the wild type, thus maintaining P700 in a more oxidized state.

In the *PGR5* expressing strain, treatments with DCMU and with DCMU plus DBMIB led to an increase of the P700<sup>+</sup> steady-state level relative to the untreated samples similar to WT, but to a lower extent, suggesting a reduction of the maximum PSI oxidation potential in the

mutant strain. This reduction was even more marked in the mutant expressing both PGRL1 and PGR5. When comparing the P700 traces under the different treatments for each analyzed genotype, a diminished difference between the steady-state and the maximal PSI oxidation levels was observed in the *PGR5* and, even more, in the *PGR5+PGRL1* mutants (Figure 3.11B). To exclude that these differences were caused by altered amounts of PSI or pigments, spectral analyses of *PGR5* and *PGR5+PGRL1* were performed. Neither the absorption spectra nor the low-temperature fluorescence emission spectra of the mutants showed significant differences with respect to the wild type (Figure 3.11C and D), suggesting that the drastic changes in P700 properties in the mutant strains are actually caused by a functional interaction of PGR5 and PGRL1 with PSI and with other components of the electron transport chain in *Synechocystis*.

#### 3.3.4. Application of the strategy: 2. The *psaA* gene

In the case of the *PGRL1* mutants, the double recombination strategy was used to introduce in *Synechocystis* two photosynthesis-related proteins from *Arabidopsis* that are not naturally present in this organism, but the core photosynthetic components and functions are conserved in the two organisms. To study the function of such photosynthetic orthologs, gene replacement is normally employed. Therefore, the single-step strategy was used to replace the *Synechocystis psaA* (*Syn psaA*) gene with the corresponding homolog from the green plant *Arabidopsis thaliana* (*At psaA*). As already mentioned, the *psaA* gene is, in both cyanobacteria and plants, part of the *psaA/psaB* operon which codes for PsaA and PsaB, the core subunits of PSI (for a review, see Chitnis, 2001).

By transforming the glucose-tolerant WT *Synechocystis* strain with the vector pDS<sub>psaA</sub>, analogously to the experiments described above, knockout (*psaA<sup>prim</sup>*) and replacement (*psaA<sup>sec</sup>*) mutants were subsequently obtained (Figure 3.12A). The knockout line *psaA<sup>prim</sup>* was generated with the first recombination event, in which the integrated construct replaced the endogenous *psaA* gene. Only the *psaA* coding sequence was affected by the replacement, whereas the surrounding genomic regions and all the endogenous regulatory elements remained unchanged. In the *psaA<sup>prim</sup>* mutant, the integrated *At psaA* gene was non-functional, being split in two parts separated by the *nptI-sacB* cassette. As expected, the same severe  $\Delta$ *psaA* mutant phenotype was observed in the *psaA<sup>prim</sup>* strain that was turquoise-blue and highly light sensitive. The blue phenotype of the first-round recombinant resulted from the lack of Chl *a*, with the phycobilisome chromophore phycocyanin (PC) being the predominant pigment present (Figure 3.12B). After complete segregation of the first replacement, the

second recombination event was permitted by removal of the selective pressure and subsequent negative selection on sucrose-containing medium yielded colonies in which excision of the *nptI-sacB* cassette led to the reconstitution of the *At psaA* gene, replacing the endogenous one. These mutants, named *psaA<sup>sec</sup>*, were also bluish, having a drastically reduced Chl *a*/PC ratio with respect to the wild type, but they were able to accumulate more chlorophyll than the *psaA<sup>prim</sup>* strain (Figure 3.12B). The second-round recombinants could grow under normal light conditions.

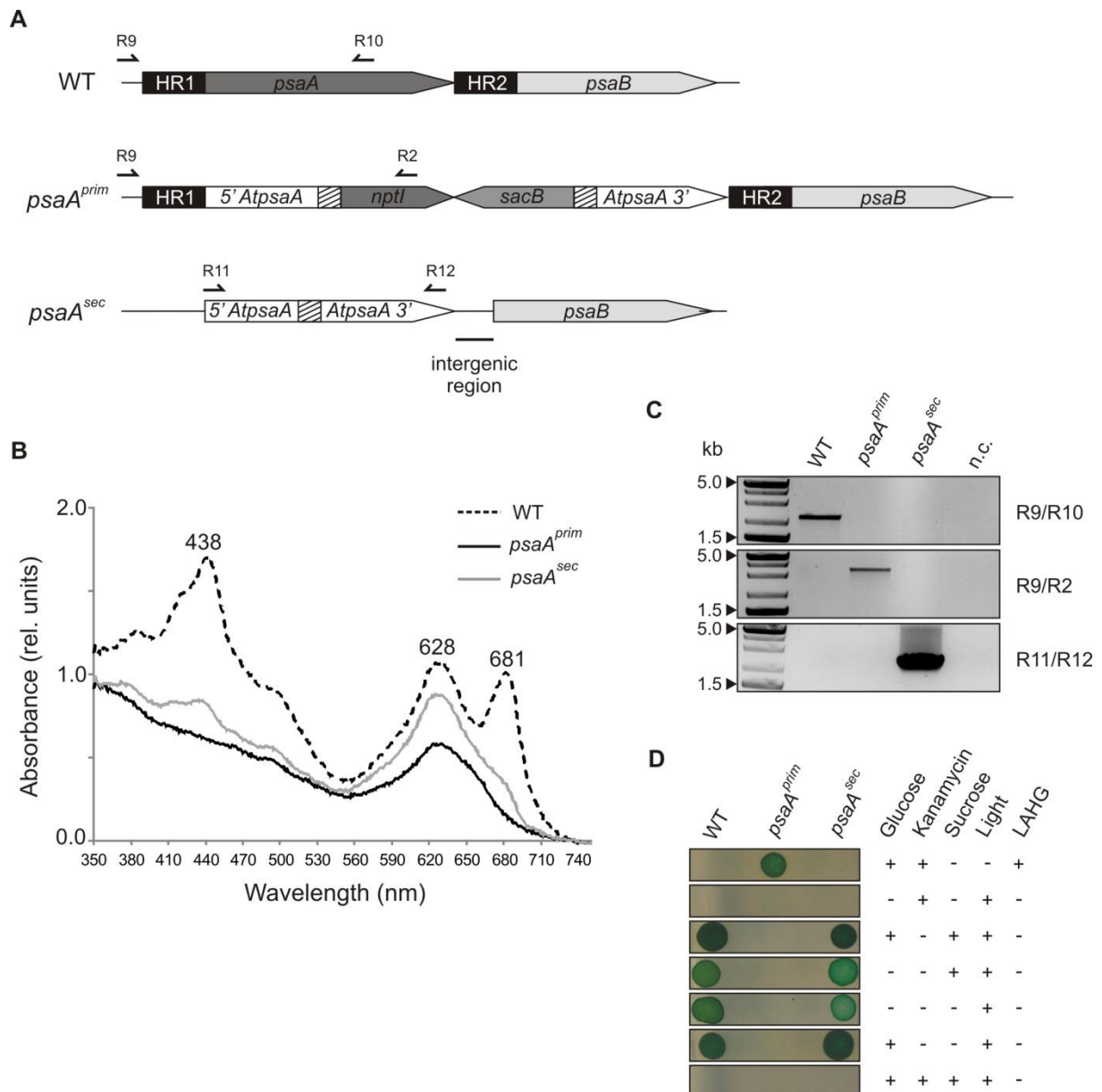


Figure 3.12 Analysis of the *psaA* strains (Viola et al., 2014)

(A) Schematic depiction of mutant strains after the first and second rounds of recombination following transformation with the *psaA* construct. The *psaA* construct is integrated in the *Synechocystis* *psaA* gene. In *psaA<sup>prim</sup>* the *nptI-sacB* cassette interrupts the *At psaA* gene. In *psaA<sup>sec</sup>*, loss of the cassette leads to the

reconstitution of the entire *At psaA* under the control of the native cyanobacterial promoter. Positions of the primers used for genotyping (R2, R9-12) are indicated.

(B) *In vivo* absorption spectra of WT, *psaA<sup>prim</sup>* and *psaA<sup>sec</sup>* *Synechocystis* strains. The peaks at 438 and 681 nm correspond to the maxima of Chl *a* absorption, the peak at 628 nm corresponds to the absorption maximum of PC. The spectra were normalized to the absorbance at 730 nm.

(C) Complete segregation of the generated *Synechocystis psaA* strains, as demonstrated by PCR analysis. Primer positions are given in (A). Complete segregation of the generated *Synechocystis psaA* strains, as demonstrated by PCR analysis. Primer positions are given in A. Expected sizes of the amplicons generated by the used primer pairs were: P9/P10, 2 kb; P9/P2, 3 kb; P11/P12, 2.3 kb. Negative control (n.c.) was included.

(D) Drop test of WT, *psaA<sup>prim</sup>* and *psaA<sup>sec</sup>* *Synechocystis* strains on selective media and under different light conditions. Liquid cultures at OD<sub>730</sub> of 0.4 were washed with BG11 without glucose and spotted (15  $\mu$ l each) on non-selective BG11 medium or on BG11 containing 100  $\mu$ g/ml kanamycin or 5 % sucrose. When tested for autotrophic growth, cells were grown in continuous light at 30  $\mu$ mol photons m<sup>-2</sup> s<sup>-1</sup> on BG11 without glucose. When grown in Light Activated Heterotrophic Growth (LAHG) conditions, the cells were incubated in the dark on BG11 supplemented with 5 mM glucose, and exposed to light for 5 min every 24 hours.

The correct segregation of the *psaA* genetic manipulations performed was confirmed by genomic PCR using three primer pairs. The region (2 kb) spanning the upstream homologous region used for integration of the construct (HR1) and the endogenous *psaA* gene could be amplified with the primer pair R9+R10 only in WT, confirming that in both mutant strains the knockout was complete. In *psaA<sup>prim</sup>*, but not in WT and in the *psaA<sup>sec</sup>* mutant, the primer pair R9+R2 generated an amplicon (3 kb) spanning HR1, the flanking 5' *At psaA* segments and the 5' region of the *nptI-sacB* cassette. Primers R11 and R12 amplified the fully reconstituted *psaA* gene from *A. thaliana*, generating a PCR product of 2.2 kb that was detectable only in the *psaA<sup>sec</sup>* recombinants (Figure 3.12C).

The growth phenotypes of the mutant strains were analyzed by spotting them on BG11-agar plates under different selective and trophic conditions (Figure 3.12D). The *psaA<sup>prim</sup>* mutant displayed resistance to kanamycin, deriving from the integrate *nptI* resistance gene, but, being PSI-deficient, it only grew heterotrophically in LAHG conditions. Like the  $\Delta$ *psaA* knockout strain, *psaA<sup>prim</sup>* was unable to grow in continuous bright light and without glucose. Excision of the *nptI-sacB* cassette with the second recombination rendered the *psaA<sup>sec</sup>* mutant sensitive to kanamycin but able to grow on BG11 containing sucrose, whereas the presence of 5 % sucrose was lethal to the knockout strain. None of the mutants, as in the previous examples, was viable in presence of both kanamycin and 5 % sucrose. Interestingly, *psaA<sup>sec</sup>* resembled the already described *AB<sub>opt</sub>* mutants in its ability to grow in full light and photoautotrophically on BG11 agar plates containing no sugar, suggesting that the *At PsaA* protein can functionally replace the *Synechocystis* protein and even interact with the cyanobacterial PsaB in the formation of the PSI core.

### 3.3.5. Discussion: advantages of the single-step replacement strategy

Targeted gene and genome manipulation via homologous recombination in bacteria relies on the use of marker genes. In marker-less gene replacement, a negative and a positive selection marker are employed, in a process that normally involves two transformation steps with two DNA suicide vectors. In this work, we developed an alternative strategy for marker-less gene replacement in *Synechocystis*, based on the use of a single plasmid and a single transformation step.

The technique was tested by inserting the *luxAB* operon from *Vibrio fischeri* into the neutral receptor site *slr0168*. To this end the wild type strain was transformed with the vector pDSlux and the transformation efficiency with this integration vector was in the range of  $10^{-5}$ , while the average frequency of the second recombination event was  $10^{-6}$  (see Table 1). This ten-fold difference could be due to the fact that the first recombination event involves a double crossover between the genomic DNA and the plasmid vector, whereas the second recombination presumably involves a single intra-genomic crossover (Clerico et al., 2007). Thus, a difference in efficiency between these two recombination mechanisms could explain the results obtained. In addition, other factors like length, position and relative concentration of the homology regions might contribute to the difference in efficiency (Kufryk et al., 2002). In comparison with standard procedures, the single-step marker-less gene replacement strategy described here has several advantages. The requirement of only one vector for each gene replacement makes the cloning procedure faster and more facile, especially when one needs to sequentially replace many genes. Our single-step approach merely requires alternative selective growth conditions in addition to the transformation step, although this flexibility requires that the constructs must be assembled from numerous DNA fragments - six (plus the vector backbone) in the case of pDSlux, for instance. However, the increased complexity of the plasmid vectors required can easily be accommodated by using large-scale modular cloning technologies like the Golden Gate (Engler et al., 2009), the Gibson (Gibson et al., 2009) or the BioBrick (Shetty et al., 2008) assembly systems. Another issue that can arise during gene manipulation concerns the cloning of genes that are toxic to *E. coli*. Also in this regard, our strategy is advantageous, because the interruption of the GOI sequence by the intervening *nptI-sacB* cassette inactivates it, thus avoiding the problem of toxicity. Only the second recombination in the *Synechocystis* host cell reconstitutes both the gene sequence and function. Also for studies of biological functions for which two genes are necessary, the single-step gene replacement strategy can constitute a suitable experimental tool, as shown for the *luxAB* operon. In the *lux<sup>prim</sup>* mutants, interruption of this operon by the double selection

cassette leads to impairment of the luciferase activity, as *luxB* cannot be transcribed and therefore the heterodimeric enzyme cannot be assembled. Only after removal of the cassette by the second recombination event is the integrity of the dicistronic *luxAB* and with it the luciferase activity restored, as shown in Figure 3.9D and Table 3.2. Some background luminescence was observed in the *lux<sup>prim</sup>* recombinants, which could be due to read-through transcription of *luxB* from the *nptI* promoter. Thus, by using only one vector and performing a single transformation step it was possible to show that both *luxA* and *luxB* are necessary for luciferase function, as previously described (Engebrecht et al., 1983; Foran et al., 1988). These results confirm that, when our strategy is used to analyze a gain of function, the new function can be expected to arise only in the second recombinants and not in the first mutant strains, which can therefore serve as ideal controls.

When used to introduce in *Synechocystis* the plant-specific PGRL1 and PGR5 proteins, responsible for the NDH-independent CEF pathway in *Arabidopsis*, the technique proved to be useful in dissecting the proteins function. In *Arabidopsis*, the two thylakoid proteins PGRL1 and PGR5 participate in shuttling electrons from PSI to the Cytochrome (Cyt) *b<sub>6</sub>f* complex, forming a heterodimer (DalCorso et al., 2008; Hertle et al., 2013).

Cyanobacteria contain the NDH-dependent CEF pathway, but it is unclear whether they also possess a true pendant of the PGRL1/PGR5-dependent pathway. This is because homologues of PGRL1 have not yet been identified in cyanobacteria. However, inactivation of a cyanobacterial gene with distant homology to *PGR5* appears to perturb cyanobacterial AA-sensitive CEF (Yeremenko et al., 2005). To dissect the function of the two plant proteins in *Synechocystis*, mutants were generated expressing either PGR5 alone or PGRL1 and PGR5 together. Indeed, the *PGR5* mutants accumulated PGR5 alone, the *PGRL1* coding sequence they harboured being disrupted by the *nptI-sacB* cassette, whereas reconstitution of the *P<sub>psbA2</sub>-PGRL1* fusion led in the *PGR5+PGRL1* mutant strain to the accumulation of both PGRL1 and PGR5. When analyzing the absorption and low-temperature fluorescence emission spectra of the mutants, no significant differences with respect to the wild type could be observed. Therefore, the pigments and PSI/PSII ratios seemed not to be affected by the recombinant proteins. On the contrary, when measuring the P700 oxidation-reduction kinetics, major changes were detected in, surprisingly, both *PGR5* and *PGR5+PGRL1* recombinants. The P700<sup>+</sup>-related absorbance at 820 nm was measured with or without the addition of inhibitors blocking the electron transport at different. The PSI in the WT strain became oxidized after exposure to actinic light and then transiently re-reduced by electrons from PSII. This re-reduction did not take place after DCMU treatment, as expected.



Moreover, DCMU treatment resulted in a higher oxidation level in light and in a slower re-reduction rate after illumination was terminated, because electrons coming from the CEF alone and not also from PSII were responsible for it. When using both DCMU and DBMIB, also the re-reduction caused by CEF was prevented, the PSI oxidation level was even higher and corresponded to the maximum PSI oxidation capacity. In the strain expressing PGR5 and, even more pronouncedly, in the strain expressing both PGR5 and PGRL1, the maximum P700<sup>+</sup> signal in presence of inhibitors was markedly lower than in WT, albeit the unchanged photosystem I levels. These results were compatible with the idea that PGRL1 and PGR5, the latter even alone, prevented oxidation of PSI by reinjection of electrons into the electron transport chain. The *PGR5* and *PGR5+PGRL1* recombinants, though, displayed a faster PSI oxidation at the onset of light, with a greatly diminished re-reduction transient due to electrons coming from PSII. Although a more detailed physiological characterization of the mutants will be needed, it could be inferred from the showed results that PGR5 and PGRL1 are able to interact with the electron transport chain also in *Synechocystis*.

The single-step strategy was also employed to replace the *psaA* gene from *Synechocystis* with the homolog from *Arabidopsis thaliana*, which resides in the plastid genome of the plant. The PsaA subunit, together with PsaB, constitutes the dimeric core of PSI, and is highly conserved among photosynthetic organisms from cyanobacteria to flowering plants (Amunts and Nelson, 2008). PsaA is an essential component of PSI and is necessary for its assembly, accumulation and function, and therefore essential for photoautotrophic growth of both plants and cyanobacteria. Knockout of the *psaA* gene is lethal to higher plants, while genetic inactivation of the PSI reaction centre in *Synechocystis* generates mutants that are able to survive heterotrophically under LAHG conditions, although they have a severe phenotype and are unable to survive in the light. In the *psaA<sup>sec</sup>* mutants, replacement of the endogenous *psaA* gene with the *Arabidopsis* homolog led to a partial complementation of the *psaA<sup>prim</sup>* knockout phenotype (Figure 3.12D). Also in this case, using the single-step gene replacement strategy, both the knockout and replacement lines were generated using a single vector and a single transformation. In the case of essential genes like *psaA* the one-vector strategy confers an additional advantage because mutants with severe phenotypes can be difficult to grow in liquid cultures and therefore their transformation can be challenging. This alternative gene replacement strategy makes it possible to obtain a second recombination event simply by releasing the positive selective pressure on the segregated transformants and applying negative selection in an alternating manner.

## 4. CONCLUSIONS

In this work we established a set of tools for the identification and functional characterization of photosynthesis-related proteins from higher plants based on a cyanobacterial platform. For this purpose, the prokaryote *Synechocystis* sp. PCC 6803 was chosen, as it serves as a well-established model organism in photosynthesis research (Vermaas et al., 1986; Vermaas et al., 1987; Carpenter et al., 1993; Dühning et al., 2007; Xu et al., 2011). Cyanobacteria derive from the same ancestor as plant chloroplasts that evolved after a single endosymbiotic event (Martin et al., 2002). During this event, a photosynthetic bacterium was integrated into an ancestral eukaryotic cell, thus providing it with the complete photosynthetic machinery in the shape of a new subcellular compartment, the future chloroplast. With the subsequent evolution of land plants, the chloroplast gradually lost its genetic and physiological autonomy (Whatley and Whatley, 1981; Kleine et al., 2009) and underwent a large number of modifications in order to adapt to the new cellular (Pesaresi et al., 2007) as well as external environment. Higher plants face environmental conditions that drastically differ from the low-light, oxygen-depleted marine environment the prokaryotic photosynthetic machinery evolved in. They are confronted with fluctuating light and an oxidative environment that they cannot avert and, at the same time, with an inadequate evolutionary inheritance (Leister, 2012). As a consequence, plants developed new regulatory and protective mechanisms to optimize their photosynthetic efficiency and limit the damage caused by oxidative and light stress. Over the time, higher plants evolved an extremely complex and fine-tuned photosynthetic apparatus based on the interplay of numerous players that either derive from prokaryotic homologs or evolved independently in the eukaryotic cell (Leister, 2003; Timmis et al., 2004). Unrevealing the details of such an intricate network is a major challenge for plant scientists, since the available genetic and molecular tools seem not to keep pace with the increasing complexity of the plant photosynthesis model that is being assembled.

The generation of a cyanobacterial platform for the analysis of photosynthesis-related proteins from higher plants can constitute a versatile tool to dissect the molecular function of already identified proteins as well as for the identification of new ones whose identity has so far been elusive.

#### 4.1. Dissecting the molecular function of known proteins: the CURT1 protein family and PGRL1/PGR5-mediated CEF

The four members of the CURT1 protein family from *Arabidopsis thaliana* play an important role in the process of thylakoid membrane curvature at the grana margins (Armbruster et al., 2013). The resulting structural rearrangements represent an important adaptive mechanism to variable light conditions (Andersson, 1986; Trissl and Wilhelm, 1993; Mustárdy and Garab, 2003; Dekker and Boekema, 2005; Kargul and Barber, 2008). Although the ability of these proteins to bind membranes was demonstrated *in vitro*, the underlying mechanism is not clear yet. The expression of the major *Arabidopsis* CURT1 variant, CURT1A, in *Synechocystis* in addition (*CURT1A*) or in substitution for (*CURT1A syncurt1*) the endogenous synCURT1 homolog showed that the plant protein is able to induce thylakoid membrane curvature and to influence thylakoid architecture also in cyanobacteria. Moreover, the *Arabidopsis* and the *Synechocystis* homologs resulted to have a partially conserved function, for which a control of their cellular amounts seems to be necessary. Although expression of CURT1A did not induce the formation of grana stacks in the *Synechocystis* thylakoids, its membrane-bending properties increased in the phycobilisome-less mutants (*CURT1A syncurt1Δapc*), suggesting that physical constrains could be a main reason for the lack of grana formation. The generated *Synechocystis* CURT1 mutants represent the starting point for further analyses of the molecular function of CURT1. In the future, the introduction of different combinations of the *Arabidopsis* CURT1 isoforms will allow to dissect their specific roles. Additionally, the regulatory effects on the CURT1 function of posttranslational phosphorylation that has been postulated in plants (Armbruster et al., 2013) can be investigated. Although still controversial, phosphorylation of thylakoid proteins has been reported in cyanobacteria (Allen et al., 1985; Allen et al., 1992). In *Synechocystis*, phosphorylation of the phycobilisome linker proteins has been shown by Piven and colleagues (2005), but no PSII core phosphorylation occurs. Expression of *Arabidopsis* chloroplast kinases in the *Synechocystis* CURT1 mutant strains could help to elucidate the mechanisms that regulate the CURT1 activity in higher plants.

The PGR5 (Munekage et al., 2002) and PGRL1 (DalCorso et al., 2008; Hertle et al., 2013) proteins account for the AA-sensitive cyclic electron flow (CEF) pathway in *Arabidopsis thaliana*, which is partially redundant to the NDH-mediated CEF (Burrows et al., 1998). The two proteins interact physically with each other, which allows for the re-injection of electrons from reduced ferredoxin into the Q-cycle, with PGRL1 undergoing the reduction-oxidation reactions. The current model proposed by Hertle and colleagues (2013) suggests that a PGRL1/PGR5 dimer directly interacts with Fd and FNR in close proximity to the PSI

complex. However, the mode of interaction and the specific molecular function of PGR5 are not fully understood yet. The current state of knowledge is that in cyanobacteria only the NDH-mediated CEF pathway is present, although a protein similar to the N-terminus of PGR5 has been characterized in *Synechocystis* (Yeremenko et al., 2005).

*Synechocystis* mutants expressing either PGR5 alone (*PGR5*) or PGR5 and PGRL1 together (*PGR5+PGRL1*) were tested for a potential effect of the plant proteins on CEF around cyanobacterial PSI. The P700 oxidation-reduction kinetics were indeed altered in the two mutants, with a higher PSI oxidation level under physiological conditions but an overall reduced maximal oxidation capacity when PSI re-reduction from LEF (using DCMU) or from both LEF and CEF (using DCMU and DBMIB) were blocked. These preliminary results strongly indicate that the PGR5 and PGRL1 proteins from *Arabidopsis* interact with the photosynthetic electron transport chain of *Synechocystis*, but further analyses need to be carried out to clarify the underlying molecular mechanisms. This approach opens up interesting questions that will direct future investigations. For instance, PGR5 affects electron flow in *PGR5* mutants even in the absence of PGRL1, apparently by oxidizing PSI to a higher extent than in the wild type: is PGR5 actually the protein, among the two, that first receives electrons from Fd, as hypothesized? The maximal P700<sup>+</sup> levels in *PGR5* and *PGR5+PGRL1* are reduced also in the presence of DBMIB: is the PQ pool the actual site of electron re-injection and, if so, how can the observed phenotype in the *Synechocystis* mutants be explained? Which are the missing plant-specific components or features required for the correct function of the two introduced proteins? The newly introduced pathway competes with the NDH complex that in cyanobacteria is shared between the CEF and the respiratory pathway (Sandmann and Malkin, 1984), for the electrons deriving from PSI. Clearly, it cannot be excluded that this competition also plays a role in the observed phenotype. This aspect should be further investigated.

#### 4.2. Generating a cyanobacterium with a plant-type photosynthetic machinery: replacement of PSI

The glucose-tolerant *Synechocystis* wild type strain is able to grow heterotrophically in darkness (Williams, 1988; Anderson and McIntosh, 1991), which makes it an excellent model to study photosynthesis. The replacement of the bacterial photosynthetic apparatus with its plant-specific counterpart could provide a useful platform to determine the composition of the minimal functional photochemical apparatus. Moreover, this kind of platform might allow

identifying new plant-specific components involved in the regulation of photosynthesis that, so far, escaped identification with the currently used screening approaches.

The substitution of PSI was chosen as an initial project to establish the *Synechocystis* platform, because it is the evolutionarily most conserved photosynthetic complex but, at the same time, the least characterized. To this end, mutants were generated (*AB\_opt*) in which the PsaA and PsaB core subunits of *Synechocystis* PSI got replaced by the respective homologs of *Arabidopsis*. The characterization of these mutants showed that the plant proteins can only partially replace the bacterial counterparts. The two *Arabidopsis* genes were correctly transcribed and this partially rescued the phenotype of the PSI-less mutant (*ΔpsaA*). Although the expression of the plant *psaA-psaB* genes restored the light-tolerance phenotype and led to the accumulation of a partially assembled PSI complex, it was not possible to either detect the mature proteins by immunodecoration or any PSI-specific maxima in fluorescence emission spectra in the replacement mutant. It can be therefore presumed that the assembly of the functional PSI complex is impaired in one of the post-transcriptional steps. This can be seen as a promising starting point to identify the reasons of the lack of functionality rather than a failure of the strategy. The first working hypothesis is that At PsaA and At PsaB do not properly interact with the other *Synechocystis* subunits of PSI. To clarify this, the putative PSI complex accumulating in the *AB\_opt* mutants has to be purified and its composition to be determined. If the assembly of a chimeric PSI complex appears to be the limiting step, the additional introduction of the residual PSI subunits from *Arabidopsis* would be the next logic step. This is, indeed, the direction we are currently following and the characterization of the planned mutant strain will help to answer these questions.

Some factors that are necessary for the assembly of plant-specific PSI and that are not characterized or exert a slightly different function in cyanobacteria have previously been described (for a review, see Schöttler et al., 2011). Their requirement for the assembly of the introduced PSI could be tested by expressing them in the generated *Synechocystis* mutants. Even more interestingly, with this approach new PSI assembly factors could be identified. A library of *Arabidopsis thaliana* transcripts can, indeed, be introduced in the generated *Synechocystis* mutants in order to identify the clones that are able to rescue the PSI-deficient phenotype. The same approach could be applied in strains that show a replacement of different components of the photosynthetic apparatus, thus providing a new screening tool for novel photosynthesis-related proteins.

#### 4.3. Improving the molecular tools for large-scale gene knockout and replacement in *Synechocystis*

*Synechocystis* is naturally transformable and performs homologous recombination. To generate multiple targeted deletions and/or replacements of its genes, marker-less manipulation methods based on counter-selection are generally employed (Cai and Wolk, 1990; Matsuoka et al., 2001). Irrespectively of the markers used, the available methods are usually based on two transformation steps with two different DNA plasmids, of which the first generates the knock-out and the second one allows for the replacement of the target gene. In this study, we developed an alternative marker-less gene deletion and replacement strategy in *Synechocystis* sp. PCC 6803 which is based on a single transformation step exploiting the ability of the cyanobacterium to undergo two subsequent genomic recombination events via double and single crossing-over, by stepwise changes in the selective pressure applied. This strategy presents some convenient properties that could be profitably exploited in large-scale genomic manipulations, like during the generation of the here proposed cyanobacterial platform. A practical advantage is that only one DNA vector, and with it only one transformation step, is required for the stepwise generation of the knock-out and of the replacement *Synechocystis* mutant. This aspect can become quite relevant when manipulating a large number of genes.

When this single-vector strategy is used to analyse a gain of function mutation, the new function is expected to occur only in the second recombinants and not in the first mutant strains, which can therefore serve as ideal controls. Moreover, in the case of two-gene systems, the single-vector strategy can be used to prove that the gain of function actually depends on the functional integrity of both system components, as shown in the case of the *luxAB* reporter system.

Originally, this strategy has been conceived for the manipulation of essential photosynthetic genes, like *psaA*, whose knock-out generates mutants with severe phenotypes that are difficult to grow in liquid cultures and to manipulate and are therefore unsuitable for a second transformation procedure. This specific gene replacement mechanism allows a second recombination event simply by releasing the positive selection pressure on the segregated transformants and instead applying negative selection. The disruption, in the DNA vector employed, of the exogenous gene to introduce by the selection cassette allows obtaining, in the first recombination step, the knockout of the target cyanobacterial gene. Moreover, this disruption could prove itself useful when cloning genes that are toxic in *Escherichia coli*.

Taken together, the implementation of a double recombination event by a simple stepwise change of growth conditions can be exploited to address various biological questions and could also be employed for large-scale gene replacement approaches. Thanks to the tight counter-selection against incomplete second-round recombinants and transformants bearing multiple genomic integrations, the method could indeed be applied in semi-automated systems.

In this work we established the basis for a new approach to study higher plant photosynthesis that relies on the transfer of the plant photosynthetic machinery into the simplified context of a unicellular prokaryote. Although the presented work only touches the surface of the possibilities that are innate to this strategy and the presented results are clearly provisional, encouraging hints of a future successful development are already present. Plant scientists need to keep up with the increasing complexity of the biological processes they investigate by developing new research tools. The here presented approach might just be one of such possible alternatives to achieve this aim.

## REFERENCES

- Adir, N.** (2005). Elucidation of the molecular structures of components of the phycobilisome: reconstructing a giant. *Photosynth Res* **85**, 15-32.
- Ajlani, G., and Vernotte, C.** (1998). Construction and characterization of a phycobiliprotein-less mutant of *Synechocystis* sp. PCC 6803. *Plant Mol Biol* **37**, 577-580.
- Ajlani, G., Vernotte, C., DiMagno, L., and Haselkorn, R.** (1995). Phycobilisome core mutants of *Synechocystis* PCC 6803. *Biochim Biophys Acta* **1231**, 189-196.
- Albertsson, P.A., and Andreasson, E.** (2004). The constant proportion of grana and stroma lamellae in plant chloroplasts. *Physiol Plant* **121**, 334-342.
- Albus, C.A., Ruf, S., Schöttler, M.A., Lein, W., Kehr, J., and Bock, R.** (2010). Y3IP1, a nucleus-encoded thylakoid protein, cooperates with the plastid-encoded Ycf3 protein in photosystem I assembly of tobacco and *Arabidopsis*. *Plant Cell* **22**, 2838-2855.
- Allen, J.F., Sanders, C.E., and Holmes, N.G.** (1985). Correlation of membrane protein phosphorylation with excitation energy distribution in the cyanobacterium *Synechococcus* 6301. *FEBS J* **193**, 271-275.
- Allen, J.F.** (1992). Protein phosphorylation in regulation of photosynthesis. *Biochim Biophys Acta* **1098**, 275-335.
- Allen, J.F., and Pfannschmidt, T.** (2000). Balancing the two photosystems: photosynthetic electron transfer governs transcription of reaction centre genes in chloroplasts. *Philos Trans R Soc Lond B Biol Sci* **355**, 1351-1359.
- Allen, J.F., and Forsberg, J.** (2001). Molecular recognition in thylakoid structure and function. *Trends Plant Sci* **6**, 317-326.
- Allen, J.F., de Paula, W.B., Puthiyaveetil, S., and Nield, J.** (2011). A structural phylogenetic map for chloroplast photosynthesis. *Trends Plant Sci* **16**, 645-655.
- Amann, K., Lezhneva, L., Wanner, G., Herrmann, R.G., and Meurer, J.** (2004). ACCUMULATION OF PHOTOSYSTEM ONE1, a member of a novel gene family, is required for accumulation of [4Fe-4S] cluster-containing chloroplast complexes and antenna proteins. *Plant Cell* **16**, 3084-3097.
- Amunts, A., and Nelson, N.** (2008). Functional organization of a plant photosystem I: evolution of a highly efficient photochemical machine. *Plant Physiol Biochem* **46**, 228-237.
- Amunts, A., and Nelson, N.** (2009). Plant photosystem I design in the light of evolution. *Structure* **17**, 637-650.
- Amunts, A., Drory, O., and Nelson, N.** (2007). The structure of a plant photosystem I supercomplex at 3.4 Å resolution. *Nature* **447**, 58-63.
- Andersen, B., Scheller, H.V., and Møller, B.L.** (1992). The PSI-E subunit of photosystem I binds ferredoxin:NADP<sup>+</sup> oxidoreductase. *FEBS Lett* **311**, 169-173.
- Anderson, S.L., and McIntosh, L.** (1991). Light-activated heterotrophic growth of the cyanobacterium *Synechocystis* sp. strain PCC 6803: a blue-light-requiring process. *J Bacteriol* **173**, 2761-2767.



- Andersson, J.M.** (1986). Photoregulation of the composition, function, and structure of thylakoid membranes. *Annu Rev Plant Physiol* **37**, 93-136.
- Armbruster, U., Labs, M., Pribil, M., Viola, S., Xu, W., Scharfenberg, M., Hertle, A.P., Rojahn, U., Jensen, P.E., Rappaport, F., Joliot, P., Dormann, P., Wanner, G., and Leister, D.** (2013). *Arabidopsis* CURVATURE THYLAKOID1 proteins modify thylakoid architecture by inducing membrane curvature. *Plant Cell* **25**, 2661-2678.
- Arnon, D.I., Allen, M.B., and Whatley, F.R.** (1954). Photosynthesis by isolated chloroplasts. *Nature* **174**, 394-396.
- Arnon, D.I., Tsujimoto, H.Y., and Tang, G.M.** (1981). Oxygenic photoreduction of ferredoxin independently of the membrane-bound iron-sulfur centers of photosystem I. *Biochem Biophys Res Commun* **99**, 936-945.
- Bendall, D.S., and Manasse, R.S.** (1995). Cyclic photophosphorylation and electron transport. *Biochim Biophys Acta* **1229**, 23-38.
- Boudreau, E., Takahashi, Y., Lemieux, C., Turmel, M., and Rochaix, J.D.** (1997). The chloroplast *ycf3* and *ycf4* open reading frames of *Chlamydomonas reinhardtii* are required for the accumulation of the photosystem I complex. *EMBO J* **16**, 6095-6104.
- Buchanan, B.B., and Balmer, Y.** (2005). Redox regulation: a broadening horizon. *Annu Rev Plant Biol* **56**, 187-220.
- Büchel, C., and Kühlbrandt, W.** (2005). Structural differences in the inner part of photosystem II between higher plants and cyanobacteria. *Photosynth Res* **85**, 3-13.
- Burrows, P.A., Sazanov, L.A., Svab, Z., Maliga, P., and Nixon, P.J.** (1998). Identification of a functional respiratory complex in chloroplasts through analysis of tobacco mutants containing disrupted plastid *ndh* genes. *EMBO J* **17**, 868-876.
- Butler, P.J., and Kühlbrandt, W.** (1988). Determination of the aggregate size in detergent solution of the light-harvesting chlorophyll a/b-protein complex from chloroplast membranes. *Proc Natl Acad Sci U S A* **85**, 3797-3801.
- Cai, Y.P., and Wolk, C.P.** (1990). Use of a conditionally lethal gene in *Anabaena* sp strain PCC 7120 to select for double recombinants and to entrap insertion sequences. *J Bacteriol* **172**, 3138-3145.
- Campbell, W.H., and Gowri, G.** (1990). Codon usage in higher plants, green algae, and cyanobacteria. *Plant Physiol* **92**, 1-11.
- Carmeli, I., Frolov, L., Carmeli, C., and Richter, S.** (2007). Photovoltaic activity of photosystem I-based self-assembled monolayer. *J Am Chem Soc* **129**, 12352-12353.
- Carpenter, S.D., Ohad, I., and Vermaas, W.F.** (1993). Analysis of chimeric spinach/cyanobacterial CP43 mutants of *Synechocystis* sp. PCC 6803: the chlorophyll-protein CP43 affects the water-splitting system of Photosystem II. *Biochim Biophys Acta* **1144**, 204-212.
- Cavalier-Smith, T., and Lee, J.J.** (1985). Protozoa as hosts for endosymbioses and the conversion of symbionts into organelles. *J Protozool* **32**, 376-379.
- Chen, M.C., Cheng, M.C., and Chen, S.C.** (1993). Characterization of the promoter of rice plastid *psaA-psaB-rps14* operon and the DNA-specific binding proteins. *Plant Cell Physiol* **34**, 577-584.

- Chi, W., Ma, J., and Zhang, L.** (2012). Regulatory factors for the assembly of thylakoid membrane protein complexes. *Philos Trans R Soc Lond B Biol Sci* **367**, 3420-3429.
- Chitnis, P.R.** (2001). Photosystem I: Function and physiology. *Annu Rev Plant Physiol Plant Mol Biol* **52**, 593-626.
- Clerico, E.M., Ditty, J.L., and Golden, S.S.** (2007). Specialized techniques for site-directed mutagenesis in cyanobacteria. *Methods Mol Biol* **362**, 155-171.
- Collins, A.M., Liberton, M., Jones, H.D., Garcia, O.F., Pakrasi, H.B., and Timlin, J.A.** (2012). Photosynthetic pigment localization and thylakoid membrane morphology are altered in *Synechocystis* 6803 phycobilisome mutants. *Plant Physiol* **158**, 1600-1609.
- DalCorso, G., Pesaresi, P., Masiero, S., Aseeva, E., Schunemann, D., Finazzi, G., Joliot, P., Barbato, R., and Leister, D.** (2008). A complex containing PGRL1 and PGR5 is involved in the switch between linear and cyclic electron flow in *Arabidopsis*. *Cell* **132**, 273-285.
- Daum, B., and Kühlbrandt, W.** (2011). Electron tomography of plant thylakoid membranes. *J Exp Bot* **62**, 2393-2402.
- Day, A., and Goldschmidt-Clermont, M.** (2011). The chloroplast transformation toolbox: selectable markers and marker removal. *Plant Biotechnol J* **9**, 540-553.
- Debus, R.J.** (1992). The manganese and calcium ions of photosynthetic oxygen evolution. *Biochim Biophys Acta* **1102**, 269-352.
- Dekker, J.P., and Boekema, E.J.** (2005). Supramolecular organization of thylakoid membrane proteins in green plants. *Biochim Biophys Acta* **1706**, 12-39.
- Depege, N., Bellafiore, S., and Rochaix, J.D.** (2003). Role of chloroplast protein kinase Stt7 in LHCII phosphorylation and state transition in *Chlamydomonas*. *Science* **299**, 1572-1575.
- Dolganov, N.A., Bhaya, D., and Grossman, A.R.** (1995). Cyanobacterial protein with similarity to the chlorophyll a/b binding proteins of higher plants: evolution and regulation. *Proc Natl Acad Sci U S A* **92**, 636-640.
- Douglas, A.E., and Raven, J.A.** (2003). Genomes at the interface between bacteria and organelles. *Philos Trans R Soc Lond B Biol Sci* **358**, 5-17; discussion 517-518.
- Dühning, U., Ossenbühl, F., and Wilde, A.** (2007). Late assembly steps and dynamics of the cyanobacterial photosystem I. *J Biol Chem* **282**, 10915-10921.
- Endo, T., Mi, H., Shikanai, T., and Asada, K.** (1997). Donation of electrons to plastoquinone by NAD(P)H dehydrogenase and by ferredoxin-quinone reductase in spinach chloroplasts. *Plant Cell Physiol* **38**, 1272-1277.
- Engbrecht, J., Neilson, K., and Silverman, M.** (1983). Bacterial bioluminescence: isolation and genetic analysis of functions from *Vibrio fischeri*. *Cell* **32**, 773-781.
- Engler, C., Gruetzner, R., Kandzia, R., and Marillonnet, S.** (2009). Golden gate shuffling: a one-pot DNA shuffling method based on type II restriction enzymes. *PLoS One* **4**, e5553.

- Eriksson, J., Salih, G.F., Ghebramedhin, H., and Jansson, C.** (2000). Deletion mutagenesis of the 5' *psbA2* region in *Synechocystis* 6803: identification of a putative cis element involved in photoregulation. *Mol Cell Biol Res Commun* **3**, 292-298.
- Ewart, G.D., and Smith, G.D.** (1989). Purification and properties of soluble hydrogenase from the cyanobacterium *Anabaena cylindrica*. *Arch Biochem Biophys* **268**, 327-337.
- Fischer, N., Hippler, M., Setif, P., Jacquot, J.P., and Rochaix, J.D.** (1998). The PsaC subunit of photosystem I provides an essential lysine residue for fast electron transfer to ferredoxin. *EMBO J* **17**, 849-858.
- Folea, I.M., Zhang, P., Aro, E.M., and Boekema, E.J.** (2008). Domain organization of photosystem II in membranes of the cyanobacterium *Synechocystis* PCC6803 investigated by electron microscopy. *FEBS Lett* **582**, 1749-1754.
- Foran, D.R., and Brown, W.M.** (1988). Nucleotide sequence of the LuxA and LuxB genes of the bioluminescent marine bacterium *Vibrio fischeri*. *Nucleic Acids Res* **16**, 777.
- Fouet, A., Arnaud, M., Klier, A., and Rapoport, G.** (1984). Characterization of the precursor form of the exocellular levansucrase from *Bacillus subtilis*. *Biochem Biophys Res Commun* **119**, 795-800.
- Foyer, C.H., Neukermans, J., Queval, G., Noctor, G., and Harbinson, J.** (2012). Photosynthetic control of electron transport and the regulation of gene expression. *J Exp Bot* **63**, 1637-1661.
- Fristedt, R., Willig, A., Granath, P., Crevecoeur, M., Rochaix, J.D., and Vener, A.V.** (2009). Phosphorylation of photosystem II controls functional macroscopic folding of photosynthetic membranes in *Arabidopsis*. *Plant Cell* **21**, 3950-3964.
- Fujita, Y., Murakami, A., Ohki, K., and Hagiwara, N.** (1988). Regulation of photosystem composition in cyanobacterial photosynthetic system: evidence indicating that photosystem I formation is controlled in response to electron transport state. *Plant Cell Phys* **29**, 557-564.
- Fukushima, A., Kusano, M., Nakamichi, N., Kobayashi, M., Hayashi, N., Sakakibara, H., Mizuno, T., and Saito, K.** (2009). Impact of clock-associated *Arabidopsis* pseudo-response regulators in metabolic coordination. *Proc Natl Acad Sci U S A* **106**, 7251-7256.
- Funatsu, G., and Wittmann, H.G.** (1972). Ribosomal proteins .33. Location of amino-acid replacements in protein S12 isolated from *Escherichia coli* mutants resistant to streptomycin. *J Mol Biol* **68**, 547-&.
- Gan, C.** (1989). Gene gun accelerates DNA-coated particles to transform intact cells. *Scientist* **3**, 25.
- Gay, P., Lecoq, D., Steinmetz, M., Ferrari, E., and Hoch, J.A.** (1983). Cloning structural gene *sacB*, which codes for exoenzyme levansucrase of *Bacillus subtilis*: expression of the gene in *Escherichia coli*. *J Bacteriol* **153**, 1424-1431.
- Gibson, D.G., Young, L., Chuang, R.Y., Venter, J.C., Hutchison, C.A., and Smith, H.O.** (2009). Enzymatic assembly of DNA molecules up to several hundred kilobases. *Nature Methods* **6**, 343-U341.
- Grossman, A.R., Karpowicz, S.J., Heinnickel, M., Dewez, D., Hamel, B., Dent, R., Niyogi, K.K., Johnson, X., Alric, J., Wollman, F.A., Li, H., and Merchant, S.S.** (2010). Phylogenomic analysis of the *Chlamydomonas* genome unmasks proteins potentially involved in photosynthetic function and regulation. *Photosynth Res* **106**, 3-17.

- Hankamer, B., Morris, E., Nield, J., Gerle, C., and Barber, J.** (2001). Three-dimensional structure of the photosystem II core dimer of higher plants determined by electron microscopy. *J Struct Biol* **135**, 262-269.
- Hanley, J., Setif, P., Bottin, H., and Lagoutte, B.** (1996). Mutagenesis of photosystem I in the region of the ferredoxin cross-linking site: modifications of positively charged amino acids. *Biochemistry* **35**, 8563-8571.
- He, Q.F., Schlich, T., Paulsen, H., and Vermaas, W.** (1999). Expression of a higher plant light-harvesting chlorophyll *a/b*-binding protein in *Synechocystis* sp PCC 6803. *Eur J Biochem* **263**, 561-570.
- Heathcote, P., Jones, M.R., and Fyfe, P.K.** (2003). Type I photosynthetic reaction centres: structure and function. *Philos Trans R Soc Lond B Biol Sci* **358**, 231-243.
- Herbert, S.K., Martin, R.E., and Fork, D.C.** (1995). Light adaptation of cyclic electron transport through Photosystem I in the cyanobacterium *Synechococcus* sp. PCC 7942. *Photosynth Res* **46**, 277-285.
- Herbert, S.K., Samson, G., Fork, D.C., and Laudenbach, D.E.** (1992). Characterization of damage to photosystems I and II in a cyanobacterium lacking detectable iron superoxide dismutase activity. *Proc Natl Acad Sci U S A* **89**, 8716-8720.
- Herranen, M., Tyystjarvi, T., and Aro, E.M.** (2005). Regulation of photosystem I reaction center genes in *Synechocystis* sp. strain PCC 6803 during light acclimation. *Plant Cell Physiol* **46**, 1484-1493.
- Herranen, M., Battchikova, N., Zhang, P., Graf, A., Sirpio, S., Paakkarinen, V., and Aro, E.M.** (2004). Towards functional proteomics of membrane protein complexes in *Synechocystis* sp. PCC 6803. *Plant Physiol* **134**, 470-481.
- Hertle, A.P., Blunder, T., Wunder, T., Pesaresi, P., Pribil, M., Armbruster, U., and Leister, D.** (2013). PGRL1 is the elusive ferredoxin-plastoquinone reductase in photosynthetic cyclic electron flow. *Mol Cell* **49**, 511-523.
- Hill, R., and Bendall, F.** (1960). Crystallization of a photosynthetic reductase from a green plant. *Nature* **187**, 417.
- Hippler, M., Drepper, F., Haehnel, W., and Rochaix, J.D.** (1998). The N-terminal domain of PsaF: precise recognition site for binding and fast electron transfer from cytochrome *c6* and plastocyanin to photosystem I of *Chlamydomonas reinhardtii*. *Proc Natl Acad Sci U S A* **95**, 7339-7344.
- Hippler, M., Reichert, J., Sutter, M., Zak, E., Altschmied, L., Schroer, U., Herrmann, R.G., and Haehnel, W.** (1996). The plastocyanin binding domain of photosystem I. *EMBO J* **15**, 6374-6384.
- Holland, H.D.** (2006). The oxygenation of the atmosphere and oceans. *Philos Trans R Soc Lond B Biol Sci* **361**, 903-915.
- Holzenburg, A., Bewley, M.C., Wilson, F.H., Nicholson, W.V., and Ford, R.C.** (1993). Three-dimensional structure of photosystem II. *Nature* **363**, 470-472.
- Howe, C.J., Barbrook, A.C., Koumandou, V.L., Nisbet, R.E., Symington, H.A., and Wightman, T.F.** (2003). Evolution of the chloroplast genome. *Philos Trans R Soc Lond B Biol Sci* **358**, 99-106; discussion 106-107.
- Ihnatowicz, A., Pesaresi, P., Varotto, C., Richly, E., Schneider, A., Jahns, P., Salamini, F., and Leister, D.** (2004). Mutants for photosystem I subunit D of *Arabidopsis thaliana*: effects on photosynthesis, photosystem I stability and expression of nuclear genes for chloroplast functions. *Plant J* **37**, 839-852.

- Jensen, P.E., Bassi, R., Boekema, E.J., Dekker, J.P., Jansson, S., Leister, D., Robinson, C., and Scheller, H.V.** (2007). Structure, function and regulation of plant photosystem I. *Biochim Biophys Acta* **1767**, 335-352.
- Joliot, P., and Johnson, G.N.** (2011). Regulation of cyclic and linear electron flow in higher plants. *Proc Natl Acad Sci U S A* **108**, 13317-13322.
- Jordan, P., Fromme, P., Witt, H.T., Klukas, O., Saenger, W., and Krauss, N.** (2001). Three-dimensional structure of cyanobacterial photosystem I at 2.5 Å resolution. *Nature* **411**, 909-917.
- Kaneko, T., Sato, S., Kotani, H., Tanaka, A., Asamizu, E., Nakamura, Y., Miyajima, N., Hirose, M., Sugiura, M., Sasamoto, S., Kimura, T., Hosouchi, T., Matsuno, A., Muraki, A., Nakazaki, N., Naruo, K., Okumura, S., Shimpo, S., Takeuchi, C., Wada, T., Watanabe, A., Yamada, M., Yasuda, M., and Tabata, S.** (1996). Sequence analysis of the genome of the unicellular cyanobacterium *Synechocystis* sp. strain PCC6803. II. Sequence determination of the entire genome and assignment of potential protein-coding regions (supplement). *DNA Res* **3**, 185-209.
- Kargul, J., and Barber, J.** (2008). Photosynthetic acclimation: structural reorganisation of light harvesting antenna--role of redox-dependent phosphorylation of major and minor chlorophyll a/b binding proteins. *FEBS J* **275**, 1056-1068.
- Kargul, J., Turkina, M.V., Nield, J., Benson, S., Vener, A.V., and Barber, J.** (2005). Light-harvesting complex II protein CP29 binds to photosystem I of *Chlamydomonas reinhardtii* under State 2 conditions. *FEBS J* **272**, 4797-4806.
- Kerfeld, C.A., and Krogmann, D.W.** (1998). Photosynthetic cytochromes *c* in cyanobacteria, algae, and plants. *Annu Rev Plant Physiol Plant Mol Biol* **49**, 397-425.
- Kirsch, W., Seyer, P., and Herrmann, R.G.** (1986). Nucleotide sequence of the clustered genes for two P700 chlorophyll a apoproteins of the photosystem I reaction center and the ribosomal protein S14 of the spinach plastid chromosome. *Current Genetics* **10**, 843-855.
- Klaus, S.M., Huang, F.C., Golds, T.J., and Koop, H.U.** (2004). Generation of marker-free plastid transformants using a transiently cointegrated selection gene. *Nat Biotechnol* **22**, 225-229.
- Kleine, T., Maier, U.G., and Leister, D.** (2009). DNA transfer from organelles to the nucleus: the idiosyncratic genetics of endosymbiosis. *Annu Rev Plant Biol* **60**, 115-138.
- Komenda, J., Sobotka, R., and Nixon, P.J.** (2012). Assembling and maintaining the Photosystem II complex in chloroplasts and cyanobacteria. *Curr Opin Plant Biol* **15**, 245-251.
- Kouril, R., Zygadlo, A., Arteni, A.A., de Wit, C.D., Dekker, J.P., Jensen, P.E., Scheller, H.V., and Boekema, E.J.** (2005). Structural characterization of a complex of photosystem I and light-harvesting complex II of *Arabidopsis thaliana*. *Biochemistry* **44**, 10935-10940.
- Krech, K., Ruf, S., Masduki, F.F., Thiele, W., Bednarczyk, D., Albus, C.A., Tiller, N., Hasse, C., Schöttler, M.A., and Bock, R.** (2012). The plastid genome-encoded Ycf4 protein functions as a nonessential assembly factor for photosystem I in higher plants. *Plant Physiol* **159**, 579-591.
- Krysan, P.J., Young, J.C., and Sussman, M.R.** (1999). T-DNA as an insertional mutagen in *Arabidopsis*. *Plant Cell* **11**, 2283-2290.

- Kufryk, G.I., Sachet, M., Schmetterer, G., and Vermaas, W.F.J.** (2002). Transformation of the cyanobacterium *Synechocystis* sp PCC 6803 as a tool for genetic mapping: optimization of efficiency. *FEMS Microbiol Lett* **206**, 215-219.
- Kunert, A., Hagemann, M., and Erdmann, N.** (2000). Construction of promoter probe vectors for *Synechocystis* sp PCC 6803 using the light-emitting reporter systems Gfp and LuxAB. *J Microbiol Methods* **41**, 185-194.
- Labarre, J., Chauvat, F., and Thuriaux, P.** (1989). Insertional mutagenesis by random cloning of antibiotic-resistance genes into the genome of the cyanobacterium *Synechocystis* strain PCC 6803. *J Bacteriol* **171**, 3449-3457.
- Lalioi, M.D., and Heath, J.K.** (2001). A new method for generating point mutations in bacterial artificial chromosomes by homologous recombination in *Escherichia coli*. *Nucl Acids Res* **29**.
- Leister, D.** (2003). Chloroplast research in the genomic age. *Trends Genet* **19**, 47-56.
- Leister, D.** (2012). How can the light reactions of photosynthesis be improved in plants? *Front Plant Sci* **3**, 199.
- Lewin, R.A.** (2002). Prochlorophyta - a matter of class distinctions. *Photosynth Res* **73**, 59-61.
- Lezhneva, L., and Meurer, J.** (2004). The nuclear factor HCF145 affects chloroplast *psaA-psaB-rps14* transcript abundance in *Arabidopsis thaliana*. *Plant J* **38**, 740-753.
- Lezhneva, L., Amann, K., and Meurer, J.** (2004). The universally conserved HCF101 protein is involved in assembly of [4Fe-4S]-cluster-containing complexes in *Arabidopsis thaliana* chloroplasts. *Plant J* **37**, 174-185.
- Liberton, M., Howard Berg, R., Heuser, J., Roth, R., and Pakrasi, H.B.** (2006). Ultrastructure of the membrane systems in the unicellular cyanobacterium *Synechocystis* sp. strain PCC 6803. *Protoplasma* **227**, 129-138.
- Liu, H., Zhang, H., Niedzwiedzki, D.M., Prado, M., He, G., Gross, M.L., and Blankenship, R.E.** (2013). Phycobilisomes supply excitations to both photosystems in a megacomplex in cyanobacteria. *Science* **342**, 1104-1107.
- Lunde, C., Jensen, P.E., Haldrup, A., Knoetzel, J., and Scheller, H.V.** (2000). The PSI-H subunit of photosystem I is essential for state transitions in plant photosynthesis. *Nature* **408**, 613-615.
- Mannan, R.M., Whitmarsh, J., Nyman, P., and Pakrasi, H.B.** (1991). Directed mutagenesis of an iron-sulfur protein of the photosystem I complex in the filamentous cyanobacterium *Anabaena variabilis* ATCC 29413. *Proc Natl Acad Sci U S A* **88**, 10168-10172.
- Maple, J., and Møller, S.G.** (2007). Mutagenesis in *Arabidopsis*. *Methods Mol Biol* **362**, 197-206.
- Martin, W.** (2003). Gene transfer from organelles to the nucleus: frequent and in big chunks. *Proc Natl Acad Sci U S A* **100**, 8612-8614.
- Martin, W., Rujan, T., Richly, E., Hansen, A., Cornelsen, S., Lins, T., Leister, D., Stoebe, B., Hasegawa, M., and Penny, D.** (2002). Evolutionary analysis of *Arabidopsis*, cyanobacterial, and chloroplast genomes reveals plastid phylogeny and thousands of cyanobacterial genes in the nucleus. *Proc Natl Acad Sci U S A* **99**, 12246-12251.

- Matsuoka, M., Takahama, K., and Ogawa, T.** (2001). Gene replacement in cyanobacteria mediated by a dominant streptomycin-sensitive *rps12* gene that allows selection of mutants free from drug resistance markers. *Microbiology* **147**, 2077-2087.
- Maxwell, P.C., and Biggins, J.** (1976). Role of cyclic electron transport in photosynthesis as measured by the photoinduced turnover of P700 in vivo. *Biochemistry* **15**, 3975-3981.
- Meeks, J.C., Elhai, J., Thiel, T., Potts, M., Larimer, F., Lamerdin, J., Predki, P., and Atlas, R.** (2001). An overview of the genome of *Nostoc punctiforme*, a multicellular, symbiotic cyanobacterium. *Photosynth Res* **70**, 85-106.
- Mullineaux, C.W.** (2005). Function and evolution of grana. *Trends Plant Sci* **10**, 521-525.
- Mullineaux, C.W.** (2008). Phycobilisome-reaction centre interaction in cyanobacteria. *Photosynth Res* **95**, 175-182.
- Munekage, Y., Hojo, M., Meurer, J., Endo, T., Tasaka, M., and Shikanai, T.** (2002). *PGR5* is involved in cyclic electron flow around photosystem I and is essential for photoprotection in *Arabidopsis*. *Cell* **110**, 361-371.
- Murakami, A.** (1997). Quantitative analysis of 77K fluorescence emission spectra in *Synechocystis* sp. PCC 6714 and *Chlamydomonas reinhardtii* with variable PS I/PS II stoichiometries. *Photosynth Res* **53**, 141-148.
- Murat, D., Byrne, M., and Komeili, A.** (2012). Cell biology of prokaryotic organelles. *Cold Spring Harb Perspect Biol* **2**, a000422.
- Mustárdy, L., and Garab, G.** (2003). Granum revisited. A three-dimensional model-where things fall into place. *Trends Plant Sci* **8**, 117-122.
- Mustárdy, L., Buttle, K., Steinbach, G., and Garab, G.** (2008). The three-dimensional network of the thylakoid membranes in plants: quasihelical model of the granum-stroma assembly. *Plant Cell* **20**, 2552-2557.
- Naver, H., Boudreau, E., and Rochaix, J.D.** (2001). Functional studies of Ycf3: its role in assembly of photosystem I and interactions with some of its subunits. *Plant Cell* **13**, 2731-2745.
- Nelson, N., and Ben-Shem, A.** (2002). Photosystem I reaction center: past and future. *Photosynth Res* **73**, 193-206.
- Nevo, R., Charuvi, D., Shimoni, E., Schwarz, R., Kaplan, A., Ohad, I., and Reich, Z.** (2007). Thylakoid membrane perforations and connectivity enable intracellular traffic in cyanobacteria. *EMBO J* **26**, 1467-1473.
- Nickelsen, J., and Rengstl, B.** (2013). Photosystem II assembly: from cyanobacteria to plants. *Annu Rev Plant Biol* **64**, 609-635.
- Nickelsen, J., Rengstl, B., Stengel, A., Schottkowski, M., Soll, J., and Ankele, E.** (2010). Biogenesis of the cyanobacterial thylakoid membrane system--an update. *FEMS Microbiol Lett* **315**, 1-5.
- Nixon, P.J., Rogner, M., and Diner, B.A.** (1991). Expression of a higher-plant *psba* gene in *Synechocystis* 6803 yields a functional hybrid photosystem-II reaction center complex. *Plant Cell* **3**, 383-395.
- Niyogi, K.K., Li, X.P., Rosenberg, V., and Jung, H.S.** (2005). Is PsbS the site of non-photochemical quenching in photosynthesis? *J Exp Bot* **56**, 375-382.

- Ogawa, T.** (1991). A gene homologous to the subunit-2 gene of NADH dehydrogenase is essential to inorganic carbon transport of *Synechocystis* PCC6803. *Proc Natl Acad Sci U S A* **88**, 4275-4279.
- Oie, T., Maggiora, G.M., and Christoffersen, R.E.** (1982). Structural characterization of a special-pair chlorophyll dimer model of P700. *Int J Quantum Chem* **22**, 157-171.
- Olive, J., Ajlani, G., Astier, C., Recouvreur, M., and Vernotte, C.** (1997). Ultrastructure and light adaptation of phycobilisome mutants of *Synechocystis* PCC 6803. *Biochim Biophys Acta - Bioenergetics* **1319**, 275-282.
- Ossenbühl, F., Inaba-Sulpice, M., Meurer, J., Soll, J., and Eichacker, L.A.** (2006). The *Synechocystis* sp PCC 6803 *oxal* homolog is essential for membrane integration of reaction center precursor protein pD1. *Plant Cell* **18**, 2236-2246.
- Ozawa, S., Onishi, T., and Takahashi, Y.** (2010). Identification and characterization of an assembly intermediate subcomplex of photosystem I in the green alga *Chlamydomonas reinhardtii*. *J Biol Chem* **285**, 20072-20079.
- Peredo, E.L., Les, D.H., King, U.M., and Benoit, L.K.** (2012). Extreme conservation of the *psaA/psaB* intercistronic spacer reveals a translational motif coincident with the evolution of land plants. *J Mol Evol* **75**, 184-197.
- Pesaresi, P., Schneider, A., Kleine, T., and Leister, D.** (2007). Interorganellar communication. *Curr Opin Plant Biol* **10**, 600-606.
- Pinto, F.L., Thapper, A., Sontheim, W., and Lindblad, P.** (2009). Analysis of current and alternative phenol based RNA extraction methodologies for cyanobacteria. *BMC Mol Biol* **10**, 79.
- Piven, I., Ajlani, G., and Sokolenko, A.** (2005). Phycobilisome linker proteins are phosphorylated in *Synechocystis* sp. PCC 6803. *J Biol Chem* **280**, 21667-21672.
- Powles, S.B.** (1984). Photoinhibition of photosynthesis induced by visible light. *Annu Rev Plant Physiol* **35**, 15-44.
- Rakhimberdieva, M.G., Boichenko, V.A., Karapetyan, N.V., and Stadnichuk, I.N.** (2001). Interaction of phycobilisomes with photosystem II dimers and photosystem I monomers and trimers in the cyanobacterium *Spirulina platensis*. *Biochemistry* **40**, 15780-15788.
- Ried, J.L., and Collmer, A.** (1987). An *nptI-sacB-sacR* cartridge for constructing directed, unmarked mutations in gram-negative bacteria by marker exchange- eviction mutagenesis. *Gene* **57**, 239-246.
- Rippka, R., Deruelles, J., Waterbury, J.B., Herdman, M., and Stanier, R.Y.** (1979). generic assignments, strain histories and properties of pure cultures of cyanobacteria. *J Gen Microbiol* **111**, 1-61.
- Ruf, S., Kössel, H., and Bock, R.** (1997). Targeted inactivation of a tobacco intron-containing open reading frame reveals a novel chloroplast-encoded photosystem I-related gene. *J Cell Biol* **139**, 95-102.
- Sambrook, J., Fritsch, E.F., and Maniatis, T.** (1989). *Molecular Cloning: A Laboratory Manual* (Cold Spring Harbor Laboratory Press).
- Sandmann, G., and Malkin, R.** (1984). Light inhibition of respiration is due to a dual function of the cytochrome *b<sub>6</sub>f* complex and the plastocyanin/cytochrome *c<sub>553</sub>* pool in *Aphanocapsa*. *Arch Biochem Biophys* **234**, 105-111.



- Sato, S., Nakamura, Y., Kaneko, T., Asamizu, E., and Tabata, S.** (1999). Complete structure of the chloroplast genome of *Arabidopsis thaliana*. *DNA Res* **6**, 283-290.
- Schaffner, W., and Weissmann, C.** (1973). A rapid, sensitive, and specific method for the determination of protein in dilute solution. *Anal Biochem* **56**, 502-514.
- Schagger, H., and von Jagow, G.** (1987). Tricine-sodium dodecyl sulfate-polyacrylamide gel electrophoresis for the separation of proteins in the range from 1 to 100 kDa. *Anal Biochem* **166**, 368-379.
- Schagger, H., Aquila, H., and Von Jagow, G.** (1988). Coomassie blue-sodium dodecyl sulfate-polyacrylamide gel electrophoresis for direct visualization of polypeptides during electrophoresis. *Anal Biochem* **173**, 201-205.
- Scherer, S.** (1990). Do photosynthetic and respiratory electron transport chains share redox proteins? *Trends Biochem Sci* **15**, 458-462.
- Schöttler, M.A., Albus, C.A., and Bock, R.** (2011). Photosystem I: its biogenesis and function in higher plants. *J Plant Physiol* **168**, 1452-1461.
- Schwabe, T.M., and Kruij, J.** (2000). Biogenesis and assembly of photosystem I. *Indian J Biochem Biophys* **37**, 351-359.
- Shapiro, A.L., Vinuela, E., and Maizel, J.V., Jr.** (1967). Molecular weight estimation of polypeptide chains by electrophoresis in SDS-polyacrylamide gels. *Biochem Biophys Res Commun* **28**, 815-820.
- Shen, G., Boussiba, S., and Vermaas, W.F.** (1993). *Synechocystis* sp PCC 6803 strains lacking photosystem I and phycobilisome function. *Plant Cell* **5**, 1853-1863.
- Shetty, R.P., Endy, D., and Knight, T.F., Jr.** (2008). Engineering BioBrick vectors from BioBrick parts. *J Biol Eng* **2**, 5.
- Shikanai, T.** (2007). Cyclic electron transport around photosystem I: genetic approaches. *Annu Rev Plant Biol* **58**, 199-217.
- Shimoni, E., Rav-Hon, O., Ohad, I., Brumfeld, V., and Reich, Z.** (2005). Three-dimensional organization of higher-plant chloroplast thylakoid membranes revealed by electron tomography. *Plant Cell* **17**, 2580-2586.
- Smart, L.B., and McIntosh, L.** (1993). Genetic inactivation of the *psaB* gene in *Synechocystis* sp. PCC 6803 disrupts assembly of photosystem I. *Plant Mol Biol* **21**, 177-180.
- Smart, L.B., Anderson, S.L., and McIntosh, L.** (1991). Targeted genetic inactivation of the photosystem I reaction center in the cyanobacterium *Synechocystis* sp PCC 6803. *EMBO J* **10**, 3289-3296.
- Soll, J., and Schleiff, E.** (2004). Protein import into chloroplasts. *Nat Rev Mol Cell Biol* **5**, 198-208.
- Steinmetz, M., Lecoq, D., Aymerich, S., Gonzytreboul, G., and Gay, P.** (1985). The DNA sequence of the gene for the secreted *Bacillus subtilis* enzyme levansucrase and its genetic control sites. *Mol Gen Genet* **200**, 220-228.
- Stöckel, J., Bennewitz, S., Hein, P., and Oelmüller, R.** (2006). The evolutionarily conserved tetratricopeptide repeat protein Pale Yellow Green7 is required for photosystem I accumulation in *Arabidopsis* and copurifies with the complex. *Plant Physiol* **141**, 870-878.

- Tagawa, K., Tsujimoto, H.Y., and Arnon, D.I.** (1963). Analysis of photosynthetic reactions by the use of monochromatic light. *Nature* **199**, 1247-1252.
- Terasaki, N., Yamamoto, N., Tamada, K., Hattori, M., Hiraga, T., Tohri, A., Sato, I., Iwai, M., Taguchi, S., Enami, I., Inoue, Y., Yamanoi, Y., Yonezawa, T., Mizuno, K., Murata, M., Nishihara, H., Yoneyama, S., Minakata, M., Ohmori, T., Sakai, M., and Fujii, M.** (2007). Bio-photosensor: Cyanobacterial photosystem I coupled with transistor via molecular wire. *Biochim Biophys Acta* **1767**, 653-659.
- Thomas, D.J., Avenson, T.J., Thomas, J.B., and Herbert, S.K.** (1998). A cyanobacterium lacking iron superoxide dismutase is sensitized to oxidative stress induced with methyl viologen but is not sensitized to oxidative stress induced with norflurazon. *Plant Physiol* **116**, 1593-1602.
- Thompson, J.D., Gibson, T.J., and Higgins, D.G.** (2002). Multiple sequence alignment using ClustalW and ClustalX. *Curr Protoc Bioinformatics* **Chapter 2**, Unit 2.3.
- Tillett, D., and Neilan, B.A.** (2000). Xanthogenate nucleic acid isolation from cultured and environmental cyanobacteria. *J Phycol* **36**, 251-258.
- Timmis, J.N., Ayliffe, M.A., Huang, C.Y., and Martin, W.** (2004). Endosymbiotic gene transfer: organelle genomes forge eukaryotic chromosomes. *Nat Rev Genet* **5**, 123-135.
- Timms, A.R., Steingrimsdottir, H., Lehmann, A.R., and Bridges, B.A.** (1992). Mutant sequences in the *rpsL* gene of *Escherichia coli* B/r: mechanistic implications for spontaneous and ultraviolet light mutagenesis. *Mol Gen Genet* **232**, 89-96.
- Trissl, H.W., and Wilhelm, C.** (1993). Why do thylakoid membranes from higher plants form grana stacks? *Trends Biochem Sci* **18**, 415-419.
- Vallejos, R.H., Ceccarelli, E., and Chan, R.** (1984). Evidence for the existence of a thylakoid intrinsic protein that binds ferredoxin-NADP<sup>+</sup> oxidoreductase. *J Biol Chem* **259**, 8048-8051.
- van der Est, A., Bock, C., Golbeck, J., Brettel, K., Setif, P., and Stehlik, D.** (1994). Electron transfer from the acceptor A1 to the iron-sulfur centers in photosystem I as studied by transient EPR spectroscopy. *Biochemistry* **33**, 11789-11797.
- Vermaas, W.** (1996). Molecular genetics of the cyanobacterium *Synechocystis* sp. PCC 6803: Principles and possible biotechnology applications. *J Appl Phycol* **8**, 263-273.
- Vermaas, W.F.J., Williams, J.G.K., and Arntzen, C.J.** (1987). Sequencing and modification of *psbB*, the gene encoding the CP-47 protein of Photosystem II, in the cyanobacterium *Synechocystis* 6803. *Plant Mol Biol* **8**, 317-326.
- Vermaas, W.F.J., Williams, J.G.K., Rutherford, A.W., Mathis, P., and Arntzen, C.J.** (1986). Genetically engineered mutant of the cyanobacterium *Synechocystis* 6803 lacks the photosystem II chlorophyll-binding protein CP-47. *Proc Natl Acad Sci U S A* **83**, 9474-9477.
- Viola S., Rühle T., Leister D.** A single vector-based strategy for marker-less gene replacement in *Synechocystis* sp. PCC 6803. Submitted.
- Wagner, D., Przybyla, D., Op den Camp, R., Kim, C., Landgraf, F., Lee, K.P., Würsch, M., Laloi, C., Nater, M., Hideg, E., and Apel, K.** (2004). The genetic basis of singlet oxygen-induced stress responses of *Arabidopsis thaliana*. *Science* **306**, 1183-1185.

- Whatley, J.M., and Whatley, F.R.** (1981). Chloroplast Evolution. *New Phytol* **87**, 233-&.
- Wilde, A., Lunser, K., Ossenbühl, F., Nickelsen, J., and Börner, T.** (2001). Characterization of the cyanobacterial *ycf37*: mutation decreases the photosystem I content. *Biochem J* **357**, 211-216.
- Wilde, A., Härtel, H., Hübschmann, T., Hoffmann, P., Shestakov, S.V., and Börner, T.** (1995). Inactivation of a *Synechocystis* sp strain PCC 6803 gene with homology to conserved chloroplast open reading frame 184 increases the photosystem II-to-photosystem I ratio. *Plant Cell* **7**, 649-658.
- Williams, J.G.K.** (1988). Construction of specific mutations in photosystem II photosynthetic reaction center by genetic-engineering methods in *Synechocystis* 6803. *Methods Enzymol* **167**, 766-778.
- Wolk, C.P., Cai, Y.P., and Panoff, J.M.** (1991). Use of a transposon with luciferase as a reporter to identify environmentally responsive genes in a cyanobacterium. *Proc Natl Acad Sci U S A* **88**, 5355-5359.
- Woodson, J.D., and Chory, J.** (2008). Coordination of gene expression between organellar and nuclear genomes. *Nat Rev Genet* **9**, 383-395.
- Xu, W., Wang, Y.C., Taylor, E., Laujac, A., Gao, L.Y., Savikhin, S., and Chitnis, P.R.** (2011). Mutational analysis of photosystem I of *Synechocystis* sp PCC 6803: the role of four conserved aromatic residues in the j-helix of PsaB. *PLoS One* **6**.
- Yao, D.C., Brune, D.C., and Vermaas, W.F.** (2011). Lifetimes of photosystem I and II proteins in the cyanobacterium *Synechocystis* sp. PCC 6803. *FEBS Lett* **586**, 169-173.
- Yeremenko, N., Jeanjean, R., Prommeenate, P., Krasikov, V., Nixon, P.J., Vermaas, W.F., Havaux, M., and Matthijs, H.C.** (2005). Open reading frame *ssr2016* is required for antimycin A-sensitive photosystem I-driven cyclic electron flow in the cyanobacterium *Synechocystis* sp. PCC 6803. *Plant Cell Physiol* **46**, 1433-1436.
- Yu, L., Zhao, J., Muhlenhoff, U., Bryant, D.A., and Golbeck, J.H.** (1993). PsaE is required for in vivo cyclic electron flow around photosystem I in the cyanobacterium *Synechococcus* sp. PCC 7002. *Plant Physiol* **103**, 171-180.
- Zang, X.N., Liu, B., Liu, S.M., Arunakumara, K.K.I.U., and Zhang, X.C.** (2007). Optimum conditions for transformation of *Synechocystis* sp PCC 6803. *J Microbiol* **45**, 241-245.

## **Acknowledgements**

I would like to thank Prof. Dr. Dario Leister for giving me the opportunity and the funding to accomplish my Ph.D. in his research group and for involving me in this inspiring project.

Thanks to Prof. Dr. Jörg Nickelsen for taking over the “Zweitgutachter”.

I would like to thank Dr. Thilo Rühle for the kind and useful supervision and the motivation, support and good ideas he gave me throughout my entire Ph.D.

Thanks to all the people in the lab for the years spent together with the bad and good moments, the failures and the successes.

Thanks to Anne for the years of friendship.

Thanks to all my old and new roomies Antoine, Michi, Julia, Nina, Julian, Tobi, Alina, Olga, Antonin, Christoph and Samuel for making my life better day by day.

Thanks to Luca for being in all the previous categories.

Thanks to my friends at home, that are always there and always with me.

Thanks to Francesco, for the past, present and future time together.

A special thank to my mum and dad and to my great sisters, for everything.

## **Curriculum vitae**

### **Personal details**

Name: Stefania Viola

Date of birth: 26.02.1985

Place of birth: Brescia (BS), Italy

Citizenship: Italian

### **Education**

October 2004 – December 2007

Bachelor degree in Molecular Biology. Final grade: 110/110 with honor

Università degli studi di Padova (Padova, Italy)

October 2008 – July 2010

Master degree in Molecular Biology. Final grade: 110/110 with honor

Università degli studi di Padova (Padova, Italy)

### **Research experience**

September 2007 – December 2007

Research project: “Cloning and expression in bacterial system of a new putative peroxidase of *Arabidopsis thaliana* thylakoid membrane”

Supervisor: Dr. Elisabetta Bergantino, Università degli studi di Padova (Padova, Italy)

September 2009 – July 2010

Research project: “Further dissection of haem biosynthesis in *Arabidopsis thaliana*-Ferrochelatase II characterization”

Supervisors: Prof. Dario Leister & Dr. Tatjana Kleine

Università degli Studi di Padova (Padova, Italy)

Thesis done at Ludwig Maximilians Universität (München, Germany) as a part of the Erasmus program

## **Publications**

# **Armbruster, U.\***, **Labs, M.\***, **Pribil, M.\***, **Viola, S.\***, **Xu, W.**, **Scharfenberg, M.**, **Hertle, A.P.**, **Rojahn, U.**, **Jensen, P.E.**, **Rappaport, F.**, **Joliot, P.**, **Dormann, P.**, **Wanner, G.**, and **Leister, D.** (2013). *Arabidopsis* CURVATURE THYLAKOID1 proteins modify thylakoid architecture by inducing membrane curvature. *Plant Cell* **25**, 2661-2678.

# **Viola S.**, **Rühle T.**, **Leister D.** (2014). A single vector-based strategy for marker-less gene replacement in *Synechocystis* sp. PCC 6803. *Microb Cell Fact* **13**:4

\* Authors contributed equally

# Publications related to this dissertation

**Declaration / Eidesstattliche Erklärung**

Ich versichere hiermit an Eides statt, dass die vorgelegte Dissertation von mir selbständig und ohne unerlaubte Hilfe angefertigt ist.

München, den

Stefania Viola